NATHALIE FERREIRA SILVA DE MELO

PREPARATION AND CHARACTERIZATION OF DIFFERENT MODIFIED RELEASE SYSTEMS FOR LOCAL ANESTHETIC ARTICAINE

PREPARO E CARACTERIZAÇÃO DE DIFERENTES SISTEMAS DE LIBERAÇÃO MODIFICADA PARA O ANESTÉSICO LOCAL ARTICAÍNA

Campinas
2014

UNIVERSIDADE ESTADUAL DE CAMPINAS
Instituto de Biologia

UNICAMP

NATHALIE FERREIRA SILVA DE MELO

PREPARATION AND CHARACTERIZATION OF DIFFERENT MODIFIED RELEASE SYSTEMS FOR LOCAL ANESTHETIC ARTICAINE

PREPARO E CARACTERIZAÇÃO DE DIFERENTES SISTEMAS DE LIBERAÇÃO MODIFICADA PARA O ANESTÉSICO LOCAL ARTICAÍNA

Thesis presented to the Biology Institute of the University of Campinas in partial fulfillment of the requirements for the degree of Doctor, in Functional and Molecular Biology, in the area of Biochemistry.

Tese apresentada ao Instituto de Biologia da Universidade Estadual de Campinas como parte dos requisitos exigidos para a obtenção do título de Doutora em Biologia Funcional e Molecular, área de Bioquímica.

Supervisor/*Orientador:* Prof. Dr. Leonardo Fernandes Fraceto

ESTE EXEMPLAR CORRESPONDE À VERSÃO FINAL DA TESE DEFENDIDA PELA ALUNA NATHALIE FERREIRA SILVA DE MELO, E ORIENTADA PELO PROF. DR. LEONARDO FERNANDES FRACETO.

Campinas
2014

Informações para Biblioteca Digital

Título em outro idioma: Preparation and characterization of different modified release systems for local anesthetic articaine
Palavras-chave em inglês:
Drug delivery systems
Polymeric nanoparticles
Solid lipid nanoparticles
Gels
Carticaine
Área de concentração: Bioquímica
Titulação: Doutora em Biologia Funcional e Molecular
Banca examinadora:
Leonardo Fernandes Fraceto [Orientador]
Marco Vinícius Chaud
Nelson Eduardo Durán Caballero
Marcelo Henrique Napimoga
Michelle Franz Montan Braga Leite
Data de defesa: 08-08-2014
Programa de Pós-Graduação: Biologia Funcional e Molecular

Campinas, 08 de agosto de 2014

BANCA EXAMINADORA

Prof. Dr. Leonardo Fernandes Fraceto (Orientador)

_____
Assinatura

Prof. Dr. Marco Vinícius Chaud

_____
Assinatura

Prof. Dr. Nelson Eduardo Durán Caballero

_____
Assinatura

Prof. Dr. Marcelo Henrique Napimoga

_____
Assinatura

Dra. Michelle Franz Montan Braga Leite
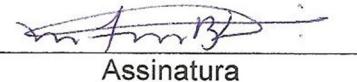
_____
Assinatura

Profa. Dra. Luciana de Matos Alves Pinto

_____
Assinatura

Dra. Milene Heloísa Martins
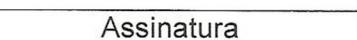
_____
Assinatura

Dra. Cíntia Maria Saia Cereda

_____
Assinatura

v
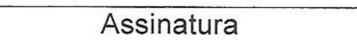
RESUMO

Os anestésicos locais (AL) são fármacos utilizados no controle da dor crônica ou aguda. A articaína (ATC) é um AL da classe das amino-amidas que possui maior potência e menor toxicidade que a lidocaína e tem sido um fármaco de escolha em procedimentos odontológicos e anestesia epidural. As características desejáveis para um AL incluem controle da dor durante procedimentos clínicos e a diminuição da toxicidade local e/ou sistêmica. Assim, uma alternativa que tem se mostrado capaz de promover estes efeitos desejáveis é a veiculação destes fármacos em sistemas de liberação modificada. Neste sentido, as nanopartículas poliméricas (NP), nanopartículas lipídicas sólidas (NLS) e lipossomas unilamelares pequenos (SUV) são sistemas nanocarreadores capazes de promover modificação do perfil de liberação de fármacos e possuem diâmetro inferior a 1 µm. As NP são classificadas como nanoesferas (NE), compostas por uma matriz polimérica e nanocápsulas (NC), constituídas por um invólucro polimérico disposto ao redor de um núcleo oleoso ou aquoso. As NLS são constituídas por uma matriz lipídica que se apresenta sólida em temperatura ambiente. As SUV são estruturas vesiculares compostas por bicamadas de fosfolipídios que se arranjam espontaneamente em meio aquoso. Os hidrogéis são redes poliméricas que quando dispersas em mio aquoso assumem uma conformação doadora de viscosidade à formulação. O objetivo deste trabalho foi preparar e caracterizar diferentes sistemas de liberação modificada para a ATC (neutra e ionizada) incluindo NP, NLS, SUV e hidrogéis (contendo ATC livre e encapsulada) com a finalidade de melhorar suas propriedades farmacológicas visando uma futura aplicação clínica por via infiltrativa e/ou tópica. A otimização das suspensões de NP e SUV foi alcançada através de planejamento fatorial e analisada as propriedades: diâmetro médio, polidispersão, potencial zeta e eficiência de encapsulação do fármaco. Todas as suspensões foram preparadas com ATC a 2%. Foram obtidas partículas de diâmetro compreendido entre 100 e 400 nm e índice de polidispersão abaixo de 0,2. A eficiência de encapsulação alcançada foi bastante satisfatória (entre 50 e 70%). As propriedades físico-químicas das suspensões foram avaliadas em função do tempo, a fim de determinar a estabilidade das partículas. As formulações escolhidas não apresentaram grandes alterações dessas propriedades, sendo consideradas estáveis por um período de até 120 dias de armazenamento à temperatura ambiente. Ensaios de liberação *in vitro* demonstraram menor velocidade de liberação da ATC quando encapsulada em NP, NLS e SUV, em relação à ATC livre. Testes de citotoxicidade *in vitro* em culturas de células 3T3 e CHO revelaram que a ATC livre induz morte celular de maneira concentração dependente, efeito este que foi parcialmente revertido com a encapsulação da ATC em NP, NLS e SUV, indicando menor toxicidade das formulações propostas. Os hidrogéis contendo ATC livre e encapsulada demonstraram boa consistência, homogeneidade e estabilidade. Nos testes reológicos, os géis apresentaram comportamento pseudoplástico com tixotropia, o que pode melhorar a eficácia do fármaco. O gel contendo NC-PCL com ATC apresentou início de permeação mais rápido e liberação mais lenta (até 8 horas). Os resultados obtidos mostraram que foi possível preparar nanocarreadores e hidrogéis para a ATC, sendo obtidos bons resultados com alteração no perfil de liberação do fármaco e diminuição da citotoxicidade, sendo uma futura alternativa para o controle da dor.

Palavras-chave: nanopartículas poliméricas, nanopartículas lipídicas sólidas, lipossomas, poli (ε-caprolactona), alginato/quitosana, hidrogéis, anestésicos locais, articaína.

ABSTRACT

Local anesthetics (LA) are drugs used in controlling chronic or acute pain. The articaine (ATC) is an LA of amino-amides class which have lower toxicity and higher potency than lidocaine and has been the drug of choice in dental procedures and epidural anesthesia. Desirable features for LA include pain control during clinical procedures and the reduction of local and/or systemic toxicity. Thus, an alternative that has been shown to promote these desirable effects is the placement of these drugs in modified release systems. In this regard, polymeric nanoparticles (PN), solid lipid nanoparticles (SLN) and small unilamellar liposomes (SUV) are nanocarriers systems able to promote modification of the drug release profile and have a diameter of less than 1 µM. NP is classified as nanospheres (NS), comprising a polymeric matrix and nanocapsules (NC), consisting of a polymeric shell around an oily or aqueous core. SLN are formed by a lipid matrix which appears solid at room temperature. SUV are vesicular structures composed of phospholipids bilayers which spontaneously arrange themselves in an aqueous medium. Hydrogels are polymeric networks that when dispersed in aqueous medium assume a conformation donor viscosity of the formulation. The objective of this work was to prepare and characterize different modified delivery systems for ATC (neutral and ionized form) including PN, SLN, SUV and hydrogels (containing free and encapsulated ATC) in order to improve its pharmacological properties targeting future clinical application for infiltrating and/or topically. The optimization of PN and SUV suspensions was achieved through a factorial design and analyzed the properties: mean diameter, polydispersity, zeta potential and encapsulation efficiency of the drug. All suspensions were prepared with ATC 2%. Particles were obtained with diameter between 100-400 nm and polydispersity index lower than 0.2. The encapsulation efficiency was achieved quite satisfactory (between 50 and 70%). The physico-chemical properties of the suspensions were assessed as function of time in order to determine the stability of the particles. The selected formulations showed no significant changes of these properties, being considered stable for a period of 120 days of storage at room temperature. *In vitro* release experiments showed slower release of ATC when encapsulated in PN, SLN and SUV, in relation to the free ATC. *In vitro* cytotoxicity tests on 3T3 and CHO cells revealed that the free ATC induces cell death concentration-dependent, an effect which was partially reversed by ATC in the encapsulation in PN, SLN and SUV, indicating low toxicity of the proposed formulations. The hydrogels containing free and encapsulated ATC showed good consistency, uniformity and stability. In the rheological tests, the gels exhibited pseudoplastic behavior with tixotropy, which can improve the effectiveness of the drug. The gel containing the NC-PCL with ATC showed faster onset of permeation and slower release (up to 8 hours). The results showed that it was possible to prepare hydrogels and nanocarriers for ATC, with good results in modification of drug release and decreased cytotoxicity profile, being a future alternative for pain control.

Keywords: polymeric nanoparticles, solid lipid nanoparticles, liposomes, poly (ε-caprolactone), alginate/chitosan, gels, local anesthetics, articaine.

x

Sumário

Dedico esta tese aos meus pais Valkíria e José Antonio, que não mediram esforços para que eu chegasse nesta etapa da minha vida.

"Nenhuma grande descoberta foi feita jamais sem um palpite ousado."

(Sir Isaac Newton)

AGRADECIMENTOS

Capítulo 1 – Introdução geral

Os sistemas de liberação de fármacos têm sido descritos na literatura com o objetivo de prolongar e melhorar o controle da administração de fármacos e diminuir a toxicidade destes. Em termos simples, os sistemas de liberação de fármacos podem ser definidos como o processo de liberação de um agente bioativo, em uma taxa específica e em um sítio específico. Muitos estudos estão sendo realizados nesta área com a finalidade de desenvolver novas formulações com vantagens frente às formulações convencionais (Rawat *et al.* 2006, Anton *et al.* 2008, Mishra *et al.* 2010, Parveen *et al.* 2012, Canfarotta *et al.* 2013).

O desenvolvimento de nanocarreadores é atualmente um dos principais tópicos na pesquisa farmacêutica para superar problemas comuns de fármacos pouco solúveis em água. Entre as diferentes abordagens, a micro e nanoencapsulação tem atraído maior atenção (Preetz *et al.* 2008, Canfarotta *et al.* 2013).

Nanocarreadores são dispositivos nanométricos compostos de diferentes materiais biodegradáveis naturais ou sintéticos e até mesmo compostos organometálicos (Figura 1). Estes nanocarreadores, nas suas diversas formas, têm a possibilidade de fornecer infinitas oportunidades na área de liberação de fármacos e, portanto, está cada vez mais sendo investigados para aproveitar o seu potencial. Devido à sua maior área superficial, mostram melhoria da farmacocinética e biodistribuição de agentes terapêuticos e, assim, são capazes de minimizar a toxicidade pelo seu acúmulo preferencial no sítio alvo (Alexis *et al.* 2008, Mishra *et al.* 2010, Parveen *et al.* 2012, Canfarotta *et al.* 2013). Eles são capazes de melhorar a solubilidade de compostos hidrofóbicos e torná-los adequadas para administração parenteral. Além disso, aumentam a estabilidade de uma variedade de agentes terapêuticos, como peptídeos e oligonucleotídeos (Koo *et al.* 2005, Mishra *et al.* 2010, Parveen *et al.* 2012). A utilização de materiais biodegradáveis minimiza as possibilidades de reações de hipersensibilidade dos tecidos e proporciona boa biocompatibilidade (Rawat *et al.* 2006, Mishra *et al.* 2010, Parveen *et al.* 2012, Canfarotta *et al.* 2013).

Figura 1: Representação dos diferentes tipos de nanocarreadores. (a) nanotubos de carbono, (b) lipossomas de fosfolipídios, (c) nanopartículas lipídicas sólidas (NLS) de lipídios sólidos, (d) nanopartículas poliméricas (i) nanoesferas e (ii) nanocápsulas, (e) micelas poliméricas, (f) dendrímero formado pela polimerização de várias unidades monoméricas, (g) nanopartícula funcionalizada. Adaptado de (Rawat *et al.* 2006).

(a) nanotubos
(b) lipossomas
(c) nanopartículas lipídicas sólidas
(d) (i) nanoesferas
(d) (ii) nanocápsulas
(e) Micelas poliméricas
(f) dendrímeros
(g) nanopartículas funcionalizadas
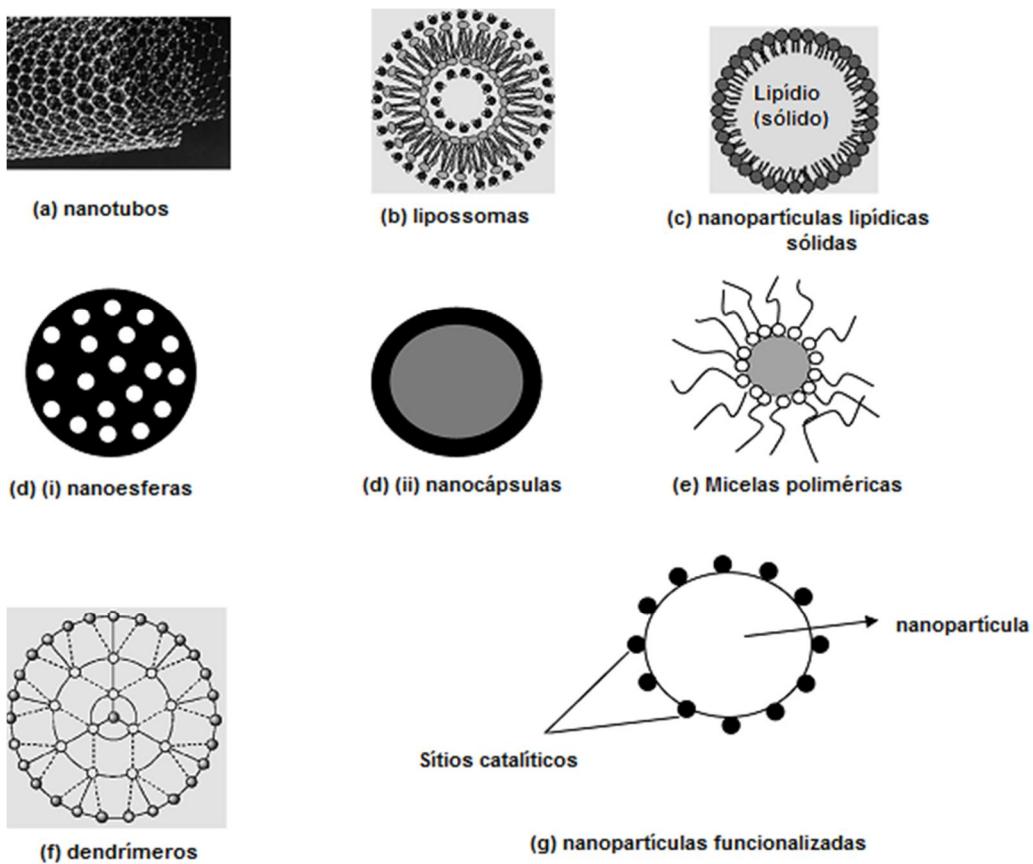
A avaliação toxicológica de partículas em escala nanométrica contribui para uma série de questões ligadas à utilização de nanomateriais em produtos comerciais. Sendo assim, o entendimento dos mecanismos de cito e genotoxicidade de um dado nanomaterial são fundamentais para a definição de seu impacto ambiental e de estratégias de proteção aos trabalhadores e a saúde humana (Seaton and Donaldson 2005, Singh *et al.* 2009, Franchi *et al.* 2012).

1.1. Nanopartículas poliméricas

As nanopartículas poliméricas (NP) são carreadoras de fármacos ou outras moléculas ativas e que apresentam tamanho compreendido entre 10 e 1000 nm. Dependendo do método de preparo e materiais empregados, podem ser obtidas nanoesferas (NE) ou nanocápsulas (NC). As NC são constituídas por um invólucro polimérico e núcleo que pode ser oleoso ou aquoso. Nestas, o fármaco pode ser encontrado dissolvido no núcleo oleoso/aquoso ou adsorvido na parede polimérica. Já as NE são constituídas de matriz polimérica densa e não apresentam óleo em sua composição. Neste sistema o fármaco pode ser encontrado retido na matriz polimérica, adsorvido ou disperso na matriz polimérica (Schaffazick *et al.* 2003, Durán *et al.* 2006, Mohanraj and Chen 2006, Morales 2007, Anton *et al.* 2008, Mishra *et al.* 2010, Parveen *et al.* 2012, Canfarotta *et al.* 2013).

Figura 2: Representação dos tipos de nanopartículas poliméricas biodegradáveis: de acordo com a organização estrutural elas são classificadas como nanocápsulas ou nanoesferas. Adaptado de (Kumari *et al.* 2010).
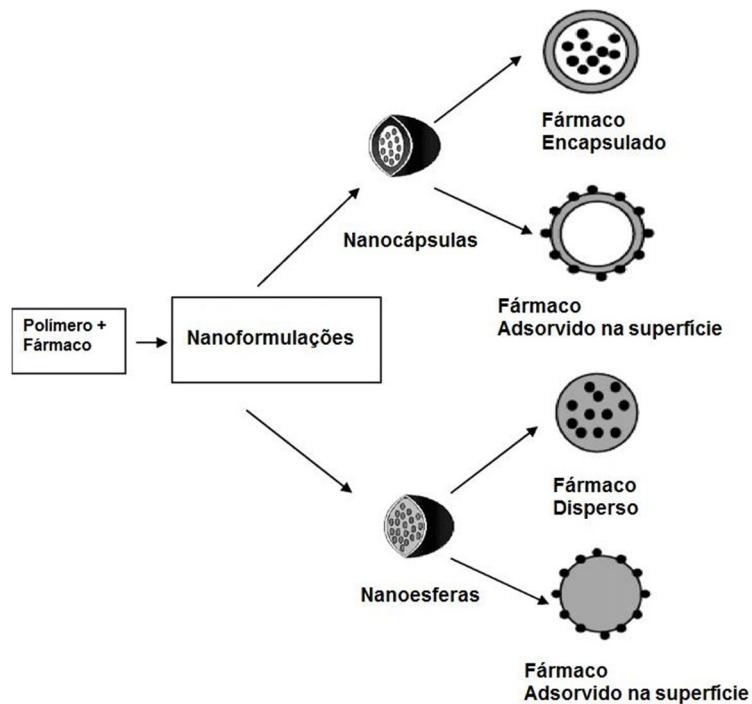
Os fármacos são liberados das NP a partir de mecanismos que envolvem a dessorção do fármaco da superfície, difusão através da matriz ou parede polimérica, desintegração,

dissolução e erosão da matriz polimérica (Gopferich 1996, Polakovic *et al.* 1999, Sonaje *et al.* 2007, Kumari *et al.* 2010).

O mecanismo de liberação pode ser modulado pela massa molecular do polímero utilizado. Quanto maior for a massa molecular, mais lento será o processo de liberação dos fármacos (Kumari *et al.* 2010, Souto *et al.* 2012).

A justificativa da aplicação de NP na terapêutica reside em algumas características como a boa estabilidade física, química e biológica, fácil preparação e boa reprodutividade, além de serem aplicáveis a uma ampla variedade de fármacos visando melhorar suas propriedades terapêuticas, e por possuírem tamanho pequeno permite a administração intravenosa, ao contrário de muitos outros sistemas coloidais (Picos *et al.* 2000, Sinha *et al.* 2004, Parveen *et al.* 2012, Canfarotta *et al.* 2013). As vantagens da aplicação de sistemas nanoparticulados poliméricos como carreadores de moléculas incluem: a) o tamanho e as características das NP podem ser facilmente manipulados e, por possuírem tamanho pequeno, permitem a administração intravenosa, ao contrário de muitos outros sistemas coloidais; b) controle e sustentação da liberação do fármaco no sítio de ação específico, alterando sua distribuição e eliminação do organismo, aumentando a eficácia terapêutica e diminuindo os efeitos colaterais resultantes do acúmulo do fármaco em tecidos não específicos; c) controle da degradação da NP e consequentemente a liberação do fármaco podem ser modulados com a escolha dos constituintes da matriz polimérica; d) os sítios específicos podem ser alcançados através da modificação da superfície de NP, onde podem ser incorporados ligantes, como partículas metálicas ou anticorpos, sendo esta uma boa estratégia, principalmente, para a terapia do câncer; e) administração por várias vias, incluindo oral, nasal, parenteral, intra-ocular e tópica; f) boa estabilidade física, química e biológica, fácil preparo e boa reprodutibilidade (Gopferich 1996, Sinha *et al.* 2004, Mohanraj and Chen 2006, Torchilin 2006, Nair and Laurencin 2007, Kumari *et al.* 2010, Parveen *et al.* 2012, Canfarotta *et al.* 2013).

1.1.1 Material utilizado na preparação das nanopartículas poliméricas

A preparação de NP como carreadores de fármacos impõe algumas restrições físico-químicas e biológicas quanto aos polímeros utilizados na preparação destes sistemas. A via de administração é um dos fatores mais importantes na escolha do polímero a ser utilizado na formulação. Em caso de administração parenteral o polímero deve ser biodegradável, já para o

caso de administração oral ou local o polímero não precisa necessariamente ser biodegradável, mas sim biocompatível. Além da via de administração a escolha do polímero deve levar em consideração as características químicas do fármaco para que associação seja satisfatória (Durán *et al.* 2006, Morales 2007, Souto *et al.* 2012).

1.1.1.1. Poliésteres alifáticos

Dentre os poliésteres alifáticos existentes, os mais utilizados são o poli(lático) (PLA), poli(glicólico), poli(lático-co-glicólico) (PLGA), poli(ε-caprolactona) (PCL), poli(hidroxivalerato) (PHV) e poli(hidroxibutirato) (PHB) (Schaffazick *et al.* 2003, Morales 2007, Kumari *et al.* 2010, Kumar and Sawant 2013).

O PCL (Figura 3) é um poliester alifático e semicristalino. O peso molecular varia de 10.000 a 80.000 g/mol. O PCL é soluvel em clorofórmio, diclorometano, tetracloreto de carbono, benzeno, tolueno e ciclohexano à temperatura ambiente. O PCL, quando empregado em sistemas de liberação de fármacos, apresenta como propriedade a alta permeabilidade a substâncias, principalmente, de baixo peso molecular (Sinha *et al.* 2004, Woodruff and Hutmacher 2010).

O PCL é amplamente utilizado em suturas devido a sua biocompatibilidade, sendo um dos mais importantes polimeros biodegradaveis na medicina (Lu and Chen 2004, Munoz-Bonilla *et al.* 2013). Poliésteres como o PCL apresentam propriedades bioadesivas. A bioadesividade confere um acréscimo na deposição das particulas em regiões do trato gastrointestinal, aumentando a absorção sistemica de fármacos (Lamprecht *et al.* 2000, Munoz-Bonilla *et al.* 2013).

Figura 3: Representação estrutural do polímero poli(ε-caprolactona).
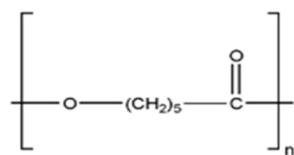
A degradação do PCL em ambientes aquosos é favorecida pelo meio alcalino e pelas altas temperaturas. A degradação ocorre por hidrólise química e/ou enzimática, principalmente

da ligação éster. Durante a degradação a diminuição da massa molar é acompanhada por uma ampla distribuição da massa molar e pelo desenvolvimento de picos de baixa massa molar (Eldsater *et al.* 2001, Woodruff and Hutmacher 2010, Munoz-Bonilla *et al.* 2013).

Os poliésteres alifáticos constituem boa estratégia para incorporação de fármacos de administarção intravenosa. No entanto, a incorporação de fármacos com solubilidade em água relativamente elevada nestes polímeros é baixa, o que promove perda de farmaco na porção aquosa durante a formação da nanopartícula e, portanto, estes casos requerem outras técnicas de encapsulação utilizando polímeros hidrofílicos como o alginato e a gelatina ou então a modificação destes poliésteres com polietilenoglicol (PEG) formando polímeros di ou tribloco (Govender *et al.* 2000, Avgoustakis *et al.* 2003, Mora-Huertas 2010, Woodruff and Hutmacher 2010).

O PEG é um polímero hidrofílico, biocompatível e aprovado pelo Food and Drug Administration (FDA) para uso interno, o qual pode ser acrescentado à estrutura do PCL formando copolímeros em dibloco PEG-PCL (Hsu *et al.* 2004, Wei *et al.* 2009). Os copolímeros PEG-PCL possuem hidrofilicidade e biodegradabilidade maiores que o homopolímero PCL, apresentando um melhor desempenho em estudos *in vitro*. Este copolímero tem sido muito estudado em desenvolvimento de sistemas de liberação de fármacos hidrofílicos, como nanocápsulas de núcleo aquoso (Yadav *et al.* 2008, Wei *et al.* 2009). Estes sistemas foram capazes de reduzir a toxicidade dos fármacos, além de aumentar o tempo de circulação uma vez que a presença do PEG na superfície da partícula impede o reconhecimento e opsonização pelas células fagocitárias (Neckel and Lemos-Senna 2005).

As nanocápsulas de núcleo aquoso conseguem promover uma elavada capacidade de encapsulação de fármacos hidrofílicos (que conseguem ficar retidos no núcleo), protegem os tecidos contra irritação provocada por fármacos altamente solúveis em água além de reduzir o efeito inicial de liberação imediata ou "burst effect", que normalmente é visto em outros tipos de nanopartículas poliméricas (Vrignaud *et al.* 2011).

Os tensoativos são fundamentais para evitar agregação das NP durante o armazenamento, sendo os tensoativos mais utilizados os de alta hidrofilia não-iônicos como os polissorbatos (Tween®), poloxamers (Pluronic®) e álcool polivinílico (PVA) (Morales 2007).

De uma maneira geral, os fármacos lipofílicos possuem maior afinidade com a matriz polimérica e com o núcleo oleoso das nanocápsulas, sendo mais eficientemente incorporados em relação aos hidrofílicos (Morales 2007, Kumari *et al.* 2010).

1.1.1.2. Alginato

O alginato (Figura 4) é um polissacarídeo linear solúvel em água derivado de algas marrons, constituído por ligações 1-4 de ácido β–D-manurônico (M) e α-L-gulurônico (G). Cada um destes monômeros apresenta uma forma diferente de se ligar a cadeia polimérica. As ligações de G são estruturadas na forma vertical, enquanto as posições de M são encontradas na horizontal (Martinsen *et al.* 1997, George and Abraham 2006, Lertsutthiwong *et al.* 2009, Sun and Tan 2013), dando origem as diferentes ligações glicosídicas α (1-4) e β (1-4).

Figura 4: Representação estrutural do polímero alginato com monômeros ácidos β-D-manurônico (M) e α-L-gulurônico (G), com as possíveis ligações glicosídicas α(1-4) e β(1-4).
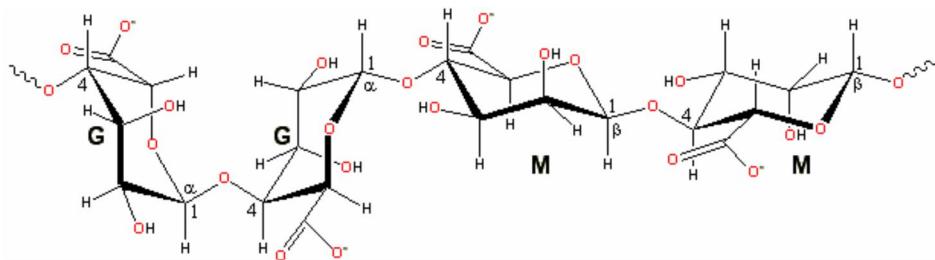
Comercialmente, o alginato pode ser extraído de três espécies de algas, que incluem *Laminaria hyperborean*, *Ascophyllum nodosum* e *Macrocystis pyrifera* (Smidsrod and Skjak-Braek 1990, George and Abraham 2006) e são muito utilizados em comidas industrializadas como emulsificante e estabilizador e são inclusos no grupo de compostos saudáveis pelo FDA, sendo biodegradável e atóxico quando administrado oralmente (ESPEVIK, 1993). Este polímero também está sendo utilizado para sistema de liberação de fármaco (Shimizu *et al.* 2003, George and Abraham 2006, Zahoor *et al.* 2007, Sun and Tan 2013) e terapia gênica (You and Peng 2005), facilitando a passagem através de barreiras biológicas, contribuindo na diminuição da toxicidade, aumentando a estabilidade e melhorando a biodisponibilidade (Alonso 2004, Durán *et al.* 2006, Sun and Tan 2013).

Estes polímeros são aniônicos e podem reagir com cátions divalentes, (levando a formação de um gel) ou com cátions polivalentes (formando ligações cruzadas) (Haug and Larsen 1962, Sun and Tan 2013). Isto ocorre porque a maioria dos cátions polivalentes consegue se ligar a esses polímeros, através de uma simples substituição entre os íons (Sun

and Tan 2013). Portanto este sistema constitui em uma técnica de encapsulação simples, que ocorre por uma transição sol-gel, formado de junções intercadeias, permitindo a entrada de fármacos ou proteínas nesta estrutura de rede (Martinsen *et al.* 1997, Sun and Tan 2013). Diferente do alginato de sódio, que é muito solúvel em água, o alginato de cálcio é insolúvel, portanto o processo de troca iônica no alginato de sódio é de fundamental importância para a aplicação na indústria de alimentos e farmacêuticas, pois, a interação entre cátions divalentes e os blocos G das moléculas formam uma estrutura de rede na forma de gel (Martinsen *et al.* 1997, George and Abraham 2006, Sun and Tan 2013).

Polímeros de alginato estão sendo altamente utilizados em aplicações biomédicas por serem biodegradáveis e biocompatíveis, mas sofrem a limitação da rápida liberação em concentrações de sais fisiológicos (Némati *et al.* 1996, De and Robinson 2003). Na presença de íons sódio, o alginato de cálcio insolúvel se converte em alginato de sódio solúvel, resultando em uma rápida desintegração do sistema (Némati *et al.* 1996, De and Robinson 2003, Sun and Tan 2013).

1.1.1.3. Quitosana

A quitosana (Figura 5) é um polissacarídeo catiônico linear composto por unidades de *D*-glicosamina e *N*-acetil-*D*-glicosamina, através de ligações glicosídicas β -(1-4). Ela pode ser obtida a partir da quitina por meio da desacetilação em meio alcalino, podendo também estar naturalmente presente em alguns fungos, como aqueles pertecentes aos gêneros *Mucor* e *Zygomicetes* (Lertsutthiwong *et al.* 2009, Saboktakin *et al.* 2011, Rampino *et al.* 2013). De acordo com o grau médio de acetilação, parâmetro empregado para caracterizar o conteúdo médio de unidades *N*-acetil-*D*-glicosamina de quitosana, podem-se obter diversas quitosanas variando-se, assim, suas propriedades físico-químicas, como solubilidade, pKa e viscosidade (Singla and Chawla 2001, Saboktakin *et al.* 2011, Rampino *et al.* 2013).

Figura 5: Representação estrutural do polímero quitosana com os monômeros *D*-glicosamina com ligações glicosídicas β -(1-4).
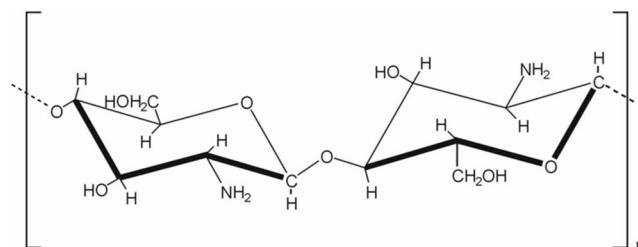
A quitosana é insolúvel em condições de pH neutro e alcalino, enquanto que é solúvel em pH ácido. A solubilidade depende da distribuição dos grupamentos amino livres e N-acetil. Em meio ácido, ocorre a protonação dos grupamentos amino e a molécula pode ser solubilizada (Saboktakin *et al.* 2011). A quitosana vem ganhando importância dentro da área farmacêutica por ser um polímero catiônico não-tóxico com boa biocompatibilidade e biodegradabilidade, pois não induz reações alérgicas ou rejeição imune, além de apresentar propriedades mucoadesaivas prolongando a retenção em tecidos-alvo (Lertsutthiwong *et al.* 2009, Yang *et al.* 2011, Rampino *et al.* 2013). Ela vem sendo usada na produção de micropartículas e nanopartículas, através da formação de uma gelificação ionotrópica com polímeros negativamente carregados. Complexos poliônicos tem sido investigados como sistema de liberação de drogas, proteínas, DNA e outros oligonucleotídeos apresentando bons resultados (Janes *et al.* 2001a, Janes *et al.* 2001b, Agnihotri *et al.* 2004, Rampino *et al.* 2013). Vários tipos de complexo quitosana-poliânion foram reportados na literatura, porém a combinação de quitosana e alginato de sódio foi considerada a mais interessante para sistemas carreadores (Mi *et al.* 2002, Lertsutthiwong *et al.* 2009, Rampino *et al.* 2013). Uma vantagem adicional deste sistema são as características não tóxicas, permitindo a repetição da administração do agente terapêutico. Alguns trabalhos na literatura mostraram a encapsulação de fármacos, proteínas em nanopartículas e micropartículas de alginato-quitosana (Coppi *et al.* 2002, Gonzalez-Rodriguez *et al.* 2002, Lertsutthiwong *et al.* 2009, Rampino *et al.* 2013).

Os complexos de poliíons de alginato/quitosana obtidos a partir de gelificação ionotrópica através da interação entre os grupamentos carboxila do alginato e grupamento amino da quitosana têm a capacidade de proteger e fármaco encapsulado bem como tem características biocompatíveis e biodegradáveis e limita a liberação do fármaco de modo mais eficaz quando comparado com alginato e quitosana sozinhos. Devido à baixa toxicidade destes complexos,

nanopartículas de alginato/quitosana vem sendo estudados para encapsulação de fármacos, oligonucleotídeos e proteínas com resultados promissores (De and Robinson 2003, Gazori *et al.* 2009, Rampino *et al.* 2013).

1.1.1.4. Álcool polivinílico

O álcool polivinílico (PVA) é um polímero semicristalino, hidrossolúveis, que os grupamentos hidroxilas formam ligações de hidrogênio intra e intermoleculares. O PVA tem sido utilizado como tensoativo em formulações de nanopartículas poliméricas e nanopartículas lipídicas sólidas. Como se trata de um tensoativo de massa molecular elevada (30-70 kDa), seu mecanismo para estabilizar de nanopartículas se dá por estabilização estérica (Aranha and Lucas 2001, Song and Kim 2004).

A estabilização estérica é uma consequência da interação física de cadeias longas de substâncias poliméricas adsorvidas nas partículas. Com a aproximação das partículas, as cadeias poliméricas se ordenam paralelamente umas as outras. Neste sentido, no equilíbrio termodinâmico, as partículas ficam isoladas, aumentando assim a sua estabilidade coloidal no meio (Hotza 1997).

1.1.2.. Métodos de preparação de nanopartículas poliméricas

Os métodos de preparação de NP podem ser baseados na polimerização *in situ* de monômeros ou na precipitação de polímeros pré-formados naturais ou sintéticos (Morales 2007, Souto *et al.* 2012).

Métodos de polimerização *in situ* envolvem a formação do polímero no momento da preparação das NP e podem ser obtidos por polimerização em emulsão ou polimerização interfacial. As limitações desses métodos envolvem a exigência de solventes orgânicos tóxicos para o preparo e a dificuldade de purificação, levando a presença de moléculas residuais tóxicas (monômeros) decorrentes da polimerização deficiente. Devido a estas limitações foram propostos o uso de polímeros pré-formados para o preparo de NP e estes são os mais utilizados atualmente (Reis *et al.* 2006).

Dentre os métodos baseados em polímeros pré-formados podemos citar a emulsificação/ evaporação do solvente e a gelificação ionotrópica (Schaffazick *et al.* 2003, Reis *et al.* 2006, Souto *et al.* 2012).

O **método emulsificação/evaporação do solvente** compreende a preparação de uma solução orgânica do polímero contendo o fármaco hidrofóbico dissolvido e a sua dispersão sobre forma de microgotas em um meio de não-solvente (meio de suspensão), um liquido em que o polímero seja insolúvel, geralmente estabilizado com um agente de suspensão. Posteriormente ocorre a eliminação do solvente através de evaporação sob pressão reduzida ou agitação contínua. A água e o cloreto de metileno são os não-solventes e solventes, respectivamente mais utilizados. As emulsões O/A são vantajosas porque utilizam a água como não-solvente, ou seja, o processo é econômico e não necessita de reciclagem, e as partículas dificilmente se aglomeram (Reis *et al.* 2006, Morales 2007, Souto *et al.* 2012).

O **método de gelificação ionotrópica** é apresentado como estratégia para preparo de NP a partir de polímeros naturais hidrofílicos como o alginato, quitosana e a gelatina. O processo envolve a mistura de duas fases aquosas onde uma contém um polímero aniônico, como o alginato e a outra um polímero catiônico como a quitosana. Os grupamentos amino carregados positivamente da quitosana interagem com os grupamentos carregados negativamente do alginato para formar aglomerados em escala nanométrica. Estes aglomerados são formados devido à interação eletrostática entre duas fases aquosas onde a gelificação ionotrópica envolve a transição do material da fase líquida para a fase gel em temperatura ambiente (Calvo *et al.* 1997, Mohanraj and Chen 2006, Sun and Tan 2013).

A formação das NP se dá durante a fase de aglomeração, onde há precipitação do polímero da fase contínua para formação de uma película que se aglomera em NP e são estabilizadas por ligações covalentes, que podem ser alcançadas por alteração de pH ou temperatura ou então adição de um agente capaz de realizar ligações cruzadas (Mora-Huertas 2010).

A evolução dos métodos de preparo de NP se deve a vários aspectos: necessidade do uso de reagentes menos tóxicos, simplicidade do processo, por permitirem economia, escalonamento e otimização para obter maior rendimento e eficiência de associação. Dependendo das características físico-químicas do fármaco é possível escolher o método de preparo que levará a uma associação eficiente. O método escolhido deve minimizar a perda de fármaco e garantir sua atividade farmacológica. Além disso, passos pós-preparação como

avaliação da estabilidade e análise de solvente residual devem ser bem investigados (Reis *et al.* 2006, Morales 2007, Kumari *et al.* 2010, Souto *et al.* 2012).

1.2. Nanopartículas lipídicas sólidas

As nanopartículas lipídicas sólidas (NLS) (Figura 6) introduzidas em 1991 representam um sistema carreador alternativo para os carreadores coloidais tradicionais como emulsões, lipossomas, nano e micropartículas poliméricas (Souto *et al.* 2011). As NLS são carreadoras coloidais lipídias e apresentam-se sólidos em temperatura corporal e ambiente. Possuem um tamanho compreendido entre 50 a 1000 nm, e são feitas de materiais biocompatíveis e biodegradáveis capazes de incorporar fármacos lipofílicos. As NLS são constituídas por uma fase externa composta por um emulsificante, co-emulsificante e água e por uma fase interna composta por um por lipídio (matriz), onde o fármaco encontra-se disperso ou adsorvido na superfície (Manjunath *et al.* 2005, Souto and Doktorovova 2009, Souto *et al.* 2011, Assis *et al.* 2012, Mehnert and Mäder 2012).

Os fármacos são liberados através da saída destes da matriz lipídica, promovendo a liberação modificada dos fármacos (Jenning and Gohla 2001, Souto *et al.* 2011, Mehnert and Mäder 2012). Além disso, o potencial das NLS em liberação transdérmica tem demostrado aumento a hidratação da pele devido à maior oclusividade (formando soluções supersaturadas do fármaco carreado no local de aplicação) e melhora da fotoestabilidade de excipientes farmacêuticos (Mandawage and Patravale 2008, Souto *et al.* 2011, Mehnert and Mäder 2012).

Figura 6: Representação esquemática de nanopartículas lipídicas sólidas estabilizadas por surfactantes.
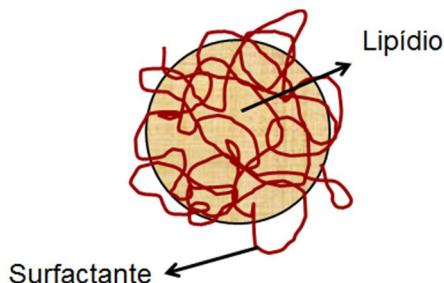
Comparado com outros sistemas coloidais, as NLS apresentam principalmente a facilidade de escalonamento (Silva *et al.* 2011a, Souto *et al.* 2011, Mehnert and Mäder 2012).

De acordo com o método de produção de NLS permitem incorporar princípios ativos polares e apolares. No entanto, devido à natureza lipídica da matriz, as NLS são particularmente adequadas para veicular ativos apolares, para os quais evidenciam uma eficiência de encapsulação elevada (Souto *et al.* 2011, Mehnert and Mäder 2012).

1.2.1. Material utilizado na preparação das nanopartículas lipídicas sólidas

As matérias-primas comuns às NLS incluem lipídio (s) sólido (s), emulsificante (s) e água. O termo lipídio inclui triglicerídeos, glicerídeos parciais, ácidos graxos, esteróides e ceras. Diversos tipos de emulsificantes têm sido utilizados para estabilizar a dispersão, entretanto a mistura de emulsificantes pode prevenir mais eficientemente a aglomeração de partículas. A escolha do emulsificante depende da forma de administração que será usada e essa é mais limitada quando se trata de administração parental (Manjunath *et al.* 2005, Souto *et al.* 2011, Assis *et al.* 2012, Mehnert and Mäder 2012).

Assim como as NP, as NLS apresentam vantagens que justificam sua aplicação na terapêutica como boa estabilidade (física, química e biológica), fácil preparação, boa reprodutividade e baixa toxicidade, uma vez que a matriz lipídica é composta por lipídios presentes no metabolismo humano. Estas partículas têm sido empregadas em diversos produtos comerciais, principalmente em cosméticos, além de serem aplicáveis à uma ampla variedade de fármacos visando melhorar sua propriedades terapêuticas (Mandawage and Patravale 2008, Souto and Doktorovova 2009, Mehnert and Mäder 2012).

O uso de lipídios sólidos, em vez de lipídios líquidos, aumenta o controle sobre a cinética de liberação de compostos encapsulados e melhora a estabilidade de compostos ativos lipofílicos lábeis (Helgason *et al.* 2009, Assis *et al.* 2012).

Os lipídios de composição complexa como as misturas de mono, di e triacilgliceróis e os que contêm ácidos graxos com cadeia de diferentes comprimentos originam NLS com muitas imperfeições, oferecendo mais espaço para acomodar as moléculas do princípio ativo (Souto *et al.* 2011).

1.2.1.1. Triacilglicerídeos

Os triacilglicerídeos ou triacilgliceróis são lipídios formados pela ligação de três moléculas de ácidos graxos com o glicerol, um triálcool de três carbonos, através de ligações do tipo éster (Kalo and Kemppinen 2003, Marzzoco and Torres 2007). A principal função dos triacilglicerídeos é a de reserva de energia, e são armazenados nas células do tecido adiposo, principalmente. São armazenados em uma forma desidratada, e fornece por grama aproximadamente o dobro da energia fornecida por carboidratos (Kalo and Kemppinen 2003, Marzzoco and Torres 2007).

A tripalmitina, ou tripalmitato de glicerol, é um triacilglicerídeo composto por três unidades de ácido palmítico esterificados com glicerol. É o principal componente do óleo da palma (Kellens *et al.* 1990, Basso *et al.* 2010). A tripalmitina é bastante utilizada na fabricação de cremes de barbear e sabões, devido ao tamanho médio de sua cadeia, que proporciona uma ótima ação detergente e poder espumante. Esta também é empregada em formulações de cremes e emulsões cosméticas, dando consistência e um toque suavizado à pele. Produz formulações com propriedades emolientes, umectantes e protege a pele dos efeitos irritantes dos sabões e detergentes, diminuindo a sua irritação (Basso *et al.* 2010).

1.2.2. Métodos de preparação de nanopartículas lipídicas sólidas

A preparação das NLS pode ser realizada por fusão/emulsificação ou emulsificação/evaporação do solvente (Muller *et al.* 1995, Silva *et al.* 2011a, Souto *et al.* 2011, Assis *et al.* 2012, Mehnert and Mäder 2012).

O método **fusão/emulsificação** consiste na fusão prévia do lipídio, incorporando o princípio ativo por dissolução ou por dispersão. A fase contendo o lipídio fundido é emulsificada numa fase aquosa, contendo um tensoativo polar como, por exemplo, um polissorbato ou um poloxamer (Helgason *et al.* 2009, Kuo and Chen 2009, Yoo *et al.* 2010, Souto *et al.* 2011, Mehnert and Mäder 2012). A emulsão recém-preparada é mantida à temperatura ambiente para a solidificação do lipídio e obtenção da dispersão aquosa de SLN. No processo de emulsificação utilizam-se ultrassom (Abdelbary and Fahmy 2009, Souto *et al.* 2011, Yang *et al.* 2011, Mehnert and Mäder 2012), agitação mecânica (Igartua *et al.* 2002, Jain *et al.* 2005, Souto *et al.* 2011, Mehnert and Mäder 2012) e possível operação complementar de homogeneização

à alta pressão (Attama *et al.* 2009, Hu *et al.* 2010, Souto *et al.* 2011, Mehnert and Mäder 2012). Estes procedimentos provocam o rompimento das gotículas lipídicas maiores originando gotículas pequenas dispersas no meio da fase aquosa. O ultrassom e a agitação mecânica são métodos mais simples, porém apresentam a desvantagem de originarem suspensões de NLS polidispersas (Eldem *et al.* 1991, Souto *et al.* 2011). Além disso, o uso de ultrassom é sempre acompanhado pela possibilidade de contaminação por titânio e de degradação do princípio ativo devido à elevada força de cavitação aplicada (Souto *et al.* 2011, Mehnert and Mäder 2012).

A homogeneização à alta pressão constitui um método vantajoso para preparar NLS por fusão/emulsificação, uma vez que apresenta menores dificuldades para escalonamento e permite trabalhar em condições assépticas (Shegokar *et al.* 2011, Souto *et al.* 2011, Mehnert and Mäder 2012). Para obtenção de NLS com uma distribuição homogênea de tamanhos, toda a dispersão deverá ser sujeita à mesma intensidade de energia.

A preparação de NLS por **emulsificação/evaporação do solvente** consiste na preparação de uma fase orgânica constituída pelo lipídio dissolvido em solvente orgânico imiscível com a água como, por exemplo, o diclorometano ou clorofórmio (Zhu *et al.* 2009, Varshosaz *et al.* 2010, Souto *et al.* 2011, Mehnert and Mäder 2012). Nesta fase o princípio ativo é incorporado por dissolução ou por dispersão. A fase orgânica é emulsificada numa fase aquosa que contém um tensoativo através da utilização de ultrassom ou então por homogeneização de alto cisalhamento, obtendo-se uma emulsão do tipo O/A (Yoo *et al.* 2010, Souto *et al.* 2011, Mehnert and Mäder 2012).

Para evaporar o solvente orgânico a emulsão obtida é diluída num volume grande de fase aquosa e submetida à agitação magnética, ou então a utilização de pressão reduzida sob vácuo. As NLS formam-se em consequência da precipitação do lipídio na fase externa aquosa. A evaporação do solvente orgânico deve ser realizada o mais rapidamente possível de modo a evitar a agregação das NLS recém-formadas (Souto *et al.* 2011, Mehnert and Mäder 2012).

Em comparação com o processo de preparação das NLS por fusão/emulsificação, a emulsificação/evaporação do solvente origina partículas com dimensão mais reduzida devido à menor viscosidade da fase interna, em virtude do o lipídio estar dissolvido num solvente orgânico em vez de fundido. Este método apresenta a vantagem de evitar a exposição dos princípios ativos a temperaturas elevadas apresentando, no entanto, o inconveniente relacionado com o uso de solventes orgânicos (Souto *et al.* 2011, Mehnert and Mäder 2012).

As características físico-químicas das NLS obtidas por emulsificação/evaporação do solvente são afetadas por um conjunto de parâmetros tecnológicos que incluem a solubilidade do princípio ativo, o polimorfismo do lipídio e, a natureza e concentração do lipídio e do tensoativo (Souto *et al.* 2011, Mehnert and Mäder 2012).

As características físico-químicas das NLS obtidas a partir de microemulsões são afetadas não somente pelos fatores que interferem na preparação da microemulsão, mas também pelas condições experimentais decorrentes da sua diluição na solução aquosa, pela temperatura desta última e pelo seu volume e, ainda, pelo modo como se processa a diluição. Os principais parâmetros que afetam a eficiência de encapsulação são o carregamento e o tamanho das NLS (Souto *et al.* 2011, Mehnert and Mäder 2012).

A combinação de métodos pode trazer melhora das propriedades físico-químicas das NLS, como por exemplo, a emulsificação/evaporação do solvente utilizando em uma primeira etapa o ultrassom e a homogeneização de alto cisalhamento (turrax) seguida de evaporação do solvente (Vitorino *et al.* 2011).

1.3. Lipossomas

Os lipossomas são vesículas esféricas que consistem em uma ou mais bicamadas concêntricas de fosfolipídios onde as caudas hidrofóbicas estão voltadas para o interior da bicamada e as cabeças polares para o exterior da mesma em contato com a fase aquosa, cujo tamanho compreende dimensões micrométricas ou submicrométricas (Ranade 1989, Le Bourlais *et al.* 1998a, Cereda *et al.* 2004a, Batista *et al.* 2007, Elsayed *et al.* 2007). Sua estrutura permite a incorporação de moléculas hidrofóbicas, hidrofílicas e anfifílicas (Rose *et al.* 2005, Elsayed *et al.* 2007).

A principal ação dos lipossomas como veículo é liberar determinadas concentrações de fármaco em tecidos alvo, evitando a toxicidade sistêmica, já que somente uma fração do fármaco está disponível para o local de ação (Taddio *et al.* 2005, Torchilin 2006). Devido a sua similaridade com membranas biológicas devido à presença de fosfolipídios e colesterol, os lipossomas não apresentam nenhum risco de antigenicidade ou lesões histológicas após administração destes veículos (Cereda *et al.* 2004a, Dubey *et al.* 2007).

A utilização dos lipossomas foi melhorada através da evolução de pesquisas básicas que permitiram o aumento da estabilidade e a compreensão das características físico-químicas e interação com fluidos biológicos (Lasic 1998, Batista *et al.* 2007).

Os lipossomas podem ser compostos de uma única bicamada lipídica ou bicamadas múltiplas em torno do compartimento aquoso interno sendo classificados como unilamelares e multilamelares, respectivamente. Quanto ao tamanho, as vesículas unilamelares podem ser pequenas ou grandes sendo denominadas como lipossomas unilamelares pequenos - SUV (*small unilamellar vesicles*) variando entre 50 e 200 nm, obtidas principalmente por processo de sonicação e lipossomas unilamelares grandes - LUV (*large unilamellar vesicles*) variando entre 300 e 1000 nm, obtidas principalmente por processo de extrusão (Vemuri and Rhodes 1995, Lasic 1998, Batista *et al.* 2007).

1.3.1. Materiais utilizados na preparação dos lipossomas

Os lipossomas são constituídos basicamente por fosfolipídios, colesterol e um antioxidante (Vemuri and Rhodes 1995, Batista *et al.* 2007). Os lipídios mais utilizados nas formulações de lipossomas são os que apresentam um formato cilíndrico como as fosfatidilcolinas, fosfatidilserina, fosfatidilglicerol e esfingomielina, que tendem a formar uma bicamada estável em solução aquosa. As fosfatidilcolinas são as mais empregadas em estudos de formulação de lipossomas, pois apresentam grande estabilidade frente a variações de pH ou da concentração salina (Batista *et al.* 2007).

Os fosfolipídios são caracterizados por uma temperatura de transição de fase (Tc), na qual a membrana passa de uma fase gel (onde a cadeia carbônica do lipídio está em estado ordenado) para uma fase de cristal-líquido, onde as moléculas ficam com movimentos mais livres e os radicais hidrofílicos agrupados tornam-se completamente hidratados. O comprimento e a saturação da cadeia lipídica influenciam o valor da Tc. Portanto, diferentes membranas compostas por lipídios distintos podem exibir diferentes níveis de fluidez na mesma temperatura (Lasic 1998, Frézard *et al.* 2005, Batista *et al.* 2007). A permeabilidade dos lipossomas é relativamente baixa quando a temperatura é menor que a Tc dos lipidios, sendo a mesma medida pelo fluxo ou pela taxa em que o soluto sai do compartimento aquoso, através da bicamada. Esta propriedade vai depender, no entanto, da natureza do soluto e da fluidez da membrana (Frézard *et al.* 2005, Batista *et al.* 2007).

1.3.2. Métodos de preparação de lipossomas

Muitos métodos têm sido propostos para a preparação de lipossomas, sendo que a maioria inclui a **hidratação de um filme lipídico**, onde primeiramente os lipídios são dissolvidos em solvente orgânico (clorofórmio, por exemplo) seguido da evaporação deste com a formação do filme lipídico. A hidratação deste último pode ser efetuada com água ou solução tampão, sob agitação vigorosa em vórtex, promovendo a formação da suspensão de lipossomas multilamelares (MLV). O fármaco a ser encapsulado pode estar dissolvido na fase aquosa (hidrofílicos) ou então disperso na mistura lipídica (lipofílicos) (Batista *et al.* 2007).

A partir da suspensão de MLV's, diferentes métodos são utilizados para produzir dispersões homogêneas de SUV's e LUV's, podendo-se empregar processos mecânicos, eletrostáticos ou químicos. Os mais utilizados são os processos mecânicos, em que estão incluídos: extrusão através de membranas de policarbonato com diferentes tamanhos de poros, prensa de French, microfluidificador e a sonicação (Lasic 1998, Batista *et al.* 2007).

1.4. Formulações semissólidas – géis

O contato direto de um sistema de liberação de fármacos com o tecido alvo não só maximiza a absorção como também influencia a permeação do fármaco (Ch'ng *et al.* 1985, Ganguly and Dash 2004). Neste sentido, os sistemas semissólidos, como os géis, têm sido utilizados como sistemas de liberação e direcionamento de fármacos, uma vez que mostram eficácia no tratamento e prevenção de doenças locais (Andrews *et al.* 2009, Wang *et al.* 2010).

Géis são preparações farmacêuticas semissólidas constituídas por dispersões de pequenas partículas inorgânicas ou de grandes moléculas orgânicas, encerradas e interpenetradas por um líquido (Ansel *et al.* 2000). Os semissólidos possuem propriedades estruturais reológicas que podem influenciar a liberação de fármacos na pele. Além disso, a retenção prolongada no local de aplicação (associado à área de permeação relativamente pequena) leva a uma maior eficácia terapêutica e isso pode ser alcançado uma vez que se conheça propriedade bioadesiva dos semissólidos (Andrews *et al.* 2009, Batheja *et al.* 2011). Os veículos reologicamente estruturados podem ser formulados com mistura de polímeros que forneçam uma estrutura reforçada, porém estável frente às variações de pH e/ou temperatura (Andrews *et al.* 2009, Batheja *et al.* 2011).

O desenvolvimento de sistemas de liberação para uso tópico tem um alcance limitado, uma vez que o estrato córneo, camada superior da pele, funciona como uma barreira à penetração de fármacos (Brown *et al.* 2006, Batheja *et al.* 2011). Na tentativa de superar esta barreira alguns métodos têm sido aplicados, como por exemplo, a utilização de lipossomas, microemulsões e suspensões coloidais poliméricas. Estes tipos de carreadores podem proteger fármacos contra degradação, promover liberação sustentada, reduzir irritação na pele e aumentar a liberação do fármaco no local da aplicação reduzindo a absorção sistêmica (El Maghraby *et al.* 2006, Heuschkel *et al.* 2008, Batheja *et al.* 2011).

Dispersões coloidais poliméricas e lipídicas em géis hidrofílicos podem melhorar ainda mais a liberação de fármacos na pele. O gel pode ajudar na criação de uma dispersão uniforme de carreadores na matriz e aumentar o tempo de contato com a pele, resultando em uma maior penetração dos carreadores. Além disso, podem acomodar excipientes adicionais para o desenvolvimento de formulações multicomponente. Para este fim, géis hidrofílicos (como aqueles constituídos por polímeros de ácido acrílico e/ou copolímeros de bloco como os poloxamers) têm sido bases eficazes e inertes para ativos e transportadores, incluindo nanocápsulas, lipossomas, nanopartículas lipídicas sólidas e microemulsões (Chen *et al.* 2006, Alves *et al.* 2007, Batheja *et al.* 2011).

1.4.1. Material utilizado na preparação dos géis

De maneira geral, as matérias-primas formadoras de géis são polímeros que quando dispersos em meio aquoso assumem uma estrutura capaz de alterar de viscosidade da formulação (Maia Campos *et al.* 1999, Corrêa *et al.* 2005, Batheja *et al.* 2011). Segundo as características dos polímeros, os géis podem ser de natureza iônica ou não iônica. Os géis de natureza não-iônica possuem estabilidade em ampla faixa de pH, tornando-se possível a veiculação de substâncias de caráter ácido. Já os géis iônicos são dependentes do pH, ou seja, apresentam-se estáveis em pH próximo do neutro (Maia Campos *et al.* 1999, Corrêa *et al.* 2005, Batheja *et al.* 2011).

As principais matérias-primas usadas na preparação de géis são os ácidos carboxivinílicos, ácidos poliacrílicos e ácidos sulfônicos. O tipo de polímero usado na formulação do gel pode influenciar o comportamento reológico, influenciando a estabilidade físico-química do produto e seu comportamento sobre a pele (liberação do ativo pelo veículo e

formação de filme) resultando em diferentes graus de aceitação pelos consumidores (Maia Campos *et al.* 1999, Corrêa *et al.* 2005).

1.4.1.1. Aristoflex® AVC

O Aristoflex® AVC (co-polímero do ácido sulfônico acriloildimetiltaurato e vinilpirrolidona neutralizado) é um polímero sintético pré-neutralizado inovador, que permite a formação de géis cristalinos com características de excelente consistência, toque agradável e estável em meio ácido. É utilizado como agente de gelificação para sistemas aquosos e como texturizador e espessante para as emulsões O/A. O polímero é fácil de utilizar e proporciona formulações com excelente rendimento e estabilidade superior, mesmo na ausência de emulsionante adicional (Löffler *et al.* 2001, Zanini 2007).

Formulações semissólidas preparadas com Aristoflex® AVC proporcionam efeitos de cisalhamento favoráveis e propriedades viscoelásticas. Além dos aspectos reológicos, excelentes propriedades sensoriais (sensação boa na pele, baixo grau de viscosidade e / ou aderência) caracterizam formulações contendo Aristoflex® AVC (Löffler *et al.* 2001, Zanini 2007).

O Aristoflex® AVC tem uma boa compatibilidade com os solventes orgânicos (etanol, acetona) e apresenta boa estabilidade frente para a radiação UV. A quantidade de Aristoflex® AVC utilizados em formulações para cuidados pessoais é tipicamente entre 0.5 e 5%. Este gel apresenta boa estabilidade entre pH 4.0 e 9.0 (Löffler *et al.* 2001, Zanini 2007).

1.5. Anestésicos locais

Anestésicos locais (AL) são fármacos com a capacidade de promover o bloqueio reversível da condução nervosa evitando ou aliviando o processo doloroso sem perder a consciência (Covino and Vassalo 1985, Catteral and Mackie 1996, Weinschenk 2012). O principal mecanismo envolve sua interação em um ou mais sítios específicos nos canais de sódio voltagem-dependentes presentes nas membranas neurais (Rang *et al.* 2004, Fraceto *et al.* 2006, Weinschenk 2012). Estudos recentes mostraram que os AL interagem com os canais de sódio tanto na forma ionizada quanto na forma não ionizada e, assim, estabilizam o potencial

da membrana, bloqueando a condução nervosa (Fraceto *et al.* 2006, Fraceto *et al.* 2008, Weinschenk 2012).

A cocaína, um alcalóide isolado das folhas de *Erithroxylon coca* em 1860, foi o primeiro AL e teve sua ação demonstrada ao ser utilizada como anestésico oftálmico. Após ter sido empregada na clínica durante alguns anos, foi substituída por outras substâncias, devido aos seus efeitos tóxicos como dependência física e psíquica. Em 1905, o primeiro substituto sintético, a procaína, foi obtido por síntese orgânica dando início a busca de novos compostos com propriedade anestésica (Collins 1993, Rang *et al.* 2004, de Araujo *et al.* 2008, Wiles and Nathanson 2010).

A estrutura química dos AL apresenta duas principais características: em sua maioria são moléculas anfifílicas contendo um grupamento aromático (região hidrofóbica), uma cadeia intermediária e grupamento amino (região hidrofílica). Aqueles que possuem uma ligação éster entre o grupo aromático e a cadeia intermediária são classificados como amino-ésteres (procaína, oxibuprocaína, tetracaína, etc.), e os AL que possuem uma ligação amida entre tais grupos são classificados como amino-amidas (lidocaína, ropivacaína, etidocaína, etc.) (Covino and Vassalo 1985, de Jong 1994, Malamed 2004). O perfil clínico dos AL pode ser determinado por três características: potência, velocidade de início de ação e duração da atividade anestésica. A propriedade que está relacionada à atividade anestésica e à potência é a lipossolubilidade. Vários estudos mostraram que existe correlação entre o coeficiente de partição do AL e a concentração mínima necessária para o bloqueio da condução nervosa (Covino and Vassalo 1985, de Jong 1994). Porém é preciso salientar que a solubilidade em água é essencial para o transporte do fármaco até as fibras nervosas, enquanto a solubilidade lipídica é necessária para a penetração na membrana sendo a existência de um balanço entre essas duas propriedades (caráter anfifílico) um fator essencial para a atividade dos AL (de Paula and Schreier 1995, de Araújo *et al.* 2005, de Araujo *et al.* 2008).

A toxicidade dos AL é proporcional a sua potência (Knudsen *et al.* 1997, Liu *et al.* 2013), pois a associação destes com as bicamadas lipídicas aumenta sua distribuição para os locais de ação e reduz a metabolização por esterases plasmáticas. Além disso, acredita-se que os sítios de ação de AL nos canais de sódio voltagem-dependente sejam hidrofóbicos, favorecendo assim, a interação dos AL mais hidrofóbicos e das formas não ionizadas dos mesmos. A taxa de ligação às proteínas também está relacionada com a potência anestésica devido a natureza proteica dos canais de sódio voltagem-dependentes, fazendo com que o AL

fique mais tempo interagindo com os sítios de ação (Catteral and Mackie 1996, Li *et al.* 2002, Liu *et al.* 2013).

Os principais efeitos tóxicos dos AL são decorrentes de sua absorção sistêmica, após administração regional, e pode levar à neurotoxicidade e/ou cardiotoxicidade (Rang *et al.* 2004) LIU *et al.,* 2013). A absorção dos AL pela circulação sanguínea é afetada pela lipossolubilidade, pka e taxa de ligação às proteínas plasmáticas dos compostos (McLure and Rubin 2005, Liu *et al.* 2013). A neurotoxicidade causada pelos AL pode ser evidenciada pelo aparecimento de agitação, tremores, convulsões, depressão respiratória e podendo levar ao coma e até morte. A cardiotoxicidade pode causar fibrilações e arritmias (Rang *et al.* 2004, Liu *et al.* 2013). Os mecanismos moleculares responsáveis por esses efeitos indesejáveis ainda não foram inteiramente estabelecidos. Entretanto, estudos revelaram que os AL modificam o fluxo de íons através de canais de sódio e modificam processos metabólicos intracelulares ao se ligarem a receptores β-adrenérgicos, resultando na inibição do AMP cíclico e, consequentemente, na sinalização deste segundo mensageiro. Um destes mecanismos moleculares ou a associação destes são responsáveis pelos efeitos tóxicos dos AL, e de fato, eles interferem no funcionamento celular e na homeostase (Butterworth *et al.* 1993, Renehan *et al.* 2005, Liu *et al.* 2013).

1.5.1. Articaína

A articaína, ATC, (Figura 7) é um AL da classe das amino-amidas, juntamente com a lidocaína (LDC) e ropivacaína (RVC), têm sido os fármacos de escolha na terapia da dor aguda e crônica em odontologia (Malamed 2004, de Araújo *et al.* 2005, Paxton and Thome 2010, Ashraf *et al.* 2013).

Figura 7: Estrutura química da articaína.
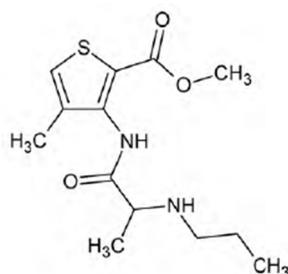
A ATC foi descoberta em 1969 por H. Rusching, mas seu uso iniciou-se apenas em 1976 na Alemanha e difundiu-se por toda Europa e na América do Sul. É o único anestésico local do tipo amino-amida que contém um grupamento éster adicional. Isto confere uma peculiaridade de biotransformação tanto no plasma quanto no fígado, pois promove uma hidrólise relativamente mais rápida (Malamed 2004, Paxton and Thome 2010). Além disso, a ATC destaca-se por ser a única que possui um anel tiofênico em vez de um anel benzênico. A presença deste anel, em sua fórmula estrutural, confere à articaína um aumento de sua potência e difusão entre os tecidos (Vasconcelos *et al.* 2002, Paxton and Thome 2010).

Tabela 1: Propriedades físico-químicas e farmacológicas da ATC (Malamed 2006).

Propriedades	ATC
Fórmula molecular	$C_{13}H_{20}N_2O_3S$
Massa (g/mol)	284,37
pKa	7,8
Início de ação (min)	2-4
Meia vida (h)	0,5
Ligação a proteínas plasmáticas (%)	95
Solubilidade aquosa (mM) (forma não ionizada)	120

A menor toxicidade sistêmica permite a utilização da ATC em concentrações maiores que outros AL, sendo utilizado clinicamente na concentração de 4% associado com epinefrina 1:100.000 e 1:200.000 (m/m) em procedimentos odontológicos e na concentração de 2% associado com epinefrina 1:200.000 (m/m) para anestesia epidural, em contraste com a LDC,

que é utilizada em concentrações menores. Isto ocorre devido à metabolização mais rápida da ATC (Vasconcelos *et al.* 2002, Malamed 2004, Paxton and Thome 2010, Ashraf *et al.* 2013). A eficácia da ATC sempre é comparada com seu predecessor, a LDC, devido à presença de propriedades muito semelhantes entre os dois AL. A ATC possui a potência de 1,5 vezes da LDC, início de ação mais rápido, e maior do sucesso da anestesia. A ação mais rápida da ATC é atribuída às propriedades físico-químicas da molécula, tendo maior lipossolubilidade (devido ao anel tiofênico) e desta forma, atingindo com maior facilidade a membrana neuronal (Isen 2000, Paxton and Thome 2010). Para anestesia epidural, apresentou um início de ação mais rápido e menor cardiotoxicidade e neurotoxicidade quando comparado com a LDC (Vree and Gielen 2005, Paxton and Thome 2010).

A melhor eficácia anestésica da ATC é baseada no fato deste anestésico apresentar uma maior difusão entre os tecidos (Malamed 2004, Paxton and Thome 2010, Ashraf *et al.* 2013). Porém, a principal complicação associada ao uso da ATC é a parestesia longa ou permanente (Malamed 2004, Ashraf *et al.* 2013). A parestesia caracteriza-se por uma sensação de dormência ou formigamento. Estudos realizados no Canadá e EUA encontraram uma relação direta entre a alta concentração utilizada de ATC e a possível causa de parestesia após a injeção para procedimentos odontológicos. A maioria dos incidentes relatados de parestesia parece estar associada ao bloqueio do nervo alveolar inferior e nervo lingual (Pogrel 2007, Diaz 2009, Ashraf *et al.* 2013).

Outra desvantagem está associada à alta concentração utilizada de ATC, uma vez que a lesão dos nervos mandibulares é concentração-dependente, aumentando o risco de ocorrência das mesmas (Johansen 2004, Paxton and Thome 2010, Ashraf *et al.* 2013).

A ATC é o único AL contra-indicado para pacientes que possuem comprovadamente alergia a medicamentos que contém enxofre (como sulfas, por exemplo) (Malamed 2004).

Como as características desejáveis para um AL incluem longa duração de ação, seletividade para o bloqueio sensorial em relação ao motor e diminuição da toxicidade sistêmica (Kuzma *et al.* 1997, de Araujo *et al.* 2003). Desta forma, uma alternativa que tem se mostrado capaz de promover estes efeitos desejáveis é a liberação modificada destes fármacos utilizando diferentes tipos de sistemas carreadores. A veiculação de anestésicos locais em sistemas carreadores tem sido estudada em diversos grupos pesquisa (Tabela 2) utilizando para isso diferentes sistemas carreadores como as: ciclodextrinas (de Araújo *et al.* 2005, Pinto *et al.* 2005, Cereda *et al.* 2012), lipossomas (Cereda *et al.* 2004a, de Araujo *et al.* 2004, Colombo *et al.* 2005, Rose *et al.* 2005, Franz-Montan *et al.* 2010, Cohen 2012), micropartículas poliméricas

(Le Guevello *et al.* 1993, Colombo *et al.* 2005, Grillo *et al.* 2009), nanopartículas poliméricas (Gorner *et al.* 1999, Govender *et al.* 1999, Polakovic *et al.* 1999, Govender *et al.* 2000, Moraes *et al.* 2009, de Melo *et al.* 2010, Grillo *et al.* 2010, de Melo *et al.* 2011, Moraes *et al.* 2011, de Melo *et al.* 2012, Campos *et al.* 2013b) e nanopartículas lipídicas sólidas (Pathak and Nagarsenker 2009, Leng *et al.* 2012). Desta forma, a veiculação do anestésico local ATC em diferentes sistemas carreadores podem melhorar a atividade anestésica deste, bem como diminuir os problemas de toxicidade sistêmica associada ao uso deste anestésico.

Muitas das novas tecnologias desenvolvidas atualmente envolvem o desenvolvimento de sistemas carreadores, têm a capacidade de alterar as propriedades terapêuticas do fármaco a eles incorporados, levando à inúmeras vantagens, como o aumento da estabilidade do fármaco, liberação mais lenta e prolongada, diminuição da toxicidade, direcionamento a tecidos-alvo, entre outras (Alonso 2004, Durán *et al.* 2006, Mishra *et al.* 2010).

Com relação à ATC, muitos estudos têm demonstrado superioridade deste AL quando comparado com outros da mesma classe na prática clínica e um crescente uso nos últimos anos principalmente em procedimentos odontológicos (Paxton and Thome 2010). Porém, a alta concentração utilizada nas formulações comerciais está relacionada com a incidência de parestesia longa ou permanente devido às lesões em nervos (Malamed 2004) o que faz com que o desenvolvimento de sistemas carreadores para este anestésico seja interessante.

Uma nova formulação contendo ATC encapsulada em nanocarreadores poderia trazer vantagens uma vez que haveria a possibilidade de redução da concentração deste AL, porém com uma mesma eficácia clínica reduzindo assim as reações adversas deste fármaco. Além disso, não há disponível comercialmente uma formulação tópica contendo ATC. Com o desenvolvimento de um hidrogel contendo este fármaco nanoencapsulado, abriria assim perspectivas de uso na prática clínica para anestesia tópica em pele.

_____

Tabela 2: Resumo de alguns estudos com AL´s associados com sistemas carreadores

Sistemas de liberação modificada				
Carreadores	**AL**	**Técnica usada**	**Principais resultados**	**Referência**
β-ciclodextrina (β-CD)	Benzocaína (BZC)	Estudo *in vitro*	O complexo de inclusão BZC:β-CD foi preparado e caracterizado. Este estudo demonstrou que a complexação foi capaz de melhorar a solubilidade aquosa da BZC, reduzir a citotoxicidade e a formação de metahemoglobina induzida por este AL.	PINTO *et al.,* 2005
Hidroxipropil-β-ciclodextrina (HP-β-CD)	Bupivacaína (BVC)	Infiltrativa: bloqueio de nervo ciático	O estudo envolveu a preparação, a caracterização e estudo *in vivo* dos complexos de inclusão da BVC (S75-R25) e da BVC (S50-R50) com HP-β-CD comparando-os com as preparações utilizadas na clínica. Os resultados demonstraram que a complexação potencializou o bloqueio nervoso e reduziu a latência, quando comparado ao AL livre.	de ARAÚJO *et al.*, 2005
Hidroxipropil-β-ciclodextrina (HP-β-CD)	Ropivacaína (RVC)	Infiltrativa: bloqueio de nervo ciático e infraorbital	Neste estudo foi desenvolvido o complexo de inclusão RVC:HP-β-CD e realizada avaliação farmacológica. Além de aumentar a solubilidade aquosa deste AL, a complexação reduziu o efeito hemolítico, reduziu a latência e prolongou a duração do bloqueio sensorial em camundongos.	de ARAÚJO *et al.*, 2008
Hidroxipropil-β-ciclodextrinas (HP-β-CD)	Bupivacaína e Ropivacaína (BVC e RVC)	Estudo *in vitro*, histopatologia	ALs foram complexados em ciclodextrinas e sua atividade miotóxica e neurotóxica foram avaliadas *in vitro* e *in vivo*. Os resultados da análise citotóxica não apresentou diferença significativa, porem os complexos reduziram os níveis séricos de creatina quinase apresentando através das analises histopatológicas uma ação miotóxica menor quando comparados aos ALs livre.	CEREDA. *et al.*, 2012
Lipossomas	Prilocaína (PLC)	Infiltrativa: bloqueio de nervo infraorbital	Neste estudo foi desenvolvida uma formulação lipossomal de PLC e avaliada sua eficácia anestésica *in vivo*. A formulação foi capaz de aumentar a duração de anestesia comparada com a PLC livre, porém não houve diferença estatística quando a formulação lipossomal foi comparada com a PLC com vasoconstritor.	CEREDA. *et al.*, 2004
Lipossomas	Bupivacaína (BVC) e Dexametasona (DEX)	Infiltrativa: bloqueio de nervo ciático	Foram preparados lipossomas contendo BVC e DEX separadamente, porém foram administrados em conjunto em camundongos. Os resultados demonstraram que a DEX encapsulada dobrou o tempo de bloqueio do nervo ciático induzido pela BVC encapsulada, além de manter excelente biocompatibilidade evidenciada pela redução da inflamação.	COLOMBO *et al.*, 2005

_____

Lipossomas	Benzocaína (BZC)	Tópica: mucosa bucal	A BZC foi encapsulada em lipossomas e foi avaliada a eficácia da anestesia tópica e pulpar em um estudo duplo-cego e randomizado. Os resultados demonstraram que a encapsulação da BZC em lipossomas foi capaz de aumentar a duração da anestesia em tecidos moles, porém não foi capaz de induzir anestesia pulpar.	FRANZ-MONTAN *et al.*, 2010
Lipossomas	Bupivacaína (BVC)	Infiltração local	O objetivo deste estudo foi comparar a ação anestésica da BVC associada a lipossomas aos opioides usados na clinica cirúrgica. Dentre os voluntários que passaram por procedimento de colectomia foi averiguado redução do custo total médio referente à BVC contra os gastos com opioides, e redução do tempo de permanência de 5 para 2 dias. Além disso, houve redução de efeitos adversos, evidenciando a efetividade do sistema de liberação prolongada.	COHEN, 2012
Lipossomas e polímeros	Lidocaína (LDC)	Estudo *in vitro*	Pesquisadores desenvolveram um sistema de liberação transdérmico para a LDC em lipossomas associados a quitosana conjugada com peptídeos. Os resultados mostraram que estes lipossomas tiveram um aumento de sua estabilidade coloidal apresentando uma boa permeação cutânea, sendo aproximadamente 4 vezes maior que a solução de AL livre.	WANG *et al.*, 2013
Nanopartículas lipídicas sólidas (SLN)	Lidocaína (LDC)	Tópica: pele	Neste trabalho, o objetivo foi desenvolver SLN contendo LDC para melhorar a liberação dérmica deste AL. As SLN foram preparadas, caracterizadas e incorporadas em hidrogel para aplicação tópica. Foram realizados experimentos de permeação *in vitro* e atividade anestésica *in vivo*. A formulação contendo SLN com LDC apresentou perfil de permeação significativamente sustentado e foi capaz de aumentar 5 vezes o tempo de anestesia *in vivo* quando comparado com uma formulação de LDC em gel comercializada.	PATHAK & NAGARSENKER, 2009
Nanopartículas lipídicas sólidas (SLN)	Lidocaína (LDC)	Infiltrativa: bloqueio epidural	Foram produzidas SLN com 3 diferentes tipos de lipídeos, sendo monoestearina (MS), palmitoestearato de glicerol (GP) e ácido esteárico (EA). As SLN contendo LDC apresentaram boa estabilidade coloidal e apresentaram efeito anestésico epidural em ratos superiores a 8 h com (MS), 12 h com (GP) e 4 h com (EA), quando comparada às 2h da LDC.	LENG *et al.*, 2012
Nanoesferas poliméricas (NE)	Bupivacaína (BVC)	Infiltrativa: bloqueio de nervo ciático	Nanoesferas de alginato/quitosana e alginato/bis(2-etilexil) sulfosuccinato (AOT) contendo BVC foram preparadas, caracterizadas e a avaliada a atividade anestésica *in vivo*. As formulações apresentaram boa estabilidade durante o período avaliado (30 dias). Além disso, essas formulações apresentaram baixa citotoxicidade *in vitro* e longo bloqueio sensorial/ motor *in vivo*.	GRILLO *et al.*, 2010
Nanocápsulas poliméricas (NC)	Benzocaína (BZC)	Infiltrativa: bloqueio de nervo ciático	O objetivo deste trabalho foi avaliar a influência da composição do núcleo oleoso nas propriedades físico-químicas e atividade anestésica da BZC encapsulada em NC de PLGA. A suspensão mais estável, perfil de liberação *in vitro* mais lento e aumento da atividade anestésica foram alcançados com NC de PLGA contendo BZC cujo núcleo era composto por óleo mineral.	de MELO *et al.*, 2011
Nanocápsulas poliméricas (NC)	Benzocaína (BZC)	Estudo *in vitro*	A fim de se obter formulação anestésica com boa característica físico-química, foi realizado um planejamento fatorial. Foram obtidas NC de PCL contendo BZC satisfatórias, sendo a melhor formulação a com tamanho de 188 (nm), potencial zeta de -32mV polidispersão 0,07 e eficiência de associação de 87%, revelando que esta estratégia é interessante para preparo de sistemas coloidal com boas propriedades.	MORAES *et al.*, 2011

_____

Nanoesferas poliméricas (NE)	Lidocaína (LDC)	Infiltrativa: bloqueio de nervo ciático	Neste trabalho foram preparadas e caracterizadas nanoesferas de PCL contendo LDC e avaliada sua eficácia anestésica *in vivo*. A suspensão apresentou bons parâmetros coloidais e boa estabilidade. O perfil de liberação *in vitro* foi mais lento que a LDC livre. Os testes de citotoxicidade e atividade farmacológica confirmaram que o sistema NE:LDC foi capaz de reduzir a toxicidade deste AL e prolongou o tempo de anestesia.	CAMPOS *et al.,* 2013
Nanocápsulas poliméricas (NC)	Benzocaína (BZC)	Infiltrativa: bloqueio de nervo ciático	Este trabalho descreve a comparação a atividade anestésica *in vivo* da BZC em NC preparadas com três polímeros diferentes (PLA, PLGA e PCL). Os sistemas foram caracterizados e bons parâmetros coloidais foram alcançados. Os ensaios farmacológicos revelaram que o sistema que obteve maior tempo de anestesia foi o de NC preparadas com o polímero PLA.	de MELO *et al.,* 2012
*Nanocápsulas poliméricas (NC)	Articaína (ATC)	Estudo *in vitro*	Neste estudo foi avaliada a influência dos fatores concentração de tensoativo e tempo de sonicação nos parâmetros coloidais de NC de PCL contendo ATC através de metodologia de planejamento experimental e superfície de resposta. Os fatores não influenciaram significativamente o diâmetro médio e a polidispersão, ao passo que a eficiência de encapsulação foi afetada pelo tempo de sonicação.	CAMPOS *et al.,* 2013
*Nanoesferas poliméricas (NE)	Articaína (ATC)	Estudo *in vitro*	O objetivo deste trabalho foi avaliar a influencia dos fatores razão de massas entre cálcio/alginato e quitosana/alginato nos parâmteros coloidais de NE de alginato/quitosana contendo ATC através de metodologia de planejamento experimental e superfície de resposta. De acordo com os resultados, o dâmetro médio, a polidispersão e a eficiência de encapsulção foram afetadas pelos 2 fatores, por outro lado o potencial zeta não foi afetado significativamente pela variação dos fatores.	de MELO *et al.,* 2013
*Nanoesferas e nanocápsulas poliméricas (NE e NC)	Articaína (ATC)	Estudo *in vitro*	Este trabalho descreve uma comparação entre dois nanocarreadores hidrofílicos para a forma ionizada da ATC, sendo NE de alginato/quitosana e NC de PEG-PCL. Os dois carreadores se mostraram promissores, com destaque para as NC que apresentaram liberação mais lenta para o AL.	de MELO *et al.,* 2014

*Trabalhos gerados a partir desta tese.

O desenvolvimento de sistemas de liberação para AL tem sido alvo de estudo do nosso grupo de pesquisa. Entre os sistemas desenvolvidos encontram-se complexos de AL com CD naturais e modificadas (de Araújo *et al.* 2005, Pinto *et al.* 2005, Moraes *et al.* 2007a, Moraes *et al.* 2007b, Moraes *et al.* 2007c, d), formulações lipossomais de AL (Cereda *et al.* 2004a, de Araujo *et al.* 2004, Cereda *et al.* 2006) e formulações nanoestruturadas poliméricas (Moraes *et al.* 2007e, Moraes *et al.* 2009, de Melo *et al.* 2010, Grillo *et al.* 2010, de Melo *et al.* 2011, de Melo *et al.* 2012, Campos *et al.* 2013a, Campos *et al.* 2013b, de Melo *et al.* 2013, de Melo *et al.* 2014).

Neste estudo pretendeu-se introduzir esta nova abordagem tecnológica de sistemas de liberação modificada nanoestruturados para o AL ATC visando a utilização por via infiltrativa e/ou tópica em pele objetivando o desenvolvimento de formulações com potencial para a atuação na prática clínica. Destaca-se ainda que até o presente momento não existiam na literatura descrição de desenvolvimento de sistemas de liberação modificada para o anestésico local ATC, tanto na forma neutra como ionizada.

Esta tese foi estruturada em capítulos, sendo cada um correspondente a um artigo já publicado e/ou submetido em periódico científico internacional ou aceito na forma de capítulo de livro.

O segundo capítulo apresenta o processo de otimização de preparo de nanocápsulas de PCL contendo ATC não ionizada. O estudo envolveu a utilização de metodologia de superfície de resposta com a finalidade de obter nanocápsulas estáveis, com boa distribuição de tamanho e elevada eficiência de encapsulação do AL ATC. Os resultados demonstraram que foi possível obter nanocápsulas com diâmetro em torno de 400 nm, índice de polidispersão abaixo de 0,2 e eficiência de encapsulação de 76 %, sendo esta formulação escolhida para estudos posteriores.

O terceiro capítulo discorre sobre o preparo e otimização de nanopartículas de alginato/quitosana contendo ATC ionizada. Da mesma forma que o capítulo anterior, a metodologia de superfície de resposta foi utilizada para otimizar o preparo das nanopartículas a fim de obter uma formulação com alta estabilidade e eficiência de encapsulação maior do que as formulações já estudadas para AL na forma ionizada. Em linhas gerais, os resultados demonstraram que foram obtidas nanopartículas com diâmetro médio de 300 nm, porém o índice de polidispersão foi maior que 0,2 devido o alginato e a quitosana serem polímeros de obtenção natural, o que pode influenciar a distribuição de tamanho das nanopartículas. A eficiência de encapsulação obtida foi de 45 %.

O quarto capítulo traz um estudo de caracterização e comparação entre dois nanocarreadores hidrofílicos para a ATC na forma ionizada. Os nanocarreadores utilizados foram nanopartículas de alginato/quitosana e nanocápsulas de polietilenoglicol-policaprolactona (PEG-PCL). Neste estudo foram avaliadas as propriedades físico-químicas (diâmetro médio, polidispersão e potencial zeta) foram avaliadas em função do tempo para verificar a estabilidade dos sistemas. As formulações mostraram-se estáveis no período de 120 dias. Foi alcançada eficiência de encapsulação satisfatória (nanocápsulas PEG-PCL 60 % e nanopartículas alginato/quitosana 45 %). Os ensaios de citotoxicidade confirmaram que a encapsulação reduz a toxicidade relative do fármaco.

No quinto capítulo, há a descrição do estudo feito para dois nanocarreadores (nanocápsulas de PCL e nanopartículas lipídicas sólidas – SLN) contendo ATC neutra. Além da caracterização físico-química das suspensões, elas foram incorporadas em uma matriz de gel com a finalidade de pré-formular uma preparação para uso tópico do AL ATC. As formulações apresentaram boas características sensoriais e reológicas, mostrando que o gel escolhido (Aristoflex® AVC) foi adequado para veicular as suspensões de nanopartículas. A formulação contendo nanocápsulas de PCL foi a que apresentou perfil de permeação mais lento, mostrando-se o mais promissor para utilização tópica da ATC.

Além da utilização de diferentes tipos de nanopartículas, neste trabalho foram avaliados também a utilização de lipossomas como carreadores para ATC. No sexto capítulo encontra-se o estudo realizado com lipossomas de fosfatidilcolina de ovo (EPV) para veicular a ATC na forma ionizada. Uma pequena modificação foi utilizada no preparo dos lipossomas. Como a ATC ionizada possui carga positiva, foram utilizados lipídios com carga negativa a fim de que aumentasse a interação eletrostática entre a ATC e o lipossoma. Para isso foram utilizados o sulfato de colesterol e o dioleil ácido fosfatídico. A otimização do preparo foi feita através de metodologia de superfície de resposta. A eficiência de encapsulação alcançada foi de 58 %, diâmetro médio de 200 nm e índice de polidispersão em torno de 0,2 indicando que os lipossomas produzidos apresentaram bons parâmetros coloidais. Os experimentos de viabilidade celular indicaram que a encapsulação reduz a toxicidade do AL em questão.

O último capítulo traz uma compilação dos dados apresentados ao longo da tese, fazendo uma comparação de todas as formulações estudadas, indicando um possível sistema mais promissor para estudos futuros com o AL ATC. Por fim, são apresentadas as considerações finais da tese.

Capítulo 2 - Nanocápsulas de poli (ε-caprolactona) contendo articaína neutra

Artigo publicado:

CAMPOS, EVR; de MELO, NFS; de PAULA, E; ROSA, AH; FRACETO, LF. Screening of conditions for the preparation of poly(ε-caprolactone) nanocapsules containing local anesthetic articaine. ***J. Colloid. Sci. Biotechnol.,*** v. 2 (2), p. 106-111, 2013.

2.1. Abstract

The local anesthetic articaine (ATC) is widely used in dentistry; however, its side effects can include paresthesia and nerve injury. Polymeric nanocapsules (PN) can be used as a carrier for drugs, and help to reduce undesirable symptoms. The objective of this study was to evaluate the influence of different factors on the average size, polydispersion and encapsulation efficiency of PN containing ATC. Poly(ε-caprolactone) (PCL) nanocapsules containing ATC were prepared by the oil-in-water emulsion/solvent evaporation method. The final ATC concentration was 2%. The preparation conditions were optimized using a central composite blocked cube-star design, which investigated the influence of two variables at five levels (2^2 factorial points (-1 and +1) and 2 replicates of the central point, 2x2 axial points (-1.414 and +1.414), with an orthogonal distribution), resulting in 10 experiments. The factors varied were (A) PVA concentration, and (B) sonication time. The nanocapsules showed a good size range, a polydispersity index less than 0.2 and high encapsulation efficiency. The values of the factors had no significant influence on either average size or polydispersion, however the encapsulation efficiency was significantly influenced by the sonication time. Improved formulations were identified using the central composite design, and the main determining factor for the choice of a suitable formulation was the encapsulation efficiency. Two of the formulations produced showed a high encapsulation efficiency of ATC in the PCL nanocapsules, and presented colloidal characteristics suitable for the route of administration.

Keywords: Articaine, PCL nanocapsules, response surface, modified release.

2.2. Introduction

Articaine (ATC) belongs to the amino-amide class of local anesthetics (LA), and is one of the drugs of choice for the treatment of acute and chronic pain in dentistry (de Araujo *et al.* 2003, Malamed 2004). ATC is the only amino-amide LA that contains an additional ester group and a thiophene ring in its structure. This influences the biotransformation of the compound in the plasma and liver, since it promotes relatively rapid hydrolysis (Malamed 2001, de Araujo *et al.* 2003, Paxton and Thome 2010). The replacement of a benzene ring by a thiophene ring increases anesthetic potency and enhances diffusion within the tissues (Vasconcelos *et al.* 2002, Paxton and Thome 2010). Lower systemic toxicity enables ATC to be used at higher concentrations than the other LA. In dental practice, it is employed at a concentration of 4% associated with epinephrine 1:100,000 and 1:200,000, while in epidural anesthesia it is used at a concentration of 2% associated with epinephrine 1:200,000 (Malamed 2001, Vasconcelos *et al.* 2002, Paxton and Thome 2010).

The greater anesthetic effectiveness of ATC is due to its ability to diffuse between tissues (Vasconcelos *et al.* 2002, Malamed 2006, Paxton and Thome 2010). However, an important drawback is that ATC can cause prolonged or permanent paresthesia (Malamed 2006), with symptoms including sensations of drowsiness and tingling. Studies undertaken in the USA and Canada have found evidence of a direct relationship between high doses of ATC and paresthesia following injection prior to dental operations. Most of the reported incidents of paresthesia appear to be associated with blockade of the inferior alveolar nerve and the lingual nerve (Pogrel 2007, Diaz 2009). Another disadvantage is related to the high concentrations of ATC employed, which increases the associated risk because mandibular nerve lesion is concentration-dependent (Johansen 2004, Paxton and Thome 2010).

The development of carrier systems for ATC could help to reduce adverse side effects, as well as enhance the effectiveness of the drug by improving delivery to the target tissues. This would permit the use of lower concentrations in pharmaceutical formulations (Kuzma *et al.* 1997, de Araújo *et al.* 2005). Various systems have been used as carriers for local anesthetics, including polymeric materials (Gorner *et al.* 1999, Govender *et al.* 1999, Polakovic *et al.* 1999). Of special interest are polymeric nanocapsules (NC), where the active principle can be either dissolved in the oily nucleus or adsorbed on the wall of the particle. Nanocapsules are therefore excellent carriers for hydrophobic substances such as the neutral form of articaína (Schaffazick

et al. 2003, Durán *et al.* 2006, Mohanraj and Chen 2006, Morales 2007, Anton *et al.* 2008, Mishra *et al.* 2010).

In medical formulations, particles in the 100–500 nm size range are considered nanoparticles, since their behavior is governed by quantum effects. These particles share the same functionality in pharmaceutical applications (Roco 1999, Bawa 2007, Buse and El-Aneed 2010).

Statistical design is used to plan experiments in order to identify the most important contributing factors, and offers advantages including a reduction of the number of experiments required as well as more reliable results (Rotthauser *et al.* 1998). The popularity of response surface methodology (RSM) is due to its simplicity and efficiency (Box and Drapper 1987). The effect of a given factor (*k*) on a response is determined by varying the level of the factor, and observing the effect on the response. The number of tests required to perform a full 2*k* factorial design increases according to the number of factors investigated (Barros-Neto *et al.* 2007).

In the present work, poly(ε-caprolactone) nanocapsules containing articaine (at a final concentration of 2%) were manufactured after screening the preparation conditions and optimizing the formulation using a response surface methodology employing rotational central composite design (RCCD). The effects of PVA concentration and sonication time on particle polydispersity, size, and ATC encapsulation efficiency were investigated. The objective was to obtain formulations of NC containing ATC that showed improved colloidal stability and encapsulation efficiency, with a view to their use in *in vivo* experiments.

2.3. Experimental details

2.3.1. Materials

The articaine used was kindly donated by DFL Indústria Química e Farmacêutica Ltda. (Brazil). Poly (ε-caprolactone), Myritol oil, and polyvinyl alcohol (PVA) were obtained from Sigma Aldrich. Acetone and chloroform were analytical grade. The solvents used for the chromatographic analyses were HPLC grade acetonitrile (J.T. Baker) and Milli-Q water.

2.3.2. Methodology

2.3.2.1. Preparation of the PCL nanocapsules containing ATC

The nanocapsules were prepared according to the oil-in-water emulsion method, with solvent evaporation, described by Zhou et al. 400 mg of PCL polymer was dissolved in 20 mL of chloroform, and another solution containing 200 mg of ATC and 200 mg of Myritol 318 was prepared by dissolution of the components in 10 mL of acetone. The two solutions were sonicated for one minute in a sonicator (at 100 W), in order to form a pre-emulsion. The pre-emulsion was then added to 50 mL of aqueous solutions containing different concentrations of PVA (in accordance with the experimental design described below) as surfactant, and submitted to sonication for different time intervals in order to form a double emulsion containing the nanocapsules. The emulsion was maintained under magnetic stirring for 10 minutes, after which the organic solvent was removed under reduced pressure, with the aid of a rotary evaporator. The solution was concentrated to a final volume of 10 mL, containing ATC at a concentration of 2% (Zhou *et al.* 2010).

2.3.2.2. Optimization of formulation preparation: response surface methodology and rotational central composite design

The ideal values of the proportion of PVA used in the aqueous phase, and the sonication time, were determined using a rotational central composite design (Table I). Five levels were employed for these two factors, while constant values were used for the volumes of the aqueous and organic phases, as well as for the ATC and polymer concentrations. The responses obtained using the RCCD were evaluated in terms of particle size, polydispersity index, and efficiency of encapsulation of ATC in the PCL nanocapsules. Each experiment was performed in duplicate, and the formulations were prepared in random order.

Table 1: Matrix of the rotational central composite design applied to the preparation of the polymeric nanocápsulas containing articaine.

Formulation	PVA	Sonication
1	1 (175 mg)	1 (10 min)
2	-1 (125 mg)	-1 (6 min)
3	-1 (125 mg)	1 (10 min)
4	1 (175 mg)	-1 (6 min)
5	0 (150 mg)	0 (8 min)
6	0 (150 mg)	1.4 (12 min)
7	0 (150 mg)	-1.4 (4 min)
8	1.4 (200 mg)	0 (8 min)
9	0 (150 mg)	0 (8 min)
10	-1.4 (100 mg)	0 (8 min)

2.3.2.3. Measurements of particle size and polydispersion

The dynamic light scattering technique was used to determine the average particle size (as hydrodynamic diameter) and polydispersion, with dilution of the nanocapsule suspensions (with or without ATC) in Milli-Q water (at a ratio of 1:1000, v/v). The analysis employed a Malvern ZetaSizer ZS 90 instrument, with a fixed angle of 90º and a temperature of 25 ºC. The size distributions and polydispersity indices were expressed as the averages of three measurements (Gorner *et al.* 1999, Govender *et al.* 2000, Venkatraman *et al.* 2005).

2.3.2.4. Encapsulation efficiency of articaine in the PCL nanocapsules

The encapsulation efficiency was determined by the ultrafiltration/centrifugation method. Samples of the nanocapsules containing ATC were centrifuged in regenerated cellulose ultrafiltration units (30 kDa molecular exclusion pore size, Microcon, Millipore). The filtrate was collected, and articaine was quantified by high performance liquid chromatography (HPLC). The

encapsulation rate of the drug was calculated from the difference between the amount of articaine in the filtrate, and the total concentration (100 %) of the drug in the formulation (Gamisans *et al.* 1999, Schaffazick *et al.* 2003).

The chromatographic analyses employed a mobile phase consisting of a 12:88 (v/v) ratio of acetonitrile and 0.02 mol/L sodium dihydrogen phosphate solution adjusted to pH 3.0 with phosphoric acid, at a flow rate of 2 mL/min. ATC was measured at a wavelength of 273 nm using an UV detector. The injection volume was 100 µL. Total articaine (100 %) present in the PCL nanocapsule suspension was determined following dilution in acetonitrile, with quantification using an analytical curve that had been previously validated according to Resolution 899/2003 of the Brazilian National Health Surveillance Agency (ANVISA).

2.3.2.5. Analysis of the results using RCCD

Statistical analysis of the effects on the measured parameters of variations in sonication time and surfactant concentration, as well as interactions between the factors, was performed using StatGraphics Plus (version 5.1) software, considering a significance level of 95 % ($p < 0.05$).

2.3.2.6. ATR-FTIR analysis

Spectra for ATC, the polymer, PCL nanocapsules, PCL nanocapsules loaded ATC and a physical mixture of ATC and the polymer were investigated by FTIR analysis using a Varian 660-IR spectrometer equipped with an attenuated total reflectance (ATR) device (diamond crystal, 2.2 x 3.0 mm, nominal incident angle of 45°). The equipament was operated in transmittance mode, with 32 accumulations in a frequency range between 4000 and 400 cm^{-1} (Campos *et al.* 2013b).

2.3.2.7. AFM imaging

The morphology of PCL nanocapsules loaded with ATC (formulation 5) was investigated by AFM using a NanoSurf Easy Scan 2 microscope in intermittent contact mode. Sample was

dried overnight in a silicon surface. The scan speed and frequency were proportional to area and 0.6 Hz respectively (Campos *et al.* 2013b).

2.4. Results and Discussion

Ten formulations were prepared in duplicate, according to the maximum and minimum levels of the factors as determined by the RCCD. Five levels were used for the quantity of surfactant and the sonication time. The effects of these factors were evaluated considering three responses: the average diameter of the nanocapsules, the polydispersivity index of the nanocapsule suspension, and the articaine encapsulation efficiency. These parameters were determined immediately following preparation of the suspensions. The results are given in Table 2.

Table 2: Matrix of the rotational central composite design, and the results obtained for the size, polydispersion (PDI), and encapsulation efficiency of PCL nanocapsules containing articaine. The numbers within parenthesis indicate formulation replicates.

Formulation	A	B	Diameter (nm)	PDI	Encapsulation efficiency (%)
1 (1)	1	1	809.3 ± 38.3	0.368 ± 0.021	68.8 ± 2.3
1 (2)	1	1	711.6 ± 23.8	0,176 ± 0.025	68.7 ± 2.6
2 (1)	-1	-1	546.9 ± 24.1	0,097 ± 0.002	79.6 ± 3.5
2 (2)	-1	-1	378.5 ± 17.2	0,144 ± 0.003	68.1 ± 3.2
3 (1)	-1	1	521.5 ± 16.9	0,232 ± 0.007	68.9 ± 2.5
3 (2)	-1	1	474.2 ± 10.3	0,105 ± 0.007	67.3 ± 2.9
4 (1)	1	-1	486.1 ± 15.6	0,514 ± 0.012	77.3 ± 3.4
4 (2)	1	-1	596.5 ±14.9	0,132 ± 0.015	70.5 ± 3.7
5 (1)	0	0	452.9 ± 13.3	0,080 ± 0.004	78.5 ± 1.3
5 (2)	0	0	445.5 ± 16.4	0,068 ± 0.006	73.5 ± 1.5
6 (1)	0	1,4	393.5 ± 11.1	0,133 ± 0.011	65.7 ± 2.8
6 (2)	0	1,4	585.8 ± 12	0,245 ± 0.015	66.4 ± 2.4
7 (1)	0	-1.4	496.5 ± 12.3	0,205 ± 0.01	71.3 ± 3.9
7 (2)	0	-1,4	485.7 ± 9.3	0,102 ± 0.014	73.9 ± 2.9
8 (1)	1,4	0	433.2 ± 10.1	0,132 ± 0.020	66.3 ± 3.4
8 (2)	1,4	0	385.7 ± 12.9	0,094 ± 0.017	64.7 ± 3.3
9 (1)	0	0	465.0 ± 8.3	0,146 ± 0.009	68.8 ± 2.1
9 (2)	0	0	431.1 ± 9.9	0,066 ± 0.010	72.5 ± 2
10 (1)	-1,4	0	765.3 ± 9.5	0,086 ± 0.015	69.0 ± 3.4
10 (2)	-1,4	0	642.4 ± 11.3	0,136 ± 0.012	73.5 ± 3.1

A: PVA; B: Sonicação

The influence of the factors (at five different levels) on nanocapsule size was assessed using RCCD, and is illustrated in the Pareto chart (Figure 1). The results of statistical analysis of

_____

the effects of the factors on particle size are provided in Table 3. Neither of the factors showed any statistically significant effect ($p < 0.05$). In earlier work, Moraes et al. also reported that the surfactant concentration did not significantly affect the particle size distribution of PLGA nanocapsules containing benzocaine (Moraes *et al.* 2009, Moraes *et al.* 2011).

Figure 1: Effects of factors on the average diameter of PCL nanocapsules containing a articaína. Results obtained at a 95% confidence level.
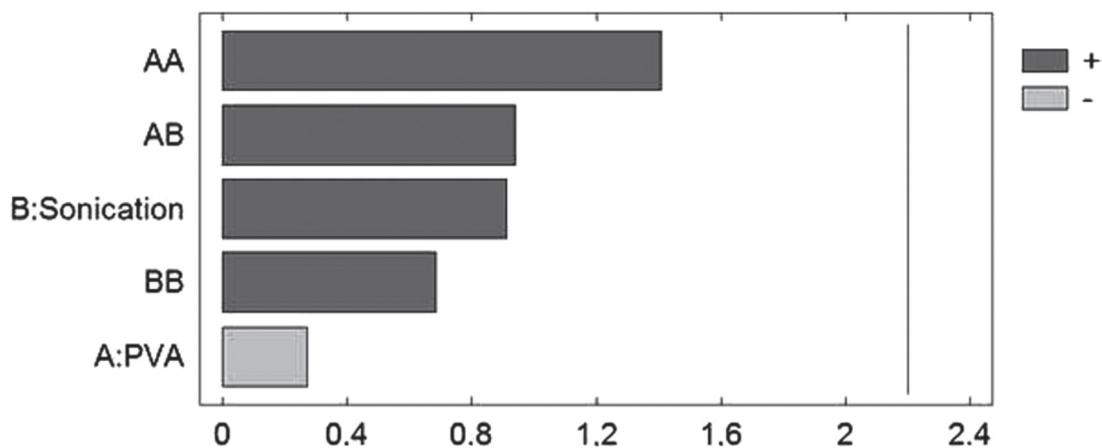
Table 3: Estimated effects of factors on the average diameter of PCL nanocapsules containing articaine, and values of *p* (ANOVA).

Source of variation	Estimated effect	p*
(A) PVA	-18.79	0.791
(B) Sonication	+ 63.07	0.381
AA	+129.05	0.186
AB	+91.07	0.367
BB	+62.79	0.507

* Results obtained at a 95% confidence level.

In the work of Ali et al. a factorial design with three levels was used to investigate the influence of sonication time and pulse rate on the average diameter and polydispersion of solid

lipid nanoparticles (SLN). It was observed that sonication time had a significant influence on average nanoparticle diameter, with a reduction in size as the sonication time and pulse rate were increased. This was attributed to the heat generated during sonication. In the same work, the influence of the composition of the formulation (in terms of surfactant and lipid) was investigated, and it was found that the average nanoparticle diameter decreased significantly ($p < 0.05$) as the concentration of Poloxamer 188 surfactant was increased (Ali *et al.* 2010).

In the present work, neither of the factors showed any statistically significant effect on average NC diameter, although there was some evidence that increased sonication time and decreased PVA concentration favored the formation of larger nanocapsules.

The effects of the factors (at five levels) on the polydispersion of the PCL nanocapsules containing ATC were evaluated by statistical analysis and construction of a Pareto chart (Figure 2, Table 4). Changes in PVA concentration and sonication time did not have any statisticall significant ($p < 0.05$) influence on polydispersion.

Figure 2: Effect of factors on the polydispersion of PCL nanocapsules containing articaine. Results obtained at a 95% confidence level.

_____
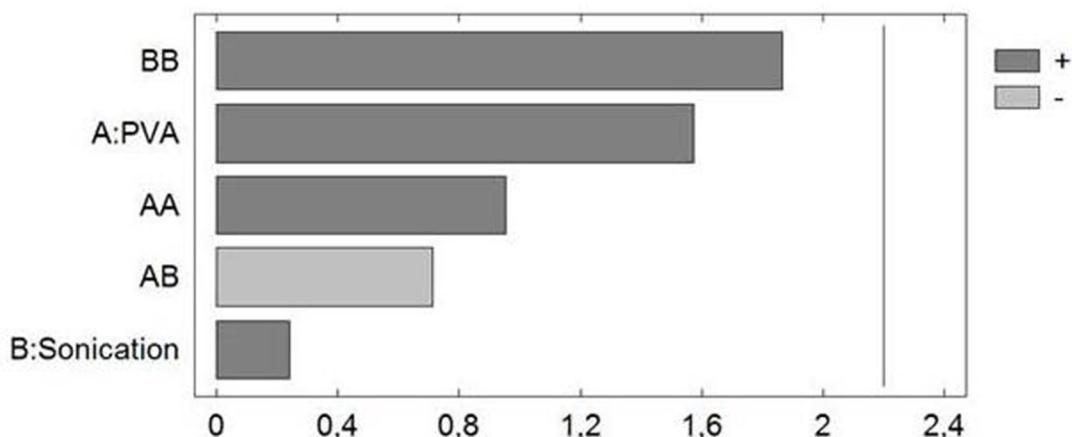
Table 4: Estimated effects of factors on the polydispersion of PCL nanocapsules containing articaine, and values of *p* (ANOVA).

Source of variation	Estimated effect	p*
(A) PVA	+0.077	0.143
(B) Sonication	+0.011	0.813
AA	+0.061	0.361
AB	+0.049	0.490
BB	+0.121	0.088*

* Results obtained at a 95% confidence level.

The results obtained for the statistical analysis of the efficiency of encapsulation of ATC in the PCL nanocapsules are presented in Figure 3 and Table 5. Only sonication time significantly influenced encapsulation efficiency, which increased when the time was reduced. When the sonication time was increased, progressively smaller amounts of ATC were encapsulated in the NC. This could probably be explained by the increase in kinetic energy associated with extended sonication, resulting in collisions and size reduction of the NC, with consequent loss of ATC to the external medium.

Figure 3: Effect of factors on the encapsulation efficiency of PCL nanocapsules containing articaine. Results obtained at a 95% confidence level.
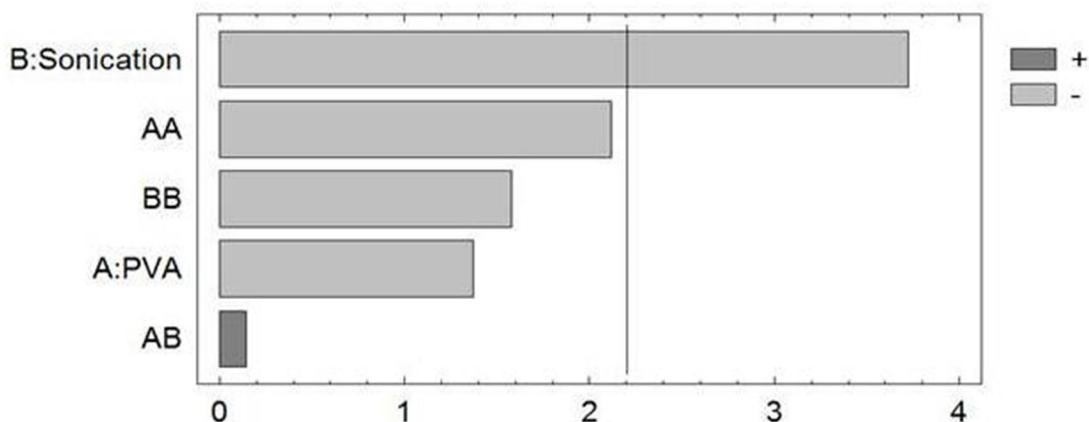
Table 5: Estimated effects of factors on the association efficiency of PCL nanocapsules containing articaine, and values of *p* (ANOVA).

Source of variation	Estimated effect	p*
(A) PVA	-1.86	0.197
(B) Sonication	-5.04	0.003*
AA	-3.79	0.057
AB	0.27	0.886
BB	-2.82	0.143

* Results obtained at a 95% confidence level.

Factorial design and response surface methodology have been widely used to investigate the effects of different preparation parameters on nanoparticle properties including size and drug encapsulation efficiency (Gamisans *et al.* 1999, Govender *et al.* 2000, Vandervoort *et al.* 2004, Venkatraman *et al.* 2005, Derakhshandeh *et al.* 2007, Moraes *et al.* 2009, Ali *et al.* 2010, Zhou *et al.* 2010, Campos *et al.* 2013b). Mondal et al. used a 2^3 factorial design to evaluate the effects of polymer and surfactant (Span 20) concentrations, as well as the proportions of the organic and aqueous phases, on the average diameter of PLGA nanoparticles. The size of the nanoparticles diminished in three circumstances (Mondal *et al.* 2008):

(1) a simultaneous increase in surfactant concentration and organic phase volume;

(2) a reduced polymer concentration together with an increase in organic phase volume; and

(3) a reduced polymer concentration together with an increased surfactant concentration.

Derakhshandeh and coworkers used a 2^4 factorial design to investigate the influence of polymer and stabilizer concentrations, as well as the volumes of the organic and aqueous phases, on the encapsulation efficiency of an anticancer drug. It was found that the efficiency of drug encapsulation in the nanoparticles was significantly improved when higher polymer concentrations and smaller volumes of the two phases were used (Derakhshandeh *et al.* 2007).

The use of statistical techniques during the development of new formulations can help to reduce costs and avoid unnecessary delays in the marketing of products. In the present work, the encapsulation efficiency was the parameter that was most sensitive to changes in production

conditions. The findings should help in the production of formulations that provide good encapsulation rates, for use in future studies of anesthetic activity.

The morphology of the nanocapsules produced using Formulation 5 (which showed the highest encapsulation efficiency) was analyzed using AFM and FTIR. The AFM results (Figure 4(a)) showed that the nanocapsules loaded with ATC were spherical, with a diameter of approximately 350 nm. This was smaller than the size determined by photon correlation spectroscopy (PCS) (Figure 4(b)), possibly due to dehydration of the nanocapsules during the AFM sample preparation procedure, or the fact that the PCS technique measures hydrodynamic diameter (Silva *et al.* 2011b, Campos *et al.* 2013b).

Figure 4: a) AFM image of PCL nanocapsules (Formulation 5) loaded with ATC, using intermittent contact mode; b) Size distribution of PCL nanocapsules loaded with ATC, obtained using the PCS technique.
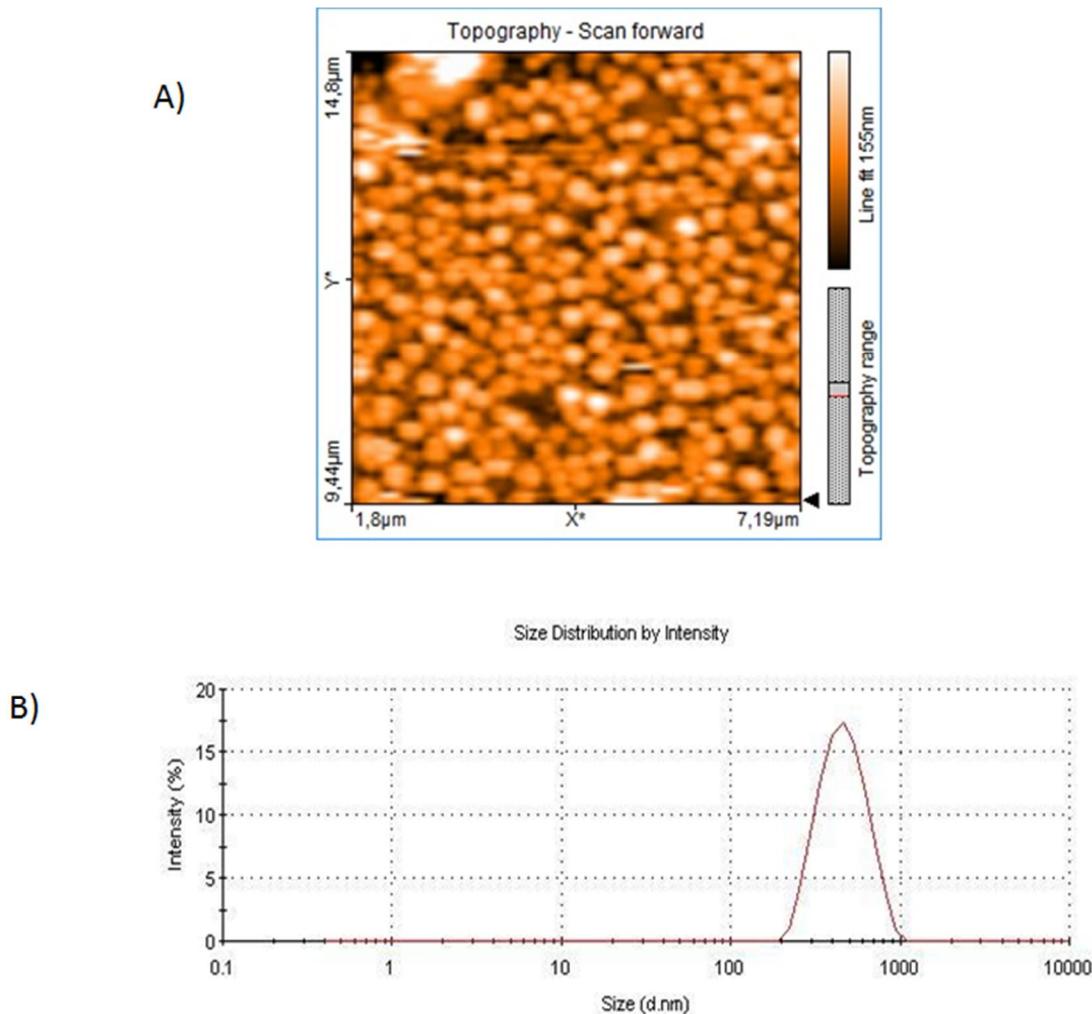
Infrared analysis of the PCL polymer revealed the characteristic bands corresponding to ester carbonyl (C=O) stretching at 1735 cm^{-1} and saturated carbon (C-H) stretching in the region between 3000 and 2800 cm^{-1} (Figure 5). The spectrum for ATC showed the carboxyl (C-O) stretching band at 1710 cm^{-1} and saturated carbon (C-H) stretching bands between 3000 and 2800 cm^{-1}. Characteristic ATC peaks were observed in the spectrum obtained for nanocapsules loaded with ATC, including a band corresponding to C-C stretching near 1600 cm^{-1}. The other peaks for the polymer showed no changes compared to the spectrum for nanocapsules without the drug.

_____

The fact that there were no changes in the absorption bands of the materials indicated that there was no degradation of the chemicals used for preparation of the nanocapsules. Similar results can be found in the literature for polymeric microparticles loaded with anti-inflammatory drugs (Poletto *et al.* 2007), as well as for polymeric nanospheres loaded with the local anesthetic lidocaine (Campos *et al.* 2013b).

Figure 5: ATR-FTIR spectra of ATC, polymer, and nanoparticles. The samples used were: a) PCL nanocapsules (Formulation 5) loaded with ATC PCL, b) PCL nanocapsules: ATC, c) ATC, d) PCL polymer and e) PCL + ATC physical mixture.
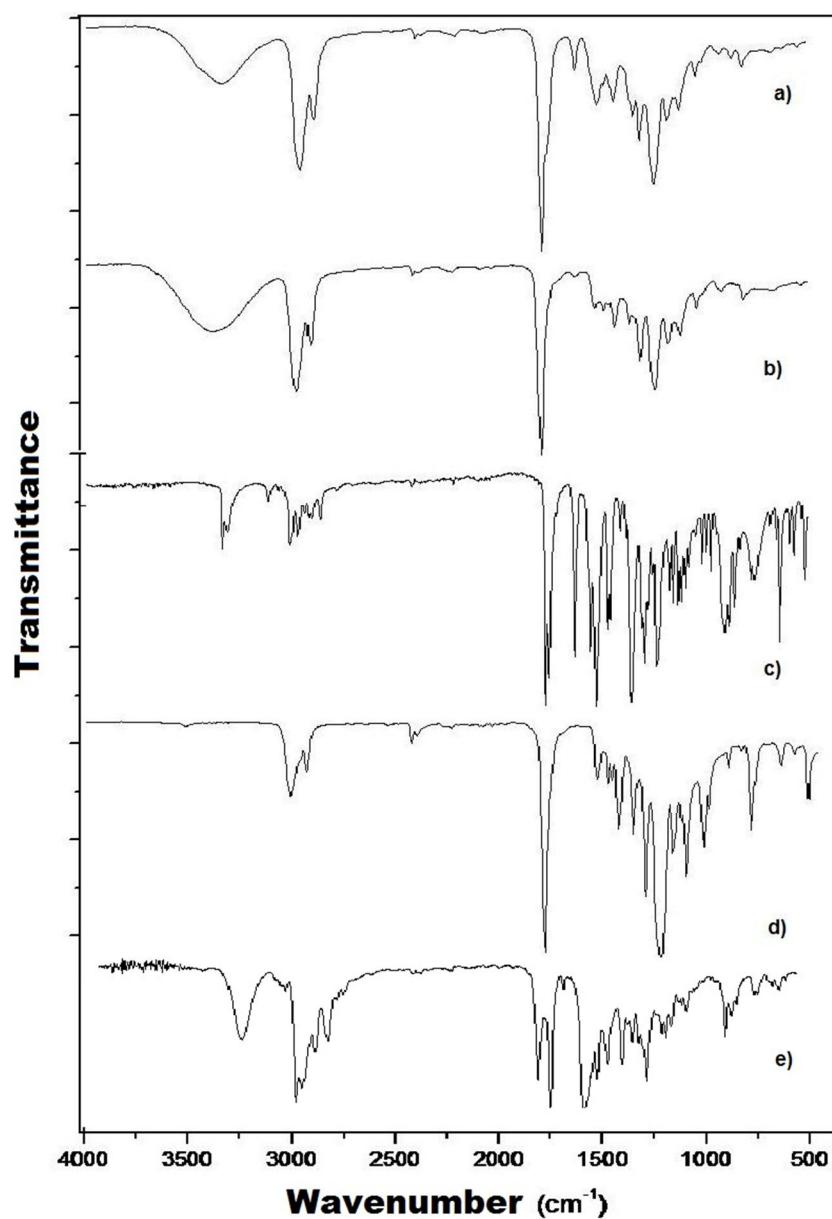
2.5. Conclusions

Response surface methodology with RCCD is a useful tool for evaluation of the different factors that influence nanocapsule characteristics including size, polydispersion and encapsulation efficiency. Determination of these parameters is important in order to predict nanoparticle stability. A satisfactory formulation should provide high encapsulation efficiency and good colloidal stability. Here, the oil-in-water emulsion technique was successfully used to produce poly(ε-caprolactone) nanocapsules containing articaine, and it was shown that nanocapsule properties were mainly influenced by sonication time, and to a lesser extent by surfactant concentration. The results of the present work provide a basis for further studies concerning the optimization of formulations employing nanocapsules, and should aid the development of new formulations that could be used in the future, in both *in vitro* and *in vivo* trials.

Acknowledgements

Capítulo 3 – Nanopartículas de alginato/quitosana contendo articaína ionizada

Artigo publicado:

3.1. Abstract

Nowadays, articaine hydrochloride (ATC) is a local anesthetic widely used in dental procedures, but its side effects include paresthesia and nerve injury. Alginate/chitosan nanoparticles (AG/CSnano) can be used as carrier for drugs, overcoming the problems. The aim of this work was to evaluate the factors (Calcium/alginate Ca^{2+}:AG and Chitosan/alginate CS:AG mass ratios) influence on the average size, polydispersity index, zeta potential and encapsulation efficiency of ATC. AG/CSnano containing ATC were prepared by ionic pregelation method. A three-level factorial design was carried out and the factors varied were Ca^{2+}/AG mass ratio and CS/AG mass ratio. There were obtained nanoparticles with size range of 340-550 nm and polydispersity index between 0.2 and 0.5, zeta potential range -19 and -22 mV and encapsulation efficiency of ATC in AG/Csnano between 22 and 45%. According to the results, the average size, polydispersity index and encapsulation efficiency were significantly affected to the variation of Ca^{2+}/AG and CS/AG mass ratio, but the zeta potential didn´t change significantly with factor variations. The factorial design showed it was possible to identify formulations that presented better results for the parameters measured. The factor chosen for the suitable formulations was the encapsulation efficiency. Through this parameter, one formulation was chosen with highest encapsulation efficiency of ATC and presented good colloidal stability parameters aiming future clinical applications.

Keywords: articaine, AG/CS nanoparticles, factorial design, drug delivery

3.2. Introduction

Polymeric nanoparticles can be used as carriers systems for active substances and showed advantages such as suitable physicochemical stability, easy preparation method, good reproducibility and application to improve chemical properties of drugs (Sinha *et al.* 2004, Silva *et al.* 2010). These systems can be obtained from natural polymers such as alginate (AG) and chitosan (CS). These biopolymers are hydrophilic, which enables encapsulation of water-soluble biomolecules and increase *in vivo* circulation times (Gazori *et al.* 2009).

Alginate polymers comprise anionic chains of guluronic and manuronic acids with (Sinha *et al.* 2004, Gazori *et al.* 2009, Woitiski *et al.* 2009, Silva *et al.* 2010) linkage between units. In the presence of divalent cations (such as calcium) form reversible hydrogels due to ionic interactions between calcium ions and the guluronic acid residues. The calcium alginate nanoparticles make its one of the most widely used carriers for release systems (Gazori *et al.* 2009, Woitiski *et al.* 2009). Alginate polymers are highly used in biomedical applications because they are biocompatible and biodegradable, but they have a limitation of rapid release into physiological salt concentrations (Némati *et al.* 1996, De and Robinson 2003). In the presence of sodium ions, insoluble calcium alginate becomes soluble sodium alginate, resulting in rapid disintegration of the drug when used in controlled release systems (Némati *et al.* 1996, De and Robinson 2003).

Chitosan is a natural cationic polymer, composed by D-glucosamine and N-acetyl glucosamine obtained by the N-deacetylation of chitin. This polymer presents biodegradable and biocompatible properties and can stabilize the alginate hydrogels for the formation of nanoparticles (Gazori *et al.* 2009, Woitiski *et al.* 2009). Chitosan is gaining importance in the pharmaceutical field for being a non-toxic cationic polymer with good biocompatibility and biodegradability, because it does not induce allergic reactions or immune rejection, in addition to presenting properties mucoadhesives prolonging retention in target tissues (Lertsutthiwong *et al.* 2009, Yang *et al.* 2011). It has been used in the production of microparticles and nanoparticles by forming an ionotropic gelation with negatively charged polymers. Polyelectrolytes complex has been investigated as a delivery system of drugs, proteins, DNA and other oligonucleotides with good results (Janes *et al.* 2001a, Janes *et al.* 2001b, Agnihotri *et al.* 2004, Zandanel and Vauthier 2012). Several types of chitosan-polyanion complex are reported in the literature but the combination of chitosan and calcium alginate was considered the most interesting systems carrier (Lertsutthiwong *et al.* 2009).

Alginate/chitosan nanoparticles (AG/CSnano) obtained from ionotropic gelation due to interaction between the alginate carboxyl groups and chitosan amino groups have the ability to protect and encapsulate drugs. The ionotropic gelation consists on the ability of polyelectrolytes to crosslink in the presence of some ions to form hydrogels. The natural polyelectrolytes contain certain anions on their chemical structure and these anions forms a structure by combination with the polyvalent cations and induce gelation by binding mainly to the anion blocks. The nanoparticles are produced by dropwise a polymeric solution into the aqueous polycationic solution. The cations diffuses into the polymeric drops, forming a three dimensional lattice of ionically crossed linked moiety (De and Robinson 2003, Gazori *et al.* 2009, Patil *et al.* 2010, Doustgani *et al.* 2012).

AG/CSnano is also biocompatible and biodegradable and limits the release of the drug more effectively when compared with alginate and chitosan alone (De and Robinson 2003, Gazori *et al.* 2009). An additional advantage of this system is low toxicity, allowing repeated administration of the therapeutic agent. Some work in the literature showed the encapsulation of drugs and proteins in alginate-chitosan nanoparticles and microparticles (Némati *et al.* 1996, Coppi *et al.* 2002, De and Robinson 2003, Woitiski *et al.* 2008, Gazori *et al.* 2009, Lertsutthiwong *et al.* 2009, Woitiski *et al.* 2009, Grillo *et al.* 2010, Nagarwal *et al.* 2012).

The composition of AG/CSnano is very important to achieve suitable properties and good stability of the formulation. Design of these nanoparticles covers processes toward developing and optimizing formulation based on physicochemical and pharmacological parameters (Woitiski *et al.* 2008, Woitiski *et al.* 2009). Experimental design has been applied for nanoparticles optimization considering the advantages such as reduction in the number of experiments that need to be performed, development of mathematical models to assess the relevance and statistical significance of the factor effects, and evaluation of interaction effect between studied factors (Woitiski *et al.* 2008, Woitiski *et al.* 2009)'.

Articaine hydrochloride (ATC) is an amino-amide local anesthetic that has been widely used in dentistry (Gupta 1991, Malamed 2001, de Araújo *et al.* 2005). This gives a peculiarity of both plasma and liver biotransformation, because it causes a relatively rapid hydrolysis (Malamed 2001, de Araújo *et al.* 2005). Furthermore, the ATC stands out because it is the only one that has a thiophenic ring instead of a benzenic ring. The presence of this ring, in its formula, gives ATC an increase in anesthetic potency and distribution among tissues (Vasconcelos *et al.* 2002, Paxton and Thome 2010).

The faster action of the ATC is attributed to the physico-chemical properties of the molecule, with a higher fat solubility (due to the thiophenic ring) and thus more easily reaching the neuronal membrane (Malamed 2004, Paxton and Thome 2010). However, the main complication associated with the use of ATC is the long or permanent paresthesia (Paxton and Thome 2010). Some studies have demonstrated the superiority of ATC when compared with others in the same class in clinical practice and an increasing use in recent years mainly in dental procedures (Malamed 2004, Paxton and Thome 2010).

However, the high concentration used in the formulations is related to the incidence of paresthesia and use of this anesthetic combined with epinephrine in dental practices may have some problems (Malamed 2004) promoting the development of carrier systems for this anesthetic is interesting, such as alginate/chitosan nanoparticles.

This study aimed to optimize AG/CSnano formulation for LA ATC, investigating the relationship between factors and experimental responses using a response surface methodology combined with 3-levels, 2-factor experimental design. Experiments were designed based on the observed important effect of polymer mass ratios and calcium on formation of the pregel with alginate and chitosan coating on the nanoparticle structure.

3.3. Materials and Methods

3.3.1. Materials

Articaine hydrochloride was obtained from donation by DFL Industry Ltd. (Brazil), sodium alginate and low molecular weight chitosan (50 kDa) were purchased from Sigma-Aldrich Chem. Co., calcium chloride was purchased from LabSynth (Brazil), acetonitrile was purchased from Tedia Company Inc. (USA). Other reagents used were analytical grade.

3.3.2. Preparation of nanoparticles

The preparation of nanoparticles was performed according to the method of ionotropic gelation (De and Robinson 2003). Initially, it was prepared a solution of sodium alginate (0.6 mg/mL) and added ATC (280 mg). Then, 2 mL of a calcium chloride solution were dropwised on the solution and was sonicated during 1 minute (Unique® 100 W). The calcium alginate pre-gel

obtained was kept stirring (300 rpm) for 30 minutes. Subsequently, 2 mL of chitosan solution (dissolved in 1% acetic acid) were added and kept stirring (300 rpm) for 30 minutes. The resulting suspension was kept under stirring overnight (300 rpm) to allow formation of uniform size nanoparticles (AG/CSnano:ATC).

3.3.3. Experimental design

The influence of the amount of some components used in the preparation of AG/CS nano:ATC was evaluated from a response surface methodology and a three-levels two factors experimental design with calcium chloride:alginate (A) and chitosan:alginate (B) mass ratios. These two variables were studied in three levels: low, central point and high (-1, 0, +1). Values of these variables are presented in Table 1. The dependent variables were mean diameter (Y_1), polydispersity index (Y_2), zeta potential (Y_3) and encapsulation efficiency (Y_4). A matrix of 10 experimental runs was constructed using quadratic model: $Y = b_0 + b_1A + b_2B + b_{12}AB + b_{11}A^2 + b_{22}B^2 + E$ where b_0 is the arithmetic mean response, b_1 and b_2 are the coefficients of the respective independent variables and b_{11}, b_{12} and b_{22} are their respective interaction terms; Y are dependent variables or responses and E the error term. The results were analyzed using one-way analysis of variance (ANOVA) and statistical significance was defined as $p < 0.05$ (Woitiski *et al.* 2008, Woitiski *et al.* 2009).

Table 1: Levels and variables of 3-level, 2-factor experimental design for the preparation of ATC loaded AG/CSnano

Levels	Variables	
	Ca^{2+}:AG (A)	CS:AG (B)
-1	0.08	0.05
0	0.10	0.10
1	0.17	0.30

Ca^{2+}:AG – calcium chloride/alginate mass ratio; CS:AG – chitosan/alginate mass ratio

The experimental design and the second order polynomial models and statistical analysis were generated with the *Statgraphics plus* 5.1 software (SAS Inc.) (Chopra *et al.* 2007, Ferreira

et al. 2007, Woitiski *et al.* 2009, Ali *et al.* 2010). With the second order polynomial models obtained were constructed response surface plots. The formulation parameters and the observations for dependent variables are showed in Table 3.

3.3.4. Validation of ATC analytical method

A high performance liquid chromatography (HPLC) analytical method for ATC quantification in nanoparticles was developed and validated following International Conference on the Harmonization of Technical Requirements for the Registration of Pharmaceuticals for Human Use and Resolution 899/2003 of the Brazilian National Health Surveillance Agency (ANVISA) guidelines (Brasil 2003, ICH 2005).

A modification of the method described previously (Richter and Oertel 1999) was performed. A Varian ProStar HPLC system was set up with Varian PS delivery solvent module, Varian PS 410 autosampler, Varian PS 210 UV detector. A reversed-phase column C18, 5 μm particle size, 150 x 4.6 mm (Gemini Phenomenex) maintained at 35°C of temperature. Mobile phase composed by sodium diigrogenophosphate (0.02 M) pH 3.0 adjusted with phosphoric acid and acetonitrile (88:12, v/v) and 2 mL/min as flow rate. The injection volume was 100 μL, and all samples were previously filtered through a 0.22 μm polyethersulfone membrane (Millipore). ATC was detected at 273 nm.

The method was validated by its linearity, limit of detection (LOD) and quantification (LOQ), accuracy and precision and the samples were analyzed in three consecutive days.

3.3.5. ATC encapsulation efficiency

The amount of ATC encapsulated was determinate by ultrafiltration/centrifugation method (Schaffazick *et al.* 2003, de Melo *et al.* 2010, de Melo *et al.* 2011). The nanoparticle suspensions were centrifuged in ultrafiltration devices composed of a regenerated cellulose membrane with molecular exclusion pore size of 10 kDa (Amicon, Millipore). Following, ATC was quantified in the filtrate using HPLC method previously validated. The ATC encapsulation efficiency (EE%) of ATC associated with the nanoparticles was calculated from the difference between the total and free ATC concentrations, measured in the dispersion and the ultrafiltrate (Eq. 1)

$$EncapsulationEfficiency(\%) = \frac{ATC:AG/CS}{ATCtotal} x100\% \qquad (1)$$

where ATC:AG/CS is the amount of ATC in AG/CS nanoparticles and ATC total is the amount of ATC used in formulation.

3.3.6. Mean diameter and zeta potential

The mean diameter (in nm) and zeta potential (in mV) were measured by photon correlation spectroscopy technique using a ZetaSizer Nano ZS-90 (Malvern Instruments Ltd.) particle analyzer at a fixed angle of 90° and temperature of 25°C. The samples were diluted 10 times and were measured in triplicate. The polydispersity index was given by particle size distribution (Schaffazick *et al.* 2003, Sankalia *et al.* 2007, de Melo *et al.* 2011).

3.4. Results and Discussion

3.4.1. Validation of analytical method

The chromatographic conditions were considered suitable as a symmetrical peak was obtained from ATC and viable, because chromatographic runs were performed in 5 minutes (data not showed). The method was considered specific since no peak corresponding to components of the mobile phase, diluent or nanoparticles co-eluted with the peak corresponding to the drug.

Linearity was evaluated by linear regression of three calibration curves performed with concentrations between 5 and 200 µg/mL. The correlation coefficient (r) of the mean analytical curve mean (n=9) was 0.99878. ANVISA recommends a correlation coefficient greater than or equal to 0.99 and all of linear correlation values are above this value (Brasil 2003, ICH 2005). Thus, the method was considered linear. The validated calibration curve was Y = 9.01274 + 1.38394X, r^2 = 0.99878, LOD = 2.55 µg/mL, LOQ = 4.51 µg/mL.

The accuracy was determined from the concentration values determined experimentally compared to the theoretical concentration as can be seen in Table

Table 2: Accuracy and precision studies for ATC analytical method validation.

ATC theoretical (µg/mL)	ATC experimental (µg/mL)	Recovery (%)	ATC experimental (µg/mL)	Recovery (%)
40.00	40.60	101.50	41.22	103.10
40.00	39.51	98.78	41.15	102.80
40.00	40.59	101.40	40.53	101.30
80.00	80.05	100.10	77.28	96.60
80.00	80.84	101.10	76.37	95.80
80.00	76.29	95.40	81.28	101.60
120.00	118.56	98.80	121.10	100.90
120.00	118.69	98.90	123.28	102.70
120.00	121.23	101.00	121.02	100.80
Mean	__	**99.66**	__	**100.62**
SD	__	**1.96**	__	**2.64**
Mean (n=18)	**100.14**			
RSD (n=18)	**3.11**			

All results are within the acceptance criteria established at the concentrations examined (95.0 to 105%), making the method accurate. Accuracy is the relationship between the average concentration determined experimentally and the corresponding theoretical concentration. The percentage recovery ranged from 95.3 to 103.1%, being within the specifications established (Brasil 2003, ICH 2005).

All validation parameters obtained from analytical method proposed were considered satisfactory for meeting the specifications established (Brasil 2003, ICH 2005). The method therefore can be considered specific linear, precise and accurate within the concentration range between 5 and 200 µg/mL of ATC was applicable to assays for determining the content of ATC loaded AG/Csnano.

3.4.2. Experimental design

Several studies use experimental designs and response surface in order to estimate the contrasts of the parameters involved in the preparation of formulations of AG/CSnano certain properties such as diameter, the drug encapsulation efficiency, among others (De and Robinson 2003, Sankalia *et al.* 2007, Gazori *et al.* 2009, Woitiski *et al.* 2009).

The AG/CSnano:ATC were prepared following ionotropic pregelation method described before. The experimental design was performed to determine the relationship between Ca^{2+}:AG and CS:AG mass ratios on response variables for the optimization of nanoparticle formulation for ATC. The choice of the variation in levels was based on preliminary testing and research literature (De and Robinson 2003, Gazori *et al.* 2009). The observed responses for mean particle size, polydispersity index, zeta potential, encapsulation efficiency are presented in Table 3.

Table 3: Experimental design and physicochemical characteristics of ATC loaded AG/CSnano stored at 25°C ($n = 3$).

Formulation	A	B	Diameter (nm)	PDI	Zeta Potential (mV)	Encapsulation Efficiency (%)
1	-1	1	405.4 ± 15.6	$0{,}281 \pm 0.002$	-21.8 ± 1.0	32.3 ± 1.3
2	0	-1	409.5 ± 4.0	$0{,}297 \pm 0.002$	-22.3 ± 0.6	38.7 ± 0.8
3	-1	-1	436.9 ± 30.0	0.508 ± 0.018	-22.4 ± 0.1	22.4 ± 3.1
4	1	1	438.8 ± 5.2	0.309 ± 0.015	-20.9 ± 0.4	30.7 ± 2.1
5	0	1	478 ± 20.1	0.418 ± 0.003	-22.6 ± 0.1	$34{,}1 \pm 1.9$
6	0	0	342.9 ± 36.4	0.275 ± 0.020	-20.7 ± 2.4	45.8 ± 1.3
7	0	0	359.8 ± 25.1	0.236 ± 0.038	-19.5 ± 2.0	42.9 ± 1.8
8	1	-1	551.1 ± 8.4	0.556 ± 0.064	-19.9 ± 2.6	29.2 ± 0.2
9	-1	0	404.6 ± 2.2	0.415 ± 0.003	-20.1 ± 0.5	32.1 ± 0.7
10	1	0	365.4 ± 9.2	0.442 ± 0.003	-22.0 ± 0.7	22.5 ± 0.3

A – Ca^{2+}:AG mass ratio; B – CS:AG mass ratio, PDI – polydispersity index

The mean diameters of the AG/CSnano: ATC was determined by photon correlation spectroscopy technique. In order to evaluate the influence of different factors at 3 levels on the particle diameter, the data from table 3 were statistically analysed using the *Statgraphics plus 5.1* software and the result obtained from factors that influence in this parameter was plotted as Pareto charts. In Pareto charts, the signal positive (+) indicate that some factor increase the effect of the measured parameter and the signal minus (-) indicates an opposite effect. Figure 1 shows the contrasts of the factors on mean diameter and the surface response estimated.

Figure 1: a) Influence of factors on the mean diameter of AG/CSnano loading ATC. Results obtained from statistics analysis from the data presented in Table 3 using the *Statgraphics plus 5.1* software. Data were presented with 95% level confidence. **b)** Estimated response surface plot showing effect of calcium:alginate (Ca^{2+}:AG) mass ratio (A) and chitosan:alginate (CS:AG) mass ratio (B) obtained from the model fitted by the data presented in Table 3 and according to Equation 2.

a)
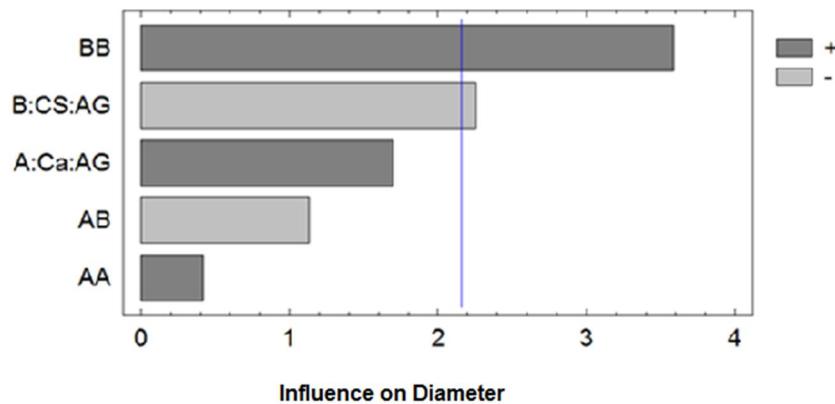
b)
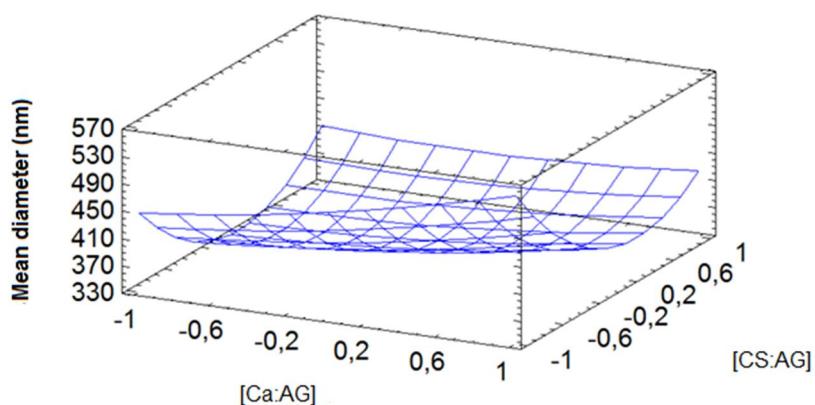
According to the results presented in Figure 1, the variation of the CS:AG mass ratio obtained p <0.05, indicating this effect is significantly different. The quadratic polynomial fit showed the effect of variation CS:AG mass ratio alone is negative, and when this factor is observed squared, the effect is positive.

The influence of the concentration of calcium chloride, bovine serum albumin and chitosan on the mean diameter, polydispersity, zeta potential, encapsulation efficiency and release profile of insulin from AG/CS nanoparticles was evaluated using a Box-Behnken design (Woitiski *et al.* 2009). The results showed that the average diameter of the nanoparticles is related to the concentration of chitosan. The complexation of chitosan contributes to an initial increase of the core alginate through the interaction between the chitosan amino groups and alginate carboxylic groups (Woitiski *et al.* 2009).

The results obtained in this study can be seen that when the factor CS:AG mass ratio is considered alone has a negative effect (see Pareto chart, Figure 1a), namely decreasing the concentration of chitosan occurs an increase in mean diameter of the nanoparticles, but when this factor is considered squared, the effect becomes positive. In previous study, Gazori and coworkers showed that the increase of chitosan concentration lead to particles more compact and with low polydispersity (Gazori *et al.* 2009). So, the differences observed in this study, could be due the presence of the ionized drug in the formulations (ATC+) that could change the ionic interactions between the polymers chains (alginate and chitosan).

From preceding discussion, second order polynomial equation was constructed based on the statistical analysis from the data presented in Table 3. This equation represent the quantitative effect of process variable (B) and interactions on the response Y_1 (Eq.2), obtained from statistical analysis of data from Table 3.

$$Y_1 = 352.73 - 74.25X_2 + 189.27X_2^2 + 32.95 \qquad (2)$$

where Y_1 is mean diameter and B is CS:AG mass ratio.

The polydispersity index was also evaluated according the influence of the variation of the factors on 3 levels. Pareto charts were constructed from the results described in the factorial design. In Figure 2, are contrasts of the factors on polydispersity and estimated response surface.

Figure 2: **a)** Influence of factors on the polydispersity index of AG/CSnano loading ATC. Results obtained from statistics analysis from the data presented in Table 3 using the *Statgraphics plus* 5.1 software. Data were presented with 95% level confidence. **b)** Estimated response surface plot showing effect of calcium:alginate (Ca^{2+}:AG) mass ratio (A) and chitosan:alginate (CS:AG) mass ratio (B) obtained from the model fitted by the data presented in Table 3 and according to Equation 3.
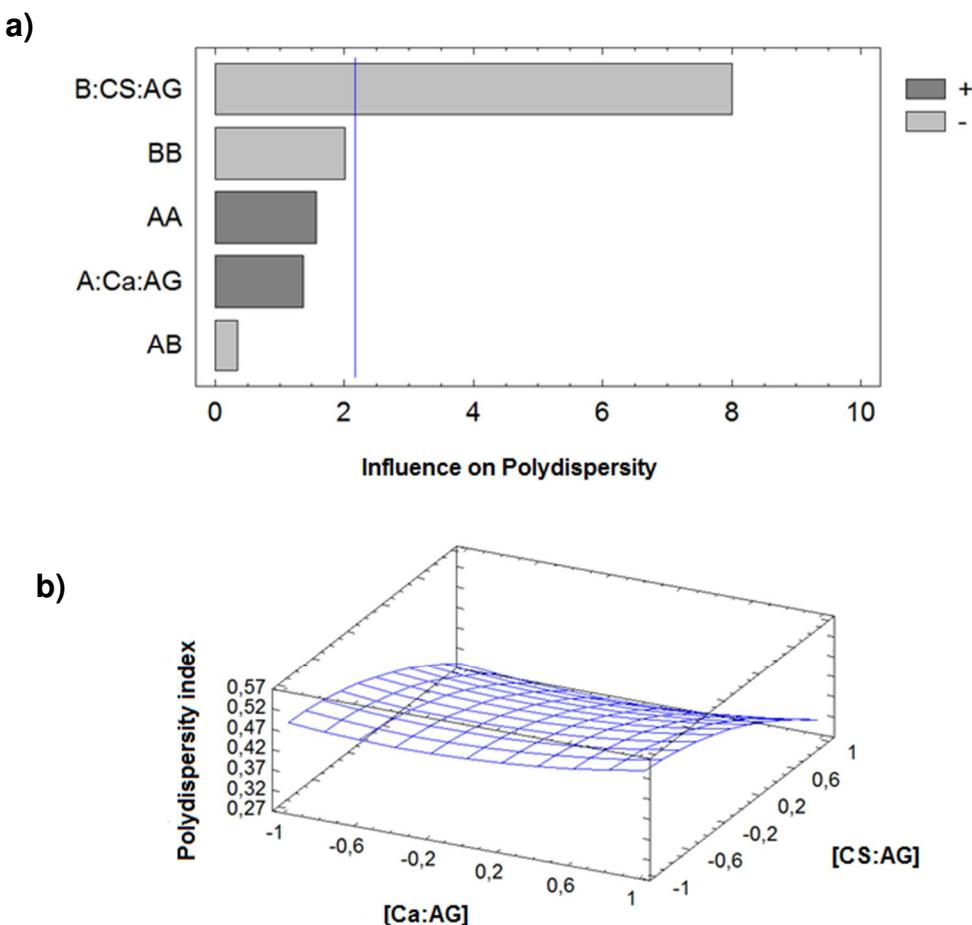
According to the results observed in Figure 2, the variation of CS:AG mass ratio obtained $p < 0.05$, indicating the decrease of chitosan concentration promote an increase in polydispersity index.

The available literature shows results d that the increase in polydispersity was achieved with high concentrations of calcium chloride due to the reduction of aggregation but was independent of the concentration of chitosan (Woitiski *et al.* 2009).

Other study investigated the change in concentration of the polymer, calcium chloride and antisense vector for growth factor receptors nanoparticles alginate/chitosan using a Box-Behnken design. The results demonstrate that chitosan may interact with the alginate at a slightly acid pH and increasing it leads to the formation of nanoparticles more compact and consequently, with narrower size distribution, leading to a reduction of the polydispersity (Gazori *et al.* 2009).

From preceding discussion, second order polynomial equations were constructed. These equations represent the quantitative effect of process variable (B) and interactions on the response Y_2 (Eq.3), obtained from statistical analysis of data from Table 3.

$$Y_2 = 0.414 - 0.198X_2 + 0.024 \qquad (3)$$

where Y_2 is polydispersity index and B is CS:AG mass ratio.

Figure 3 shows the effects of factors studied on the zeta potential and estimated response surface of the AG/CSnano:ATC.

Figure 3: **a)** Influence of factors on the zeta potential of AG/CSnano loading ATC. Results obtained with 95% level confidence. Results obtained from statistics analysis from the data presented in Table 3 using the *Statgraphics plus* 5.1 software **b)** Estimated response surface plot showing effect of calcium:alginate (Ca^{2+}:AG) mass ratio (A) and chitosan:alginate (CS:AG) mass ratio (B) obtained from the model fitted by the data presented in Table 3.
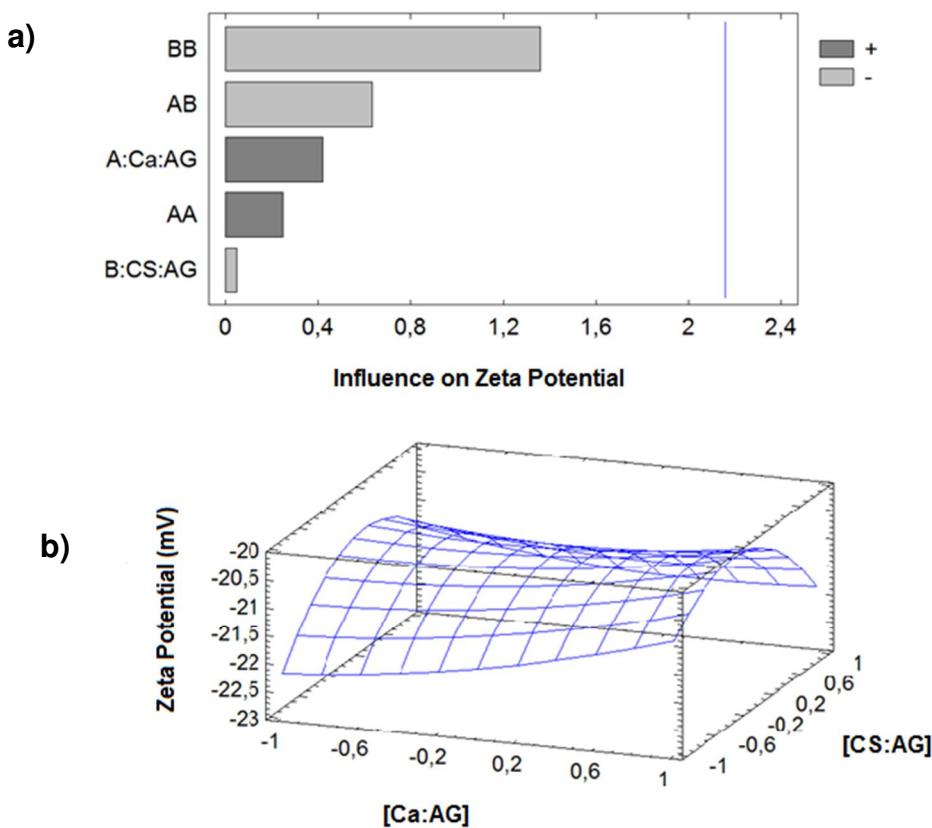
From the results shown in Figure 3, it was possible to observe that none of the variation of factors could cause significant changes in zeta potential of the AG/CSnano:ATC. Few studies report the influence of the components of formulations of nanoparticles on the zeta potential, a property it is little affected. The zeta potential of AG/CSnano is usually quite negative, suggesting high electrostatic stabilization of nanoparticles in suspension with little tendency to aggregate independent of the factors studied the levels determined by factorial design. Similar

results are found in the literature for AG/CSnano with insulin (Woitiski *et al.* 2009) and with antisense vectors (Gazori *et al.* 2009).

In the remaining parameters described above, the encapsulation efficiency of ATC in AG/CSnano was evaluated by the ultrafiltration/ centrifugation as described previously, using validated analytical methodology. To evaluate the influence of different factors at 3 levels on the encapsulation efficiency of ATC, Pareto charts were constructed from the results of factorial design and estimated response surface (Figure 4).

Figure 4: a) Influence of factors on the encapsulation efficiency of AG/CSnano loading ATC. Results obtained from statistics analysis from the data presented in Table 3 using the *Statgraphics plus* 5.1 software. Data were presented with 95% level confidence. **B)**Estimated response surface plot showing effect of calcium:alginate (Ca^{2+}:AG) mass ratio (A) and chitosan:alginate (CS:AG) mass ratio (B) obtained from the model fitted by the data presented in Table 3 and according to Equation 4.
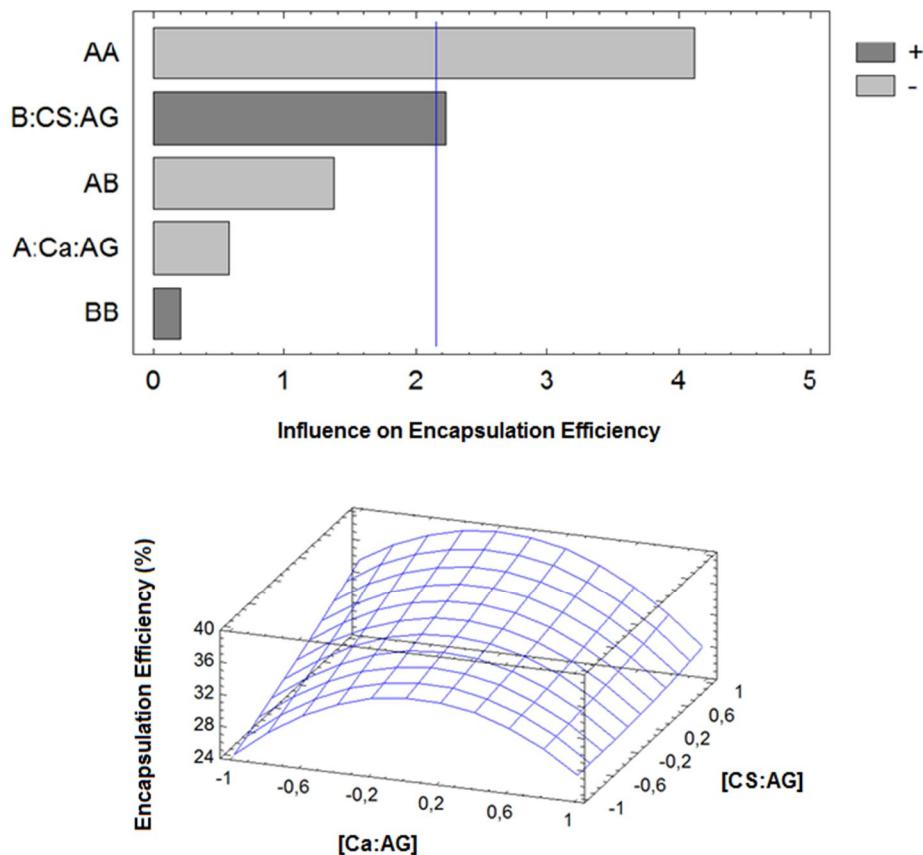
According to the results viewed in Figure 4, both variations in the Ca^{2+}:AG and CS:AG mass ratios were able to cause significant differences of the encapsulation efficiency. The model showed that the effect of Ca^{2+}:AG mass ratio was quadratic (Equation 4) on encapsulation efficiency and that the increasing in CS:AG mass ratio increases the encapsulation of ATC.

The results of previous work aforementioned (Woitiski *et al.* 2009) showed that increase in the encapsulation efficiency was achieved with high concentrations of calcium chloride, as it interacts with the guluronic acid residues present in the structure of the alginate establishing ionic bonds with carboxylic residues of insulin, increasing the association between encapsulated molecule chains and alginate. In this same work it was also observed that with increasing concentration of chitosan decreased encapsulation efficiency of insulin.

The effect of concentration of chitosan has also been observed other work (Sankalia *et al.* 2007) since the decrease of the efficiency of encapsulation of the enzyme alpha-amylase increased as the concentration of chitosan in the chitosan-alginate beads.

This effect can be attributed to an electrostatic interaction between the amino groups of chitosan and the carboxylic groups of alginate, reducing the interaction of molecules encapsulated in alginate matrix, leading to a loss to the external environment (Sankalia *et al.* 2007, Woitiski *et al.* 2009).

The results showed that increasing the concentration of chitosan favors the encapsulation efficiency while the concentration of calcium had a negative effect. Thus, it is believed that the variation in the concentration of calcium was not able to sufficiently increase the interaction between the guluronic acid residues and carboxyl residues present in the structure of the alginate and ATC, respectively. Regarding the concentration of chitosan, it is believed that the range performed in this study did not affect the interaction between the drug and the ATC alginate chains, favoring the encapsulation, however further studies should be done in order to explain this behaviour.

From preceding discussion, second order polynomial equations were constructed. These equations represent the quantitative effect of process variables (A and B) and interactions on the response Y_4 (Eq. 4), obtained from statistical analysis of data from Table 3.

$$Y_4 = 36.27 + 5.61X_2 - 16.62 X_1^2 + 4.03 \quad (4)$$

where Y_4 is encapsulation efficiency, A is Ca^{2+}:AG mass ratio and B is CS:AG mass ratio.

From the results obtained with the 3-level, 2-factor experimental design, it was observed that the quantitative composition of the AG/CSnano is important to determinate properties of nanoparticles, such as mean diameter, polydispersity, zeta potential and encapsulation efficiency.

So, the formulation corresponding to number 6 and 7 (same formulation) of the experimental design were selected for further studies, since it showed both the best encapsulation efficiency and colloidal parameters appropriate for purpose use.

3.5. Conclusion

In this study, the preparation and characterization ATC loaded AG/CSnano showed that this formulation presents good parameters for colloidal drug delivery systems. The influence of different factors on the properties of the AG/CSnano was investigated using a 3-level, 2-factor experimental design. The Ca:AG and CS:AG mass ratios and the combination of the factors had a statically significant influence on the mean diameter, polydispersity index and encapsulation efficiency in nanoparticles. The optimum formulation was achieved using 0.1 Ca:AG mass ratio and 0.1 CS:AG mass ratio. In general, the results show that ATC loaded AG/CSnano may be considered a promising carrier system for controlled release of ATC with possible further experiments.

Acknowledgements

Capítulo 4 - Carreadores hidrofílicos (nanopartículas de alginato/quitosa e nanocápsulas de PEG-PCL) para a forma ionizada da articaína

Artigo publicado:

de MELO, NFS; CAMPOS, EVR; GONÇALVES, CM; de PAULA, E; PASQUOTO, T; LIMA, R; ROSA, AH; FRACETO, LF. Development of hydrophilic nanocarriers for the charged form of the local anesthetic articaine. **Colloids Surf. B**, v. 121, p. 66-73, 2014.

4.1. Abstract

One of the current challenges in drug encapsulation concerns the development of carrier systems for hydrophilic compounds. Potential carriers include nanocapsules prepared with amphiphilic polymers, which consist of a polymeric coating surrounding an aqueous nucleus, or dense matrices such as nanospheres of alginate/chitosan, where the drug may be dispersed in the matrix or adsorbed on the surface. The development of new formulations of nanocarriers, for example the poly(ethylene glycol)-poly(ε-caprolactone) (PEG-PCL) nanocapsules and alginate/chitosan (AG/CS) nanospheres described in this work, is needed in the case of ionized drugs such as articaine. This amino amide local anesthetic is the drug of choice in dentistry for regional anesthesia as well as the relief of acute and chronic pain. Here, the physico-chemical properties of suspensions of the nanoparticles (considering diameter, polydispersion, and zeta potential) were determined as a function of time, in order to establish the stability of the systems. The formulations did not show any substantial changes in these parameters, and were stable for up to 120 days of storage at ambient temperature. Satisfactory encapsulation efficiencies were obtained for the PEG-PCL nanocapsules (60 %) and the AG/CS nanospheres (45 %). Cytotoxicity assays confirmed that the encapsulation of articaine reduced its toxicity, relative to the free drug. The most promising results were obtained using the vesicular system (PEG-PCL nanocapsules), which not only altered the release profile of the drug, but also resulted in the lowest toxicity. This carrier system therefore holds promise for use in future practical applications.

Keywords: Polymeric nanoparticles, PEG-PCL copolymer, alginate/chitosan, local anesthetic, articaine.

4.2. Introduction

Polymeric nanoparticles (NP) are used as carriers for drugs and other active molecules, and can be prepared in the form of matrix-based systems (nanospheres) or as vesicles (nanocapsules) (Schaffazick *et al.* 2003, Mohanraj and Chen 2006, Morales 2007, Anton *et al.* 2008, Mishra *et al.* 2010, Parveen *et al.* 2012, Souto *et al.* 2012). An important consideration is that the nanoparticles should be manufactured using materials whose metabolites are nontoxic and can be easily degraded. Among the most widely used materials are natural biodegradable polymers such as alginate (AG), chitosan (CS), and poly(ε-caprolactone) (PCL) (Parveen *et al.* 2012).

Alginates are polyanionic polymers extracted from brown algae. In the presence of certain divalent cations (such as Ca^{2+}) or cationic polymers (such as chitosan), these polymers undergo ionotropic gelification, with formation of inter-chain links that enable the incorporation of hydrophilic bioactive molecules by means of electrostatic and van der Waals' interactions, amongst others (Doustgani *et al.* 2012).

Alginate/chitosan (AG/CS) nanospheres can be produced by adding a solution of cations to a solution of alginate and chitosan, under agitation. The nanoparticles formed can then be used to encapsulate hydrophilic drugs (De and Robinson 2003, Gazori *et al.* 2009, Patil *et al.* 2010, Doustgani *et al.* 2012). AG/CS nanospheres are biocompatible, exhibit low toxicity, and are more effective for the modulation of drug release, compared to single component nanospheres composed of alginate or chitosan (De and Robinson 2003, Woitiski *et al.* 2008, Gazori *et al.* 2009, Lertsutthiwong *et al.* 2009, Woitiski *et al.* 2009, Nagarwal *et al.* 2012).

Poly(ε-caprolactone) is an aliphatic polyester that is widely used in drug release systems in the form of both nanospheres and nanocapsules (Sinha *et al.* 2004, Woodruff and Hutmacher 2010). Due to its hydrophobic nature, the incorporation of hydrophilic drugs in this polymer is low, and the drug is readily lost to the aqueous phase during nanoparticle formation. Alternative encapsulation methods are therefore required for these drugs (Mora-Huertas 2010, Woodruff and Hutmacher 2010). One possibility is to modify the polymer with polyethylene glycol (PEG) in order to obtain nanocapsules with aqueous nuclei that can incorporate hydrophilic compounds.

Polyethylene glycol, a biocompatible hydrophilic polymer that has been approved by the United States Food and Drug Administration, can be added to PCL to produce a PEG-PCL diblock copolymer (Hsu *et al.* 2004, Wei *et al.* 2009). This copolymer is both more hydrophilic and more biodegradable than the PCL homopolymer. Studies conducted in vitro have confirmed

its superior performance. In the form of nanocapsules with an aqueous nucleus, it has been used to develop release systems for hydrophilic drugs (Yadav *et al.* 2008, Wei *et al.* 2009), with advantages including reduced drug toxicity and increased circulation time because the presence of PEG on the particle surface hinders recognition and opsonization by phagocytic cells (Neckel and Lemos-Senna 2005). The aqueous nucleus provides these nanocapsules with a high capacity for the incorporation of hydrophilic compounds, which are retained in the nucleus, protecting the tissues from irritation caused by drugs that are highly soluble in water, as well as diminishing the "burst effect" that is frequently observed with other types of polymeric nanoparticles (Vrignaud *et al.* 2011).

Articaine hydrochloride (ATC) is an amino amide class local anesthetic, and in dental practice is often the drug of choice for control of acute and chronic pain. The compound is highly soluble in water (~5 g/L, pKa 7.8) (de Araújo *et al.* 2005, Paxton and Thome 2010). ATC is unique in that it possesses a thiophene ring, rather than a benzene ring, which enhances both its potency and its ability to diffuse amongst the tissues (Vasconcelos *et al.* 2002, Malamed 2004, Paxton and Thome 2010); this is the reason for its anesthetic effectiveness. However, a difficulty associated with the use of ATC concerns the risk of long-term or permanent paresthesia (Malamed 2004, Pogrel 2007, Diaz 2009). Another disadvantage is related to the high ATC concentration used (4%), because lesion of the mandibular nerves is concentration-dependent and the associated risks are therefore increased (Dower 2003, Johansen 2004, Paxton and Thome 2010).

A possible strategy to help mitigate these adverse effects associated with the use of ATC is to deliver the drug using modified release systems, such as polymeric nanoparticles that can be loaded with hydrophilic compounds. The objective of this work was therefore to prepare, characterize, and compare two hydrophilic nanocarriers with different structures (AG/CS nanospheres and PEG-PCL nanocapsules), using the ionized form of articaine as a model drug, as well as to evaluate the stabilities and cytotoxicities of the systems. Up to now, there have been few studies concerning the development of nanocarriers for articaine in either its neutral or ionized forms (Campos *et al.* 2013a, de Melo *et al.* 2013).

4.3. Materials and Methods

4.3.1. Materials

Articaine hydrochloride was donated by DFL Industries (Rio de Janeiro, Brazil). Sodium alginate, low molecular weight chitosan (50 kDA), poly(ε-caprolactone) (70-90 kDa), poly(ethylene glycol)-block-poly(ε-caprolactone) methyl ether (PEG ~5 kDa, PCL ~32 kDa), Tween 20, dextran 70, and triglycerides of capric and caprylic acid were purchased from Sigma-Aldrich. Calcium chloride was obtained from LabSynth and acetonitrile (HPLC grade) was acquired from Tedia Chemicals. Dulbecco's Modified Eagle Medium (DMEM), colchicine, fetal bovine serum, penicillin, and streptomycin sulfate were purchased from Cultilab Brasil. All other reagents used were either spectroscopic or analytical grade.

4.3.2. Preparation of the hydrophilic biodegradable nanocarriers

4.3.2.1. Alginate/chitosan nanospheres

The alginate/chitosan (AG/CS) nanospheres were prepared according to the ionotropic gelification method described by De & Robinson (De and Robinson 2003), with slight modifications. Briefly, ATC was added to 10 mL of a solution of sodium alginate (0.6 mg/mL) under magnetic agitation. Subsequently, 2 mL of calcium chloride solution (1.11 mg/mL) was added dropwise to the solution, under agitation, and the mixture was sonicated for 1 min (Unique sonicator, 500 W, 20 kHz). The alginate pre-gel was then maintained under magnetic agitation for 30 min. A solution of chitosan (2 mL, 0.65 mg/mL) was added dropwise to the pre-gel, after which the mixture was left under agitation overnight for stabilization of the nanospheres. The final concentration of ATC was 20 mg/mL (De and Robinson 2003, de Melo *et al.* 2013).

4.3.2.2. PEG-PCL block copolymer nanocapsules

The PEG-PCL nanocapsules were prepared according to the interfacial coacervation method described by Ma et al. (Ma *et al.* 2001), with minor modifications. Firstly, 200 mg of the PEG-PCL copolymer and 100 mg of PCL were dissolved in 10 mL of acetone, followed by

addition of 6 mL of an aqueous solution containing ATC (200 mg). The mixture was left under magnetic agitation for 30 min to form an emulsion. The emulsion was added (under magnetic agitation) to 20 mL of an aqueous phase containing Tween 20 (100 mg) and dextran 70 (200 mg), and the mixture was then kept under agitation for 10 min to obtain a suspension of nanocapsules containing ATC. This suspension was concentrated to a volume of 10 mL using a rotary evaporator, giving a final ATC concentration of 200 mg/mL (Ma *et al.* 2001).

4.3.4. Determination of nanoparticle morphology by transmission electron microscopy (TEM)

The morphologies of the AG/CS nanospheres and PEG-PCL nanocapsules were investigated using TEM. Uranyl acetate (2 %) was added to the samples to provide contrast, after which aliquots were deposited onto copper grids coated with a carbon film and dried at ambient temperature. After drying, micrographs of the samples were obtained using a JEOL 1200 EXII microscope operated at 80 kV (Silva *et al.* 2011b).

4.3.5. Characterization and stability of the particles

The chemical stability of the polymers was determined by measuring the pH of the suspensions using a potentiometer (Tecnal) that had been previously calibrated. The physicochemical stability of the suspensions of AG/CS nanospheres and PEG-PCL nanocapsules containing ATC was evaluated using measurements of average diameter, polydispersion, zeta potential, and pH, over a period of 120 days. The suspensions were stored in amber flasks at ambient temperature (de Melo *et al.* 2011, de Melo *et al.* 2012, Campos *et al.* 2013b).

The measurements of average diameter and zeta potential were performed by dynamic light scattering (photon correlation spectroscopy, PCS) after dilution of the nanoparticle suspensions in deionized water (1:100, v/v), using a ZetaSizer Nano ZS 90 analyzer (Malvern Instruments) operated at 25 °C with a fixed angle of 90°. The polydispersion indices of the samples were also measured. The results were calculated as the average of three

determinations (de Melo *et al.* 2011, de Melo *et al.* 2013) and the analyses were performed after 0, 15, 30, 60, and 120 days.

4.3.6. Analysis of the nanoparticles using ATR-FTIR and DSC

Infrared spectra were obtained for ATC, sodium alginate, chitosan, the PEG-PCL copolymer, the AG/CS nanospheres, and the PEG-PCL nanocapsules. Analyses of the nanospheres and nanocapsules were performed with and without the encapsulated drug, as well as using physical mixtures. These measurements employed a Varian 660 FTIR spectrometer equipped with an attenuated total reflectance accessory (GladiATR, Pike Technologies) and a diamond crystal (2.2 x 3.0 mm), using an incidence angle of 45°. The instrument was operated in transmittance mode, with 32 accumulations in the frequency range 4000-400 cm^{-1} and a resolution of 8 cm^{-1} (Poletto *et al.* 2007, Campos *et al.* 2013b).

Differential scanning calorimetry (DSC) analyses were performed using a TA Q20 calorimeter equipped with a cooling system. Calibration was performed using the element indium. The samples (5 mg) were placed in aluminum pans and the thermal profiles were obtained in the temperature range from -10 to 300 °C, at a heating rate of 10 °C/min, under a flow of nitrogen. An empty pan was used as a reference (Silva *et al.* 2011b).

4.3.7. ATC encapsulation efficiency and drug loading

The quantity of ATC encapsulated in the AG/CS nanospheres and PEG-PCL nanocapsules was determined by the ultrafiltration-centrifugation method (Schaffazick *et al.* 2003, de Melo *et al.* 2012). The samples were centrifuged in filter units with a molecular exclusion pore size of 10 kDa (Amicon, Millipore) and the ATC present in the ultrafiltrate was quantified by high performance liquid chromatography (HPLC). The encapsulation efficiency of the drug was then determined from the difference between the total amount of ATC present in the formulation and the amount that remained unencapsulated. All these analyses were performed in triplicate.

The drug loading was calculated from the ratio between the mass of ATC encapsulated and the final mass of the nanoparticles (de Melo *et al.* 2011, Venturini *et al.* 2011), according to:

73

$$DL\ (\%) = \frac{Wd}{W_{NP}} \times 100 \qquad\qquad (1)$$

where W_d is the mass of ATC encapsulated and W_{NP} is the final mass of the nanoparticles.

Quantification of articaine was performed by HPLC, using a Varian ProStar instrument (Agilent Technologies) equipped with an isocratic PS 210 pump and a UV-Vis detector. The column was a Phenomenex Gemini C_{18} column (NX 5µm, 110 Å, 150 x 4.6 mm), used at 35 °C. The mobile phase consisted of a solution of monobasic sodium phosphate (0.02 mol/L) at pH 3.0 (adjusted with phosphoric acid) and acetonitrile (88:12, v/v), at a flow rate of 2 mL/min. The mobile phase was filtered and degassed. The sample injection volume was 100 µL and the detector wavelength was 273 nm. The analytical methodology was previously validated and provided limits of detection and quantification of 2.55 and 4.51 µg/mL, respectively (r = 0.9999) (Richter and Oertel 1999, de Melo *et al.* 2013).

4.3.8. Cellular viability

Cellular viability was determined using the MTT reduction test performed with mouse Balb-c 3T3 cells maintained under continuous culture in DMEM medium. Approximately 2×10^4 viable cells were inoculated into 96-well plates and incubated for 48 h (de Lima *et al.* 2012, Campos *et al.* 2013b). The cells were exposed for 24 h to samples of free ATC and nanoparticles (AG/CS and PEG-PCL) containing ATC at concentrations ranging from 0.1 to 1.2 mg/mL. Viable cells were then detected using the MTT test by incubation in the presence of MTT for 2 h at 37 °C. The percentage of viable cells was determined by measuring the amount of MTT converted to formazan, using a plate reader at a wavelength of 630 nm and conversion of the absorbance values to percentages of viable cells. The data were analyzed using the Student's t-test with a significance level of p<0.05.

4.3.9. In vitro permeation kinetics and mathematical modeling

The permeation of ATC, free or encapsulated in the nanoparticles, was studied using a system composed of a donor compartment (1 mL) and an acceptor compartment (80 mL, containing 1 mM phosphate buffer at pH 7.4), separated by a cellulose membrane with a molecular exclusion pore size of 1000 Da. The system was gently agitated and maintained

under *sink* conditions (Paavola *et al.* 1995, de Melo *et al.* 2011, de Melo *et al.* 2012). Aliquots were withdrawn from the acceptor compartment after 15, 30, and 60 min, then on an hourly basis up to 1440 min. Quantification of ATC employed HPLC, as described previously, and all measurements were performed in triplicate.

The Baker-Lonsdale theoretical model was used to characterize the permeation of ATC from the nanoparticles. This model, which was developed from the Higuchi model, describes the release of an active substance from a spherical matrix. It is used to linearize the results of release assays involving micro- and nanoparticles (Costa 2002), and can be expressed as:

$$\frac{3}{2}\left[1 - \left(1 - \frac{M_t}{M_\infty}\right)^{2/3}\right] - \frac{M_t}{M_\infty} = kt, \tag{2}$$

where *Mt* and *M∞* correspond to the amounts of drug released at time *t* and at infinite time, and *k* is the release constant (Costa 2002, Siepmann and Siepmann 2008, Moreira *et al.* 2012).

4.4. Results and Discussion

4.4.1.Characterization of the nanoparticle systems

The characteristics of the nanoparticle systems, in terms of particle diameter, polydispersion, and zeta potential, are provided in Table 1. The suspension of AG/CS nanospheres was previously optimized using response surface methodology, from which an ATC encapsulation efficiency of around 45% was obtained (de Melo *et al.* 2013).

Table 1: Initial values of mean diameter (nm), polydispersivity, zeta potential (mV) and pH for AG/CS nanospheres and PEG-PCL nanocapsules formulations loading ATC. The values represent the mean of three experiments (n=3).

Formulation	Mean diameter (nm)	Polydispersivity	Zeta Potential (mV)	pH
AG/CS	326.8 ± 18.5	0.280 ± 0.008	-22.9 ± 2.1	3.9± 0.3
AG/CS:ATC	342.4 ± 20.5	0.236 ± 0.030	-21.7 ± 1.4	3.4 ± 0.3
PEG-PCL	546.9 ± 17.4	0.097 ± 0.003	-23.3 ± 2.0	4.8 ± 0.2
PEG-PCL:ATC	569.2 ± 30.5	0.144 ± 0.025	-18.9 ± 2.8	4.2 ± 0.5

4.4.2. Particle size and polydispersion

The average diameter and polydispersivity index values obtained for the AG/CS nanospheres and PEG-PCL nanocapsules containing ATC were compatible with those of colloidal suspensions and showed that encapsulation of the drug did not affect these parameters (Guterres *et al.* 1995). In the case of the AG/CS nanospheres, a polydispersivity index value of around 0.2 was indicative of a homogeneous size distribution. The PEG-PCL nanocapsules showed a more homogeneous size distribution, with a polydispersivity index value of 0.144, and the average particle diameter (569 nm) was larger than that of the AG/CS nanospheres (342 nm). This was due to the positioning of the PEG chains during formation of the nanocapsules. PEG can be present in the interior of the capsule surrounding the aqueous nucleus, as well as on the external surface, where the formation of a crown increases the hydrodynamic diameter of the particle (Vrignaud *et al.* 2011).

4.4.3. Morphological analysis of the nanoparticles

The morphology of the nanoparticles containing ATC was investigated using TEM (Figure 1).

Figure 1: Transmission electron microscopy images of (a, b) AG/CS nanoparticles with ATC and (c, d) PEG-PCL nanocapsules with ATC. Magnification: x25000 (a, c); x100000 (b, d). The bars indicate the scales of the images.

(a) (b) (c) (d)
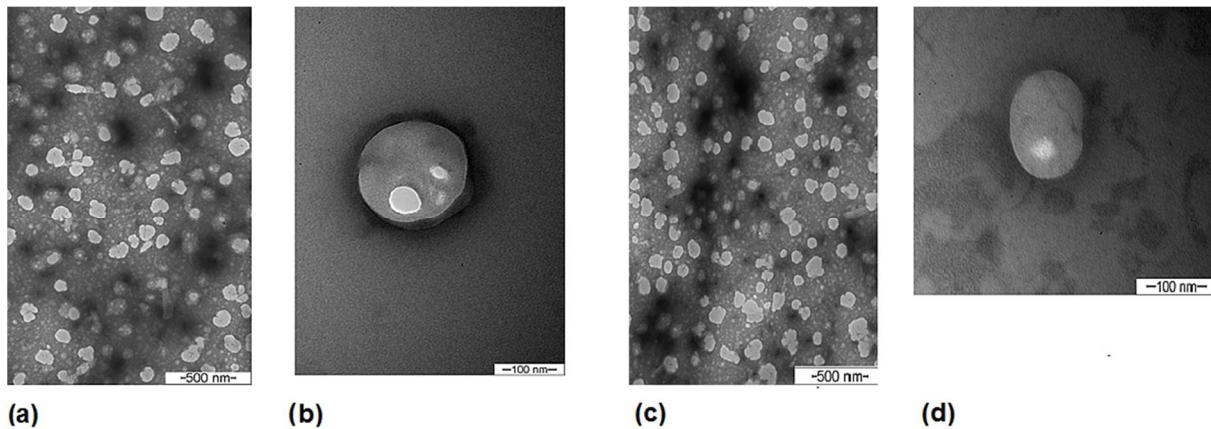
The images of the AG/CS nanospheres and PEG-PCL nanocapsules showed that both types of nanoparticle were spherical, with diameters in the range 100-300 nm. The diameters obtained from the microscopy analyses were smaller than measured by the PCS technique. This apparent difference can be explained by dehydration of the nanoparticles during the TEM sample preparation procedure. In addition, the PCS method determines the apparent (hydrodynamic) diameter, which also considers the hydration layers around the particles. In the case of the AG/CS nanospheres, whose composition is similar to that of a hydrogel, the drying process reduces the average particle size, while the removal of water from the PEG-PCL nanocapsules decreases the degree of hydration of the exposed PEG chains, as a result of which there is a decrease in the apparent size measured using TEM (Silva *et al.* 2011b). Similar findings have been reported for AG/CS nanospheres containing paraquat (Silva *et al.* 2011b) and PCL nanospheres containing lidocaine (Campos *et al.* 2013b).

4.4.4. Analysis of interactions between ATC and the nanoparticles

The ATR-FTIR technique was used to investigate the interactions between the drug and the nanoparticles. Figure S1 shows the spectra obtained for (a) ATC, (b) alginate, (c) chitosan,

(d) a physical mixture of alginate and chitosan, (e) a physical mixture of alginate, chitosan, and ATC, (f) AG/CS nanospheres, and (g) AG/CS nanospheres containing ATC.

It can be seen that ATC presented bands characteristic of stretching of ester and amide carbonyls (C=O) at 1735 cm^{-1} and 1650 cm^{-1}, respectively. Bands at 3000-3200 cm^{-1} and 2500-2700 cm^{-1} corresponded to multiple stretching peaks of quaternary amine salts. A band at 1520 cm^{-1} was related to N-H deformation. Bands at 1580 cm^{-1} and 1450 cm^{-1} were related to stretching of the C=C bond.

Alginate presented characteristic bands between 1600 and 1400 cm^{-1} related to symmetric and asymmetric carbonyl (C=O) stretching. There was also a strong broad band due to the stretching of O-H bonds at 3200 cm^{-1}, resulting from the presence of hydroxyl groups in the glycosidic moieties of the polymer.

The spectrum obtained for chitosan showed bands characteristic of the stretching and deformation of primary amine bonds (N-H) at 3400 and 1580 cm^{-1}, respectively, and a broad band due to the stretching of O-H bonds at 3200 cm^{-1}.

The spectrum for the physical mixture of alginate and chitosan showed the bands corresponding to both alginate and chitosan, while the spectrum for the physical mixture that included the drug also showed the main ATC bands.

In the spectrum for the AG/CS nanospheres, broad bands between 1600 and 1400 cm^{-1} were related to the complexation between alginate and chitosan. In the case of the AG/CS nanospheres containing ATC, the characteristic drug bands were absent; this suggests that interaction of the positively charged groups of ATC with the polymeric chains resulted in vibrational changes and superposition of the bands. There was therefore no rupture of bonds or the formation of new chemical bonding between the substances used to prepare the nanoparticles. Similar results can be found in the literature for AG/CS nanoparticles containing the herbicide paraquat (Silva *et al.* 2011b) and for alginate/gum nanoparticles containing the essential oil of *Lippia sidoides* (de Oliveira *et al.* 2014).

Figure S2 shows the spectra obtained for (a) ATC, (b) the PEG-PCL copolymer, (c) a physical mixture of ATC and the copolymer, (d) PEG-PCL nanocapsules, and (e) PEG-PCL nanocapsules containing ATC.

The spectrum for the PEG-PCL copolymer showed strong characteristic bands associated with stretching of ester carbonyl (C=O), at 1734 cm^{-1}, and O-H, at 3440 cm^{-1}. Bands in the region between 3000 cm^{-1} and 2800 cm^{-1} were due to C-H stretching of saturated carbon. Absorption bands near 3500 cm^{-1} corresponded to O-H bonds in the structure of PEG (Remant

Bahadur *et al.* 2007). For the physical mixture of ATC and the copolymer, the spectrum showed the main ATC bands as well as those of PEG-PCL. The peaks related to the polymer were also observed for the PEG-PCL nanocapsules without the drug. In the spectra for the PEG-PCL nanocapsules, with or without ATC, there was a band near 3200 cm^{-1} related to the axial deformation of O-H bonds. This was caused by the presence of residual water, because the samples were derived from aqueous suspensions. Once again, the characteristic ATC bands were absent, probably due to interaction between positively charged ATC groups and the polymeric chains, resulting in vibrational changes and superposition of the bands. As found for the AG/CS nanospheres, there was no indication of bond rupture or formation of new chemical bonds between the materials used to prepare the PEG-PCL nanocapsules. These findings confirmed that both types of nanoparticle were suitable for use as carriers of ATC.

4.4.5. Differential scanning calorimetry

The DSC analyses were used to provide information concerning the purity of the primary materials, the stability of the formulations, and the forms in which the components were present. The changes that can be detected in DSC analyses include glass transition, fusion, crystallization, and degradation. Figure S3 shows the thermal profiles obtained for ATC, alginate, chitosan, the physical mixture, and AG/CS nanospheres (with and without ATC), using the analytical conditions described previously.

The DSC analysis of ATC revealed a narrow endothermic peak at 170 ºC and another endothermic peak at 220 ºC, corresponding to the fusion and degradation of ATC, respectively. Alginate and chitosan showed broad endothermic peaks at around 85 ºC and 67 ºC, respectively, related to the loss of water associated with hydrophilic groups of the polymers, as well as exothermic peaks at around 250 ºC and 280 ºC, respectively, due to depolymerization and degradation, probably resulting from partial decarboxylation and oxidation (Sarmento *et al.* 2007, Silva *et al.* 2011b). For the physical mixture of alginate, chitosan, and ATC, the peaks present were the collective peaks observed for the individual substances.

The DSC curve obtained for the AG/CS nanospheres showed two endothermic peaks, near 70 ºC and 230 ºC, resulting from shifts of the peaks observed for the individual polymers, indicating that there had been interaction between the polymers during the process of nanoparticle formation. Similar findings have been reported previously for AG/CS nanoparticles

(Sarmento *et al.* 2007, Silva *et al.* 2011b). Analysis of the AG/CS nanospheres containing ATC showed no evidence of the narrow endothermic peak at 170 ºC, characteristic of the drug, only the broad peaks observed for the nanoparticles without ATC. This indicates that the drug was well dispersed in the polymeric matrix, and was not present in the form of crystalline arrangements. The disappearance of the endothermic ATC peaks suggests possible electrostatic interaction between the drug and the polymers (because ATC was present in the ionized form). Similar behavior has been observed for the drug bupivacaine (Grillo *et al.* 2010) and the herbicide paraquat (Silva *et al.* 2011b), when these substances were encapsulated in AG/CS nanoparticles.

The thermal profiles obtained for the PEG-PCL copolymer, ATC, the physical mixture of PEG-PCL and ATC, and PEG-PCL nanocapsules (with and without ATC) are shown in Figure S4.

The thermogram obtained for PEG-PCL showed the presence of two narrow endothermic peaks at around 50 °C, indicating fusion of the crystalline phases of PEG and PCL. This was due to the complete mixing of the constituent polymers within the copolymers, as described previously (Remant Bahadur *et al.* 2007). In the case of the PEG-PCL nanocapsules, there was an endothermic peak at around 55 ºC, indicating that formation of the nanocapsules increased the heterogeneity of the polymeric crystals, producing structures that were less perfect and that had a lower fusion temperature (Campos *et al.* 2013b). For the nanocapsules containing ATC, the endothermic fusion peak of ATC was absent, indicating that the drug was not present in its crystalline form, but was dispersed in the interior and on the surface of the nanocapsules (Byrro *et al.* 2009). In the case of the physical mixture of PEG-PCL and ATC, endothermic peaks were present for both the copolymer and the drug. Even if ATC were present in the crystalline form, superposition of peaks would hinder detection of the ATC peak in the curves obtained for the PEG-PCL nanocapsules containing the drug. Previous work has reported similar findings for polymeric microparticles containing nonsteroidal anti-inflammatory compounds (Poletto *et al.* 2007).

4.4.6. Nanoparticle encapsulation efficiency and drug loading

Quantification of the amount of drug encapsulated was achieved indirectly, considering the difference between the free fraction and the amount of ATC contained in the formulation

(100%). The encapsulation efficiencies were 45.5% and 60.5%, and the drug loadings were 44.4% and 30.2% for the AG/CS nanospheres and the PEG-PCL nanocapsules, respectively. The differences between the values obtained for the two types of nanoparticle were due to their different structures. The AG/CS nanospheres had a matrix-type structure, while the PEG-PCL nanocapsules were vesicular and could therefore more readily retain the drug in the aqueous nucleus, hence increasing the encapsulation efficiency. While the amount of ATC encapsulated was satisfactory in both cases, the best results were obtained for the PEG-PCL nanocapsules. Similar results have been reported for the encapsulation of paclitaxel in polymeric micelles of PCL-PEG-PCL (Zhang *et al.* 2012).

4.4.7. Articaine permeation profiles

The profiles of permeation of drugs from nanostructured systems are important in terms of therapeutic efficiency. Measurements of these profiles can provide fundamental information concerning the behavior of nanoparticles, including drug-carrier interactions and the mechanism of the release process (Schaffazick *et al.* 2003, Mora-Huertas 2010, Das *et al.* 2011).

The time-dependent permeation of ATC was determined in the absence and presence of the nanoparticles, using the two-compartment system in which only the drug molecules could cross the cellulose membrane separating the two chambers. The association between ATC and the nanoparticles could then be established from the permeation rate. The values were expressed in terms of the percentage of ATC released. Figure 2 shows the release profile of ATC, free or associated with the nanoparticles, as a function of time, at ambient temperature.

Figure 2: Cumulative release of ATC, free or in suspensions of AG/CS nanospheres and PEG-PCL nanocapsules, at ambient temperature (n=3).
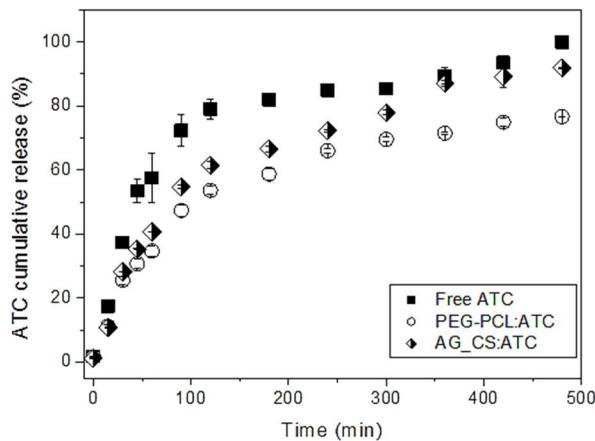
There was complete release (100%) of free ATC after 400 min, and the time required for 50% release ($t_{50\%}$) was 45 min. The $t_{50\%}$ values for the AG/CS nanospheres and the PEG-PCL nanocapsules loaded with ATC were 100 and 150 min, respectively, indicating that both formulations were able to alter the permeation profile of ATC.

The release of an active principle from a colloidal system is a complex process that is affected by a variety of factors including particle degradation, the crystallinity of the active agent, and the affinity between the agent and the colloidal matrix, amongst others (Kumari *et al.* 2010, Mishra *et al.* 2010). Here, the release of ATC was slower from the nanoparticles, compared to the free drug, with the slowest profile observed for the PEG-PCL nanocapsule formulation. The nanocapsules therefore provided both the best ATC encapsulation efficiency (60.5%) and the slowest release profile ($t_{50\%}$ = 150 min), while the corresponding values for the AG/CS nanospheres were 45.5% and 100 min, respectively. There was therefore a relationship between the release kinetics and the encapsulation efficiency, and the faster release profile obtained for the AG/CS nanospheres could be explained by the lower encapsulation efficiency (in this case, the ATC interaction was mainly due to surface electrostatic charges). The slower release profile shown by the PEG-PCL nanocapsules could be explained by greater interaction of ATC with the aqueous nucleus, which hindered release of the drug to the external medium.

Grillo et al. (Grillo *et al.* 2010) showed that the release profile of bupivacaine from AG/CS nanospheres was faster, compared to release from other types of polymeric nanoparticles, suggesting that the interaction between the active agent and the particles mainly occurred at the surface (Grillo *et al.* 2010).

4.4.8. Determination of the release mechanisms

The Baker-Lonsdale mathematical model was used to elucidate the main mechanisms involved in the release of ATC from the nanoparticle systems. This model has been used previously to linearize the results of release assays involving micro- and nanoparticles (Moreira *et al.* 2012).

The Baker-Lonsdale model was able to linearize the ATC release data. Linear regression resulted in correlation coefficient (*r*) values of 0.999 and 0.996, and release constant (*k*) values of 0.623×10^{-3} min^{-1} and 0.329×10^{-3} min^{-1}, for the AG/CS nanospheres and the PEG-PCL nanocapsules, respectively. The values of *k* indicated that diffusion was the main mechanism involved in release of the drug, as also found previously for polymeric nanoparticles containing bupivacaine (Grillo *et al.* 2010) and microparticles containing ketoprofen (Moreira *et al.* 2012).

4.4.9. Cellular viability assays

Cellular viability was evaluated using reduction of 3-(4,5-dimethylthiazol-2-yl)-2,5-diphenyltetrazolium bromide (MTT). Figure 3 shows the cellular viability data obtained using mouse 3T3 fibroblast cells incubated with free ATC and the nanoparticle formulations (with and without ATC). The tests were performed using 96-well plates, with 12 determinations for each sample.

Figure 3: Cellular viability determined using the MTT test after exposure of Balb-c 3T3 cells to free ATC and ATC incorporated in (a) AG/CS nanospheres and (b) PEG-PCL nanocapsules (n=12).
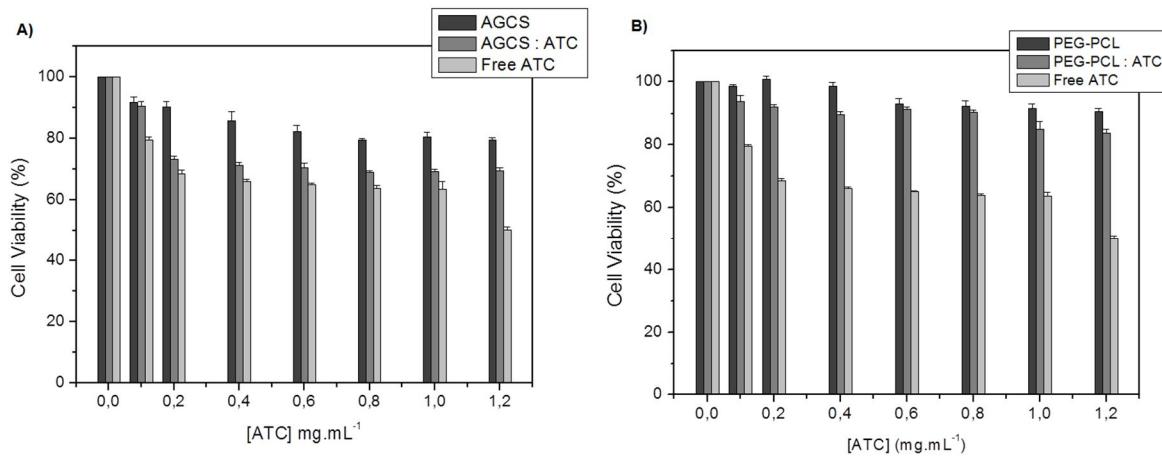
At the concentrations used, exposure of the cells to AG/CS nanospheres had a moderate effect on cellular viability, with values close to 80%. Decreases in viability of around 30% and 50% were obtained for the nanospheres loaded with ATC, and the free drug, respectively.

Nafee et al. (Nafee *et al.* 2009) found that exposure to certain ionizable groups present in polymers and pharmaceuticals can lead to loss of integrity of the cell membrane (Nafee *et al.* 2009). As the encapsulation efficiency of ATC in the AG/CS nanospheres was low (around 45%), there was a larger quantity of free drug available to interact with components of the membrane, resulting in reduced cellular viability (as also found for the free drug).

At the concentrations used, exposure of the cells to the PEG-PCL nanocapsules had no serious effect on cellular viability, with values close to 95%. However, exposure to the PEG-PCL nanocapsules loaded with ATC resulted in a reduction in cellular viability of around 20%, while a reduction of 50% was obtained for the free drug. An important point related to the in vitro cytotoxicity model is that the cytotoxic effects of ATC are dose-dependent, and that the protective effects of using ATC associated with the PEG-PCL nanocapsules can be explained by the smaller quantity of free ATC available due to the modified release provided by the nanocapsules. The higher level of toxicity observed when ATC was associated with the AG/CS nanospheres can be explained by the fact that the encapsulation efficiency was lower for this formulation, resulting in a higher concentration of free ATC. This was combined with the toxic

effect of the AG/CS nanospheres themselves, which was probably due to exposure of the cell membrane to the ionizable groups of alginate and chitosan (Nafee *et al.* 2009).

The results of the cytotoxicity assays showed that the formulation of AG/CS nanospheres containing ATC presented toxicity comparable to that of the free drug. This reflected the relatively low encapsulation efficiency, compared to the encapsulation efficiency achieved for the PEG-PCL formulation.

4.4.10. Stability of the formulations during storage

The stabilities of the two systems containing ATC were evaluated over a period of 120 days storage in amber flasks at ambient temperature. The parameters considered were the average particle diameter, polydispersion, pH, zeta potential, and encapsulation efficiency (Figure 4).

Figure 4: Values obtained for (a) average diameter, (b) polydispersion, (c) zeta potential, and (d) pH of the suspensions of AG/CS nanospheres and PEG-PCL nanocapsules containing ATC during storage for 120 days at ambient temperature (n=3).
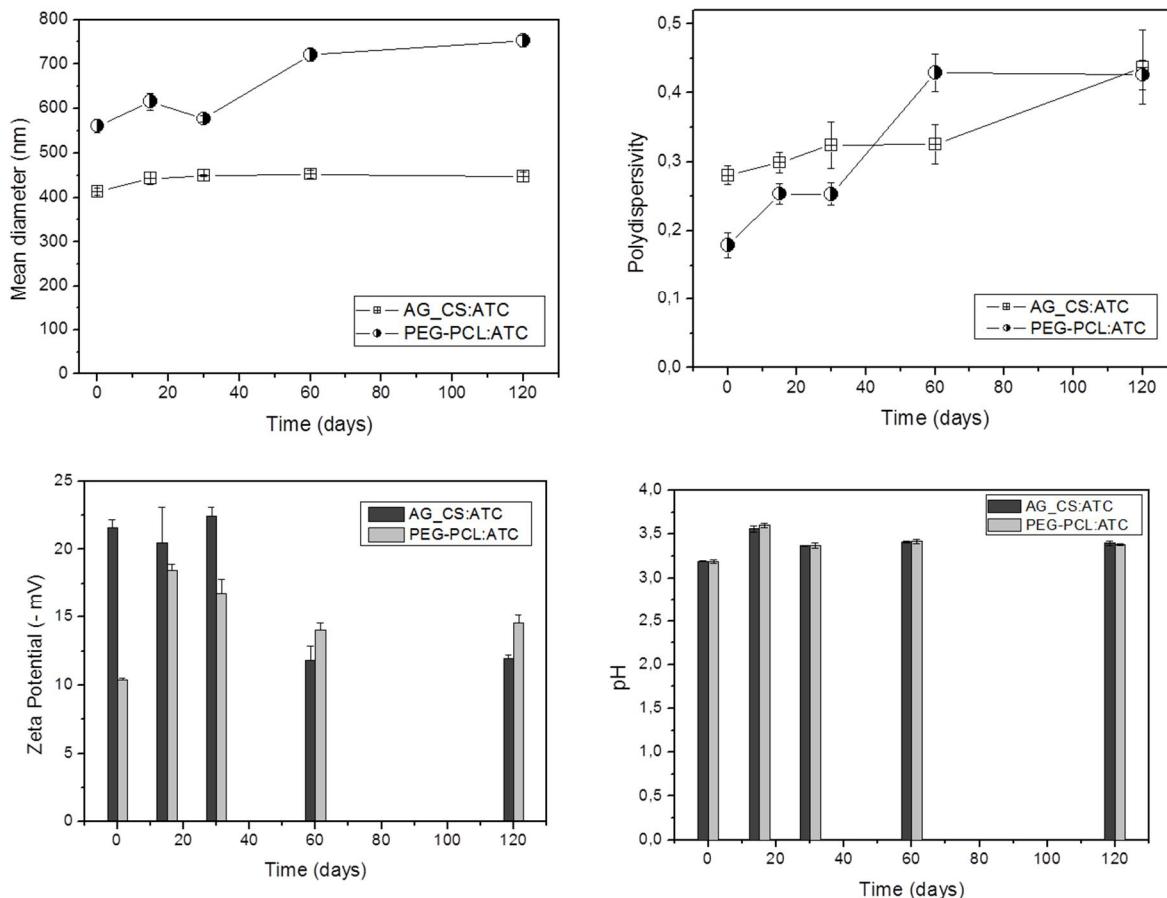
Both formulations showed changes in terms of average particle diameter, with the greatest increase after 30 days observed for the PEG-PCL nanocapsules. This increase in nanoparticle size, which could have been related to the formation of aggregates in the suspension, has also been observed in other studies (Grillo *et al.* 2010, Silva *et al.* 2011b, Zhang *et al.* 2012).

The formulations also showed changes in the polydispersion value as a function of time. Changes in polydispersion are indicative of the formation of new populations of particles with different diameters, resulting from aggregation or breakage/degradation of the particles. Both formulations studied showed initial polydispersion values above 0.2. Since these formulations were produced using polymers of natural origin (alginate and chitosan) or block copolymers, the values were expected to be slightly higher than those measured for synthetic polymers

(Schaffazick *et al.* 2003, Lertsutthiwong *et al.* 2009, Silva *et al.* 2011b, Zhang *et al.* 2012). The observed changes in polydispersion were indicative of a lack of homogeneity in the size distribution, due to particle degradation and/or aggregation.

The value of the zeta potential also provides an indication of the stability of nanoparticles in suspension. For both formulations, the zeta potential was negative and there were no major changes during the first 30 days of storage. Between 60 and 120 days, there were decreases in the zeta potential values that could be attributed to rearrangements of the polymeric chains, leading to less exposure of ionizable groups on the surfaces of the particles (Mohanraj and Chen 2006).

The analysis of pH is important in order to determine the stability of suspensions of nanocapsules, because pH changes can be indicative of polymer degradation due to hydrolysis, resulting in the release of some of the components (Schaffazick *et al.* 2003). In the present case, the pH of both formulations remained stable throughout the evaluation period, and pH values were similar to those obtained previously for polymeric nanoparticle formulations (Grillo *et al.* 2010, Silva *et al.* 2011b).

5. Conclusions

The present work provides important information concerning the preparation and characterization of nanoparticles used as carrier systems for the model drug articaine. The drug encapsulation efficiencies were satisfactory, with values of around 60% for the PEG-PCL nanocapsules and 45% for the AG/CS nanospheres. Suspensions of both formulations loaded with ATC were moderately stable over a period of 120 days. Morphological analysis using transmission electron microscopy revealed that both types of nanoparticle were spherical, with diameters in the range 100-300 nm. Use of ATR-FTIR and exploratory differential calorimetry demonstrated that there was interaction between the drug and the nanocarriers, because the infrared absorption bands of the active principle were altered and there was a reduction of the fusion temperature, indicating changes in the crystalline network. Use of the MTT reduction test showed that encapsulation of ATC reduced the cytotoxicity of the drug. The cellular viability values obtained for the PEG-PCL nanocapsule formulation were higher than obtained for ATC alone or the AG/CS nanosphere formulation. This was due to more efficient encapsulation of ATC in the PEG-PCL nanocapsules, resulting in less free ATC. The permeation profile of ATC

was modified in the presence of the nanoparticles, with slower and more sustained release compared to the permeation kinetics of free ATC. The slowest permeation profile was obtained for the PEG-PCL nanocapsule formulation. Use of a mathematical model to calculate the release constants (k) revealed that release of ATC from the nanoparticles was due to diffusion. Overall, the PEG-PCL nanocapsule formulation seems to be more promising than the AG/CS nanosphere formulation because it provided higher encapsulation efficiency, a slower permeation profile, and a greater reduction in toxicity of the model drug. This system could therefore be potentially used as a carrier for hydrophilic compounds such as articaine.

Acknowledgments

6. Supplementary information

ATR-FTIR spectra of AG/CS nanospheres

The infrared spectroscopy technique was used do investigate the interaction between drug (ATC) and nanospheres. Figure S1 shows the spectra of drug, raw materials, physical mixtures and nanospheres.

Figure S1: ATR infrared spectra for (a) ATC, (b) alginate, (c) chitosan, (d) physical mixture (alginate + chitosan), (e) physical mixture (alginate + chitosan + ATC), (f) AG/CS nanospheres, and (g) AG/CS nanospheres with ATC.
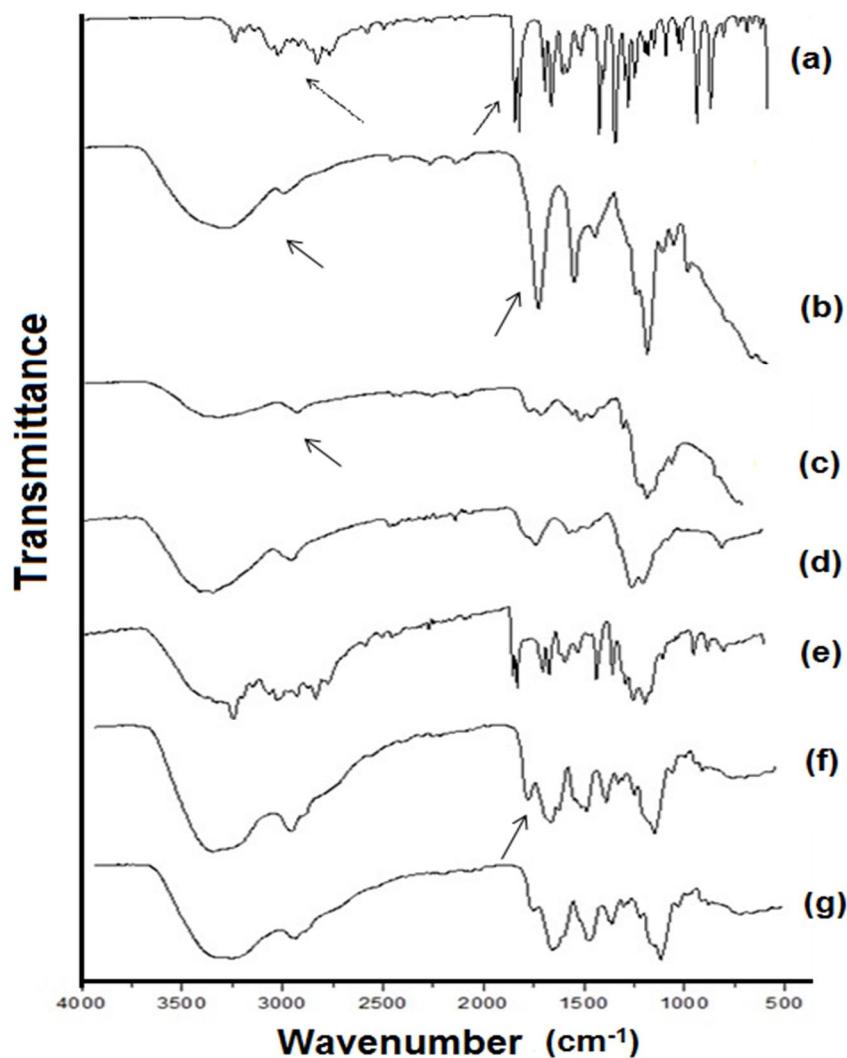
ATR-FTIR spectra of PEG-PCL nanocapsules

PEG-PCL nanocapsules loading ATC were also investigated by infrared spectroscopy. Figure S2 shows the spectra of drug, raw materials, physical mixtures and nanocapsules.

Figure S2: ATR infrared spectra for (a) ATC, (b) PEG-PCL copolymer, (c) physical mixture (ATC + copolymer), (d) PEG-PCL nanocapsules, and (e) PEG-PCL nanocapsules with ATC.
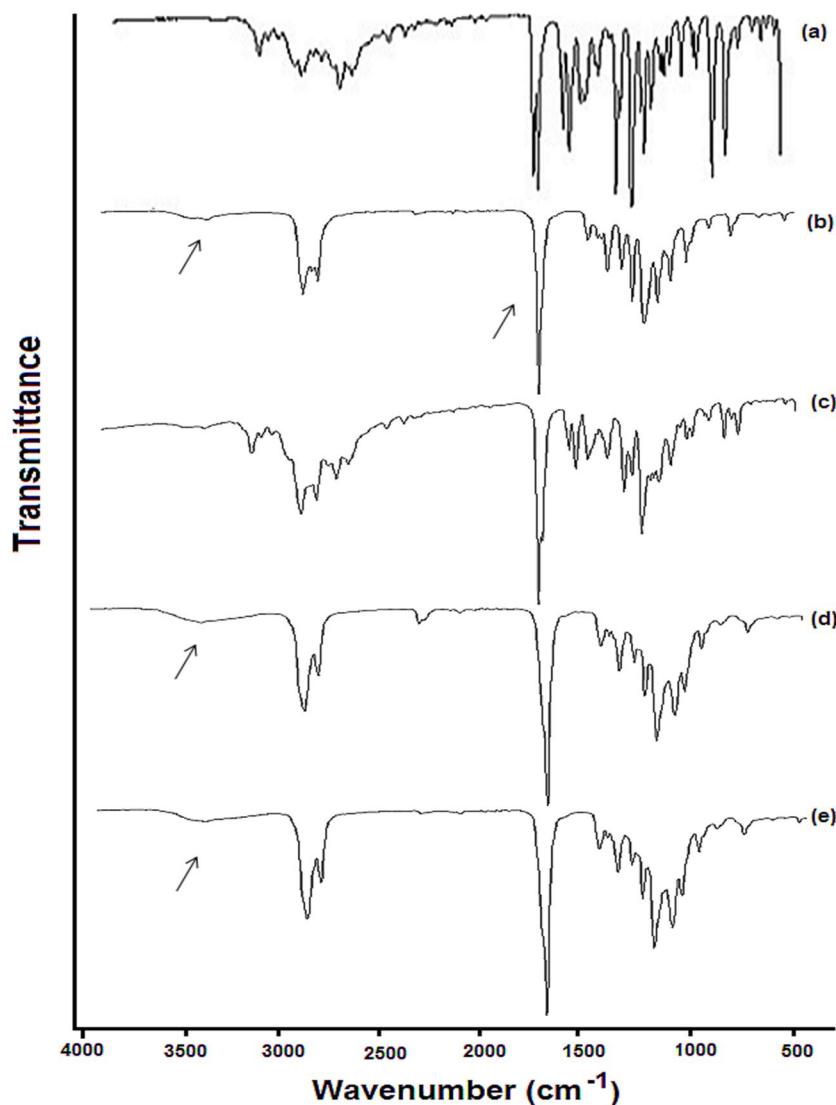
DSC curves of AG/CS nanospheres

The DSC analyses were used to provide information concerning the stability of the formulations and the forms in which the components were present. Figure S3 shows the thermal profiles obtained for the drug, raw materials, physical mixture and nanospheres.

Figure S3: DSC curves for (a) ATC, (b) alginate, (c) chitosan, (d) physical mixture (alginate + chitosan + ATC), (e) AG/CS nanospheres, and (f) AG/CS nanospheres with ATC.
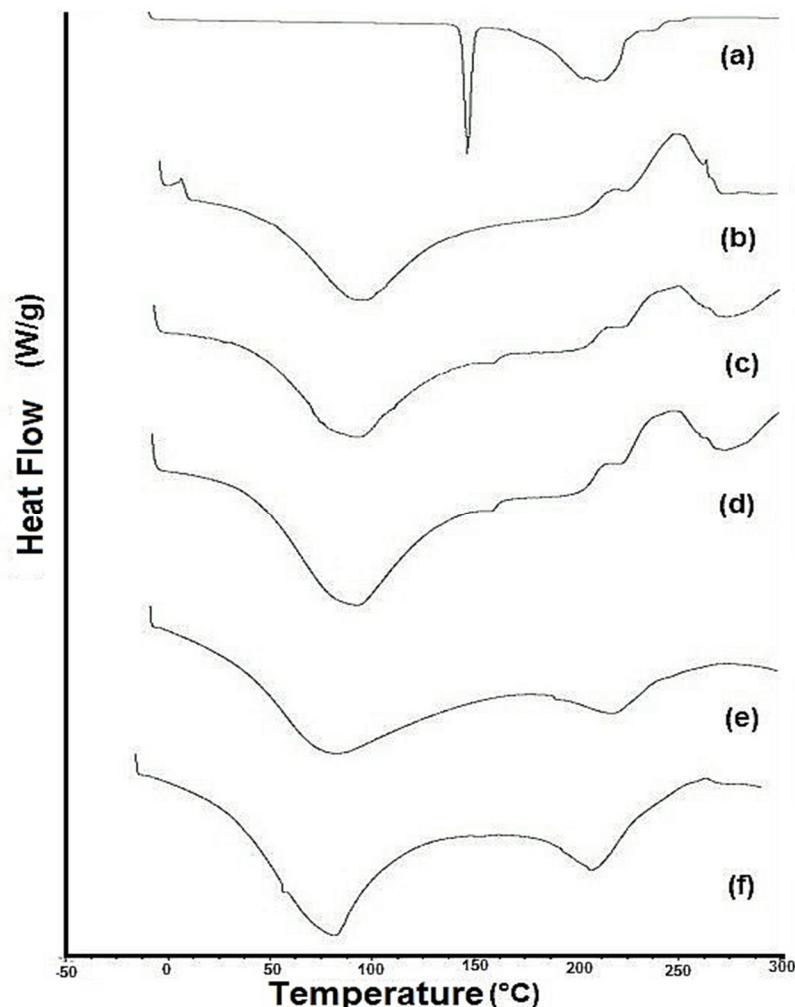
DSC curves of PEG-PCL nanocapsules

The thermal profiles were also obtained for the PEG-PCL nanocapsules loading ATC. Figure S4 shows the termal profile for the drug, raw materials, physical mixtures and nanocapsules.

Figure S4: DSC curves for (a) ATC, (b) PEG-PCL copolymer, (c) physical mixture (ATC + copolymer), (d) PEG-PCL nanocapsules, and (e) PEG-PCL nanocapsules with ATC.
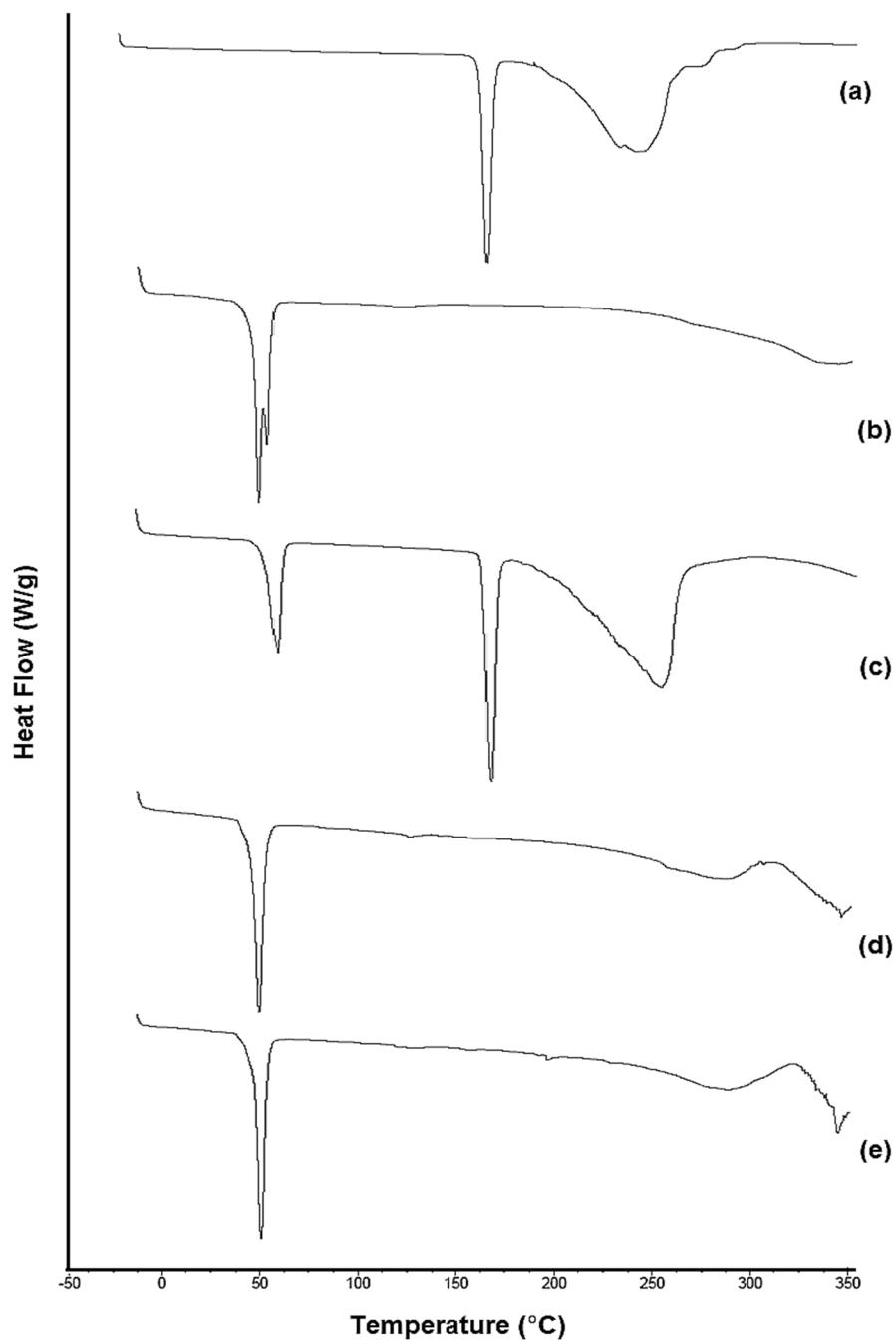
Capítulo 5 – Nanocápsulas de poli (ε-caprolactona) e nanopartículas lipídicas sólidas contendo articaína na forma neutra em formulação de hidrogel

5.1. Abstract

The objective of this work was to develop poly(ε-caprolactone) nanocapsules (PCL-NC) and solid lipid nanoparticles (SLN) as carrier systems for articaine (ATC), comparing their in vitro performance, in order to reduce the toxicity of the drug and improve its chemical stability in preformulated semi-solid preparations. The nanoparticles containing ATC were manufactured and physicochemical characterization was performed using measurements of size, polydispersity index, and pH, together with differential scanning calorimetry (DSC) and transmission electron microscopy (TEM) analyses. The stability of the nanoparticles was investigated as a function of time. Cytotoxicity was evaluated using the MTT reduction test, and the *in vitro* release kinetics was determined in two-compartment systems with donor and acceptor compartments. The nanoparticle suspensions were incorporated in gels that were characterized in terms of sensory parameters, pH, particle size and polydispersion, rheological aspects, and in vitro permeation. Colloidal stability was satisfactory, since the formulations did not present any major alterations during a storage period of 120 days. High ATC encapsulation efficiencies were achieved (78% for PCL-NC and 65% for SLN). The release profile of ATC loaded into the PCL-NC was slower, compared to the free drug and ATC incorporated in the SLN. Cytotoxicity experiments showed that both nanosystems were able to reduce the toxicity of ATC. The semi-solid formulations showed good consistency, homogeneity, and stability. In rheological tests, the gels presented pseudoplastic behavior with thixotropy, which can improve drug efficacy in clinical applications. The gel based on PCL-NC showed faster onset of permeation, which then continued for up to 8 h. The results presented here describe the initial stages of the development of new nanotechnological local anesthetic formulations possessing advantageous properties including physical and chemical stability, safety (low toxicity), and enhanced therapeutic properties. It could be concluded from the *in vitro* release experiments that the gel based on PCL-NC containing ATC helped to achieve the dual objectives of faster onset and prolonged permeation. This study opens up prospects for the future use of nanoparticles as carriers for the local anesthetic articaine.

Keywords: PCL nanocapsules, solid lipid nanoparticles, drug delivery, semi-solid formulation, hydrogel, topical anesthetics, articaine.

5.2. Introduction

The development of nanocarriers to overcome the common problem of poor drug solubility in water is currently one of the main themes in pharmaceutical research. Micro- and nanoencapsulation techniques are among the approaches that have attracted the most attention (Preetz *et al.* 2008). Polymeric nanocapsules (NC) used as carriers of drugs or other active molecules are composed of a polymeric shell and an oily core, where the active compounds are dispersed in the core or trapped in the polymeric layer (Schaffazick *et al.* 2003, Preetz *et al.* 2008, Mishra *et al.* 2010, Souto *et al.* 2012). Solid lipid nanoparticles (SLN) are structures composed of biodegradable solid lipids, stabilized using emulsifiers to disperse the active compounds in the lipid matrix(Helgason *et al.* 2009, Vitorino *et al.* 2011, Mehnert and Mäder 2012). The properties of biodegradability and biocompatibility are very important for polymers and lipids used in medical practice. Suitable compounds include poly(ε-caprolactone) (PCL), a polyester used for the preparation of NC, and glyceryl tripalmitate, used to produce SLN capable of being loaded with drugs (Lu and Chen 2004, Souto *et al.* 2012).

Articaine (ATC) is an amino-amide local anesthetic (LA) containing an additional ester group in its structure that influences its biotransformation in the plasma and liver, since it is relatively rapidly hydrolyzed. The presence in the molecule of a thiophene ring instead of a benzene ring increases anesthetic potency and enhances diffusion within the tissues. For some time, ATC has been one of the anesthetic drugs of choice in dentistry (Malamed 2004, Paxton and Thome 2010).

The fast action of ATC is due to the physicochemical properties of the molecule, which shows high solubility in lipids due to the presence of the thiophene ring. The main complication associated with the use of ATC is prolonged or permanent paresthesia, characterized by a tingling sensation. Reported incidents of paresthesia appear to have been associated with inferior alveolar and lingual nerve blockade (Malamed 2004, Pogrel 2007, Diaz 2009, Paxton and Thome 2010).

A technique that has been shown to be able to promote the desired effects of drugs is their modified release using carrier systems. The development of such systems for ATC is of considerable interest because the drug displays superior performance, compared to other anesthetics of the same class, and has been increasingly used in dental and topical procedures (Paxton and Thome 2010).

There has been substantial growth in the application of nanotechnology in topical products. Nanoencapsulated drugs applied topically can persist at the site of application for prolonged periods, while at the same time showing greater chemical stability and reduced toxicity, resulting in improved therapeutic efficacy (Vila *et al.* 2002, Alvarez-Román *et al.* 2004, Cevc and Vierl 2010).

The preformulation phase of drug development is vital in order to evaluate the compatibility of the compound with pharmaceutical adjuvants, and is used to develop new products and optimize existing formulations (Mura *et al.* 1998, Costa 2005). A wide range of raw materials are available for the preparation of gels, and the selection of a suitable substance for use in the development of a new formulation is based on considerations of the stability, release, and effectiveness of the active principle that it is intended to incorporate. It is therefore important to evaluate the physico-chemical properties of these formulations, and measure the rates of drug release, as necessary prerequisites for the purposes of quality control (de Santis 2008).

In this work, PCL-NC and SLN loaded with ATC (in its uncharged form) were manufactured after screening the preparation conditions and optimizing the composition of the formulation. The objectives were to characterize the suspensions, assess colloidal stability, compare the in vitro release profiles and cytotoxicities of free and encapsulated ATC, and to develop semi-solid formulations with a view to their use in experiments *in vivo*.

5.3. Experimental section

5.3.1. Materials

Articaine hydrochloride was kindly donated by DFL Indústria (Rio de Janeiro, Brazil). Poly(ε-caprolactone) (PCL, 70-90 kDa), triglycerides of capric and caprylic acids, glyceryl tripalmitate, polyvinyl alcohol (PVA, 30-70 kDa), propylene glycol, and methylparaben were purchased from Sigma-Aldrich Chem. Co. The gelification agent, Aristoflex® AVC, was acquired from Clariant. Acetone and chloroform (analytical grade) were obtained from LabSynth Brasil. Acetonitrile (HPLC grade) was obtained from Tedia Chemicals. DMEM (Dulbecco's Modified Eagle Medium), colchicine, fetal bovine serum, penicillin, and streptomycin sulfate were purchased from Cultilab Brasil. The water used was purified and filtered through a 0.22 µm membrane. All other reagents employed were spectroscopic or analytical grade.

5.3.2. Production of the free base form of articaine

The free base form of ATC was obtained as the hydrochloride salt. One gram of ATC hydrochloride was dissolved in deionized water and the pH value was adjusted to 8.5 using 5 mol/L NaOH. The aqueous phase was extracted three times with ethyl acetate. The organic phase was dried with sodium sulfate, filtered, and evaporated to yield an oil that was crystallized by storage at -18 °C. The ATC crystals were examined by FTIR, DSC, and HPLC, and compared with the hydrochloride salt (Larsen *et al.* 2002).

5.3.3. Preparation of PCL nanocapsules

The preparation of the PCL nanocapsules was performed according to the oil in water emulsion/solvent evaporation method, with some modifications (Zhou *et al.* 2010). ATC (200 mg) and capric/caprylic triglycerides (200 mg) were dissolved in acetone and mixed with 20 mL of chloroform containing the polymer (400 mg), using ultrasonication (1 min, 100 W). Aqueous phase (PVA solution 3 mg/mL, 50 mL) was then added and the mixture was ultrasonicated (8 min, 100 W). The resulting emulsion was placed in a rotary evaporator to remove the solvents and concentrate the suspension to 10 mL. The final ATC concentration was 20 mg/mL (Campos *et al.* 2013a)

5.3.4. Preparation of solid lipid nanoparticles

Preparation of the SLN employed the emulsification/solvent evaporation method (Vitorino *et al.* 2011). Glyceryl tripalmitate (250 mg) and ATC were dissolved in 5 mL of chloroform and mixed with 30 mL of a solution of PVA (375 mg). This mixture was sonicated (5 min, 40 W) to produce a suspension, which was then submitted to Ultra Turrax homogenization for 7 min at 18000 rpm. After this, the organic solvent was eliminated by evaporation under low pressure and the emulsion was concentrated to a final volume of 10 mL, giving a final ATC concentration of 20 mg/mL.

5.3.5. Photon correlation spectroscopy (PCS)

The average diameter and polydispersity index (PI) of the nanoparticles were determined using PCS. The PI was obtained from the size distribution of the nanoparticles. The measurements were performed at 25 °C using a ZetaSizer Nano ZS 90 analyzer (Malvern Instruments, UK), with an angle of 90°, after dilution of the samples in purified water. The results were expressed as the average of three analyses (mean ± SD) (Vitorino *et al.* 2011, de Melo *et al.* 2012, Campos *et al.* 2013a). The average diameter and polydispersion of the nanoparticles contained in the gels were also determined using the same PCS technique.

5.3.6. Transmision electron microcospy (TEM)

A JEOL 1200 EXII transmission electron microscope operated at 80 kV was used to analyze the morphology of the PCL-NC and SLN (Silva *et al.* 2011b). Prior to analysis, the samples were diluted, contrasted using uranyl acetate (2%), deposited onto copper grids coated with a carbon film, and dried at ambient temperature.

5.3.7. Encapsulation efficiency

The amount of ATC encapsulated was determined by a method combining ultrafiltration and centrifugation (de Melo *et al.* 2012, Campos *et al.* 2013a, de Melo *et al.* 2013). The suspensions were centrifuged in ultrafiltration devices (Amicon® 10 kDa molecular exclusion pore size, Millipore). ATC was then quantified in the ultrafiltrate using a Varian ProStar HPLC instrument (Agilent Technologies) fitted with a PS210 isocratic pump and a UV-Vis detector. A Phenomenex Gemini C_{18} column (NX 5μ C_{18} 110 Å, 150 x 4.6 mm) was maintained at 35 °C. The mobile phase was composed of 0.02 mol/L sodium dihydrogen phosphate (adjusted to pH 3.0 with phosphoric acid) and acetonitrile, at a ratio of 88:12 (v/v), with a flow rate of 2 mL/min. The mobile phase was filtered and degassed prior to use. The sample injection volume was 100 μL and the detector wavelength was 273 nm (de Melo *et al.* 2013).

The ATC was determined after dilution of the suspensions with acetonitrile, which caused solubilization of the polymer and released the drug into solution. Quantification of ATC employed a validated analytical curve, as described previously (de Melo *et al.* 2013).

The ATC encapsulation efficiency (*EE%*) was calculated from the difference between the total and free ATC concentrations, measured in the suspension and ultrafiltrate, respectively, according to Equation 1:

$$EE\% = \frac{W_{free}}{W_{total}} \times 100 \quad , \qquad\qquad (1)$$

where W_{free} is the mass of free ATC in solution and W_{total} is the total mass of ATC present in the suspension.

5.3.8. Differential scanning calorimetry

Portions (2 mg) of each sample (ATC, PCL polymer, glyceryl tripalmitate, empty NC, NC with ATC, empty SLN, SLN with ATC, and physical mixtures) were analyzed using a TA Instruments Q20 differential scanning calorimeter equipped with a cooler system and calibrated using indium. The samples were transferred to sealed aluminum pans and heated from -10 to 300 °C, at a rate of 10 °C/min, under a flow of nitrogen and using an empty pan as the reference (Sarmento *et al.* 2007, Silva *et al.* 2011b).

5.3.9. Stability of the suspensions

The chemical stability of the PCL-NC and SLN suspensions containing ATC was evaluated by measurements of the pH of the suspensions as a function of time, using a pH meter (Tecnal, Piracicaba, Brazil). The colloidal stability was followed over time using measurements of average diameter and polydispersity index, as described above. The stability trials were continued for a period of 120 days, during which the formulations were stored at ambient temperature (de Melo *et al.* 2012, de Melo *et al.* 2013).

5.3.10. Suspension cytotoxicity assays

Cell viability experiments employing the MTT (a yellow tetrazole) reduction test were carried out with Balb-c 3T3 cells maintained in continuous culture in DMEM. Around 2 x 10^4

viable cells were inoculated into 96-well plates and incubated for 48 h (Moraes *et al.* 2007e, Campos *et al.* 2013b). The cells were exposed for 24 h to free ATC, PCL-NC loaded with ATC, or SLN loaded with ATC, at concentrations in the range 0.1 to 1.2 mg/mL. The quantities of viable cells were determined after incubation in the presence of MTT for 2 h at 37 $^{\circ}$C, by measuring the quantity of MTT converted to purple formazan, using a plate reader at 630 nm. The absorbance values were converted into percentages of viable cells (de Lima *et al.* 2012).

5.3.11. Preparation of semi-solid formulations containing free and encapsulated articaine

The gels without the nanocarriers were prepared according to the method described by Batheja et al. (2011). The gelification agent (Aristoflex® AVC, 2%) was added to an aqueous solution containing methylparaben (0.1%), propylene glycol (1%), and ATC, and the mixture was kept under constant agitation in a porcelain mortar until a gel was formed. The gels were then left to stabilize for 24 h. Gels containing the nanocarriers were prepared by substituting the water with the suspensions of PCL-NC and SLN containing ATC. The final concentration of ATC in the gels was 20 mg/g of hydrophilic gel. The gels were stored in flasks at ambient temperature (Batheja *et al.* 2011). Aristoflex® AVC was chosen as the gelification agent due to its ease of preparation, without requiring any previous heating or neutralization steps.

5.3.12. *In vitro* permeation studies

The *in vitro* permeation studies for the PCL-NC and SLN suspensions were performed using a two-compartment model (donor and acceptor) separated by a cellulose membrane with a molecular exclusion pore size of 1000 Da (under magnetic agitation and *sink* conditions) (Paavola *et al.* 1995). The samples tested were: solution of free ATC (2%); PCL-NC:ATC suspension (2%) and SLN:ATC suspension (2%). The *in vitro* permeation studies for the hydrogels were performed using vertical Franz diffusion cells with a diffusional area of 1.76 cm^2 and an acceptor compartment volume of 5.0 mL (Venter *et al.* 2001, Stoco 2011). The diffusion cells were assembled with cellulose acetate membranes (0.45 µm pore size) impregnated with isopropyl myristate, in order to simulate the hydrophobicity of stratum corneum maintained in contact with the acceptor compartment containing 1 mM phosphate buffer at pH 7.4 and 37 °C,

under magnetic agitation. The samples tested were: gel containing free ATC (2%); gel containing PCL-NC:ATC (2%); and gel containing SLN:ATC (2%). For both experiments the samples were placed in the compartment above the membrane and 1 mL aliquots were collected from the acceptor compartment at hourly intervals, over a total period of 8 h (Stoco 2011), for analysis using the HPLC procedure described above. The data were expressed as the cumulative amounts of permeated ATC, as a function of time, and were analyzed using Equation 3:

$$J = P.Cd \tag{3}$$

where J is the flux of ATC through the membrane, P is the permeability coefficient, and Cd is the concentration of the drug used in the donor compartment (Nicoli *et al.* 2005, de Araujo *et al.* 2010).

The Higuchi theoretical model was used to analyze the behavior of ATC permeation from the nanoparticles. It is used to linearize the results of release assays involving micro- and nanoparticles and can be expressed by:

$$f_t = K_H t^{1/2}$$

where f_t correspond to the amount of drug released at time t and and K_H is the Higuchi release constant (Costa 2002).

5.3.13. Rheological measurements

Rheological measurements were performed using a Haake RheoStress 1 rheometer (Thermo-Haake, Karlsruhe, Germany) with plate-plate geometry (plate diameter 20 mm). The hydrogel formulations were submitted to continuous variation of shear rate from 0 to 300 s^{-1}, and the resulting shear stress was measured. The tests were performed in triplicate (n=3) at a constant temperature (25 ± 1 ^oC) maintained by a thermostatically-controlled water bath. The rheological behavior of the hydrogel formulations was evaluated from curves obtained by plotting the shear stress (Pa) as a function of shear rate (s^{-1}).

5.3.14. Statistical analysis

The data were expressed as means ± standard deviations (n=6). The different gel formulations were compared in terms of the permeation parameters (the flux and the lag time for

initial permeation of ATC). The results of cell viability and permeation studies were analyzed by one-way ANOVA with the Tukey-Kramer post-hoc test, using a significance level of $p < 0.05$ (Stoco 2011).

5.4. Results and Discussion

5.4.1. Characterization of the PCL-NC and SLN suspension

The two nanocarrier systems were prepared for use with the model drug ATC in its neutral (uncharged) form. After preparation, the systems were characterized in terms of average diameter, polydispersion, pH, and morphology. In a previous study, characterization of the PCL-NC formulation revealed an encapsulation efficiency of 70% (Campos *et al.* 2013a). The initial characteristics of the suspensions are described in Table 1.

Table 1: Values of mean diameter (nm), polydispersity, and pH for suspensions of PCL-NC and SLN loaded with ATC.

Suspension	Mean diameter ± SD; (polydispersity index)	pH ± SD
PCL-NC:ATC	445.5 ± 2.1 (0.068 ± 0.005)	8.1 ± 1.2
SLN:ATC	249.9 ± 2.2 (0.113 ± 0.008)	7.9 ± 0.9

The results showed that the average diameters and polydispersities of the PCL-NC and SLN containing ATC were compatible with those commonly found for colloidal suspensions. The slightly elevated pH values were due to the basicity of articaine. The polydispersity index values were below 0.2 for both suspensions, indicative of a homogeneous particle diameter distribution (Schaffazick *et al.* 2003, Vitorino *et al.* 2011, Campos *et al.* 2013b). The average particle diameter was greater for the PCL-NC than for the SLN, which could be explained by the vesicular structure of the NC and the large amount of polymer used in the formulation, compared to the amount of lipid employed in the SLN. Preliminary work has shown that the average

particle diameter increases when greater amounts of polymer are used, due to the increased viscosity of the organic phase (Campos *et al.* 2013a).

Encapsulation efficiencies of 78.1% and 65.7% were obtained for the PCL-NC and SLN, respectively. This difference could be explained by a greater affinity of ATC for the oily nucleus of the PCL-NC than for the lipid used to produce the SLN, as well as by the structural characteristics of the nanoparticles. The PCL-NC are vesicular, while the SLN have a matrix-like structure, and studies have shown that vesicular nanoparticles are able to encapsulate hydrophobic drugs more efficiently than matrix-based nanoparticles (Mora-Huertas 2010).

Transmission electron microscopy is a powerful and relatively non-invasive technique that can be used to investigate the morphology and size of nanoparticles (Vitorino *et al.* 2011). TEM micrographs obtained for the PCL-NC and SLN systems containing ATC are shown in Figure 1, together with the size distributions determined by the PCS technique. The nanoparticles were spherical, with diameters in the range 200-300 nm (Figures 1(a) and 1(c)). These sizes were consistent with the polydispersity indices and the values obtained with the PCS technique (Figures 1(b) and 1(d)). No ATC crystals were observed in the micrographs.

_____

Figure 1: Transmission electron microscope images of (a) PCL-NC:ATC and (c) SLN:ATC, at magnifications of x15,000 and x60,000, respectively. The bars indicate the scales of the images. Size distributions obtained for (b) PCL-NC:ATC and (d) SLN:ATC using the PCS technique.
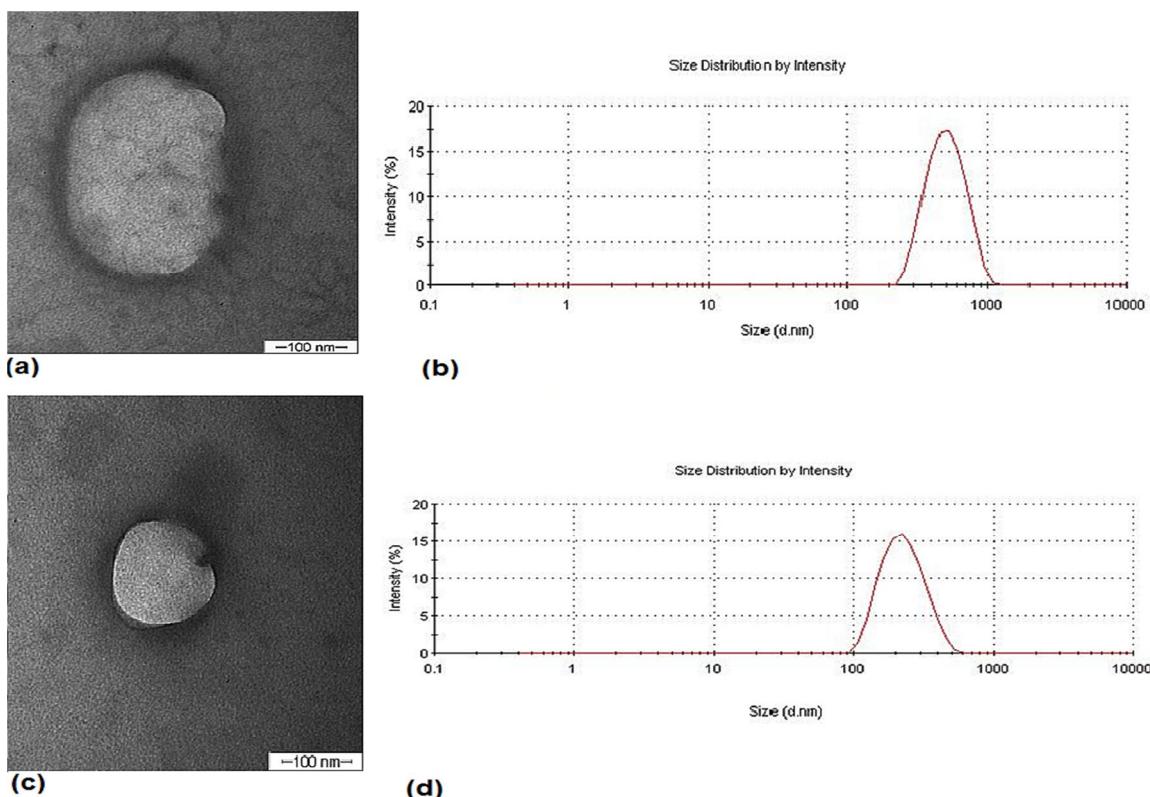
5.4.2. Stability of the suspension

The stability of the formulations was determined from measurements of particle diameter, polydispersity index, and pH immediately after preparation and during 120 days of storage at room temperature. Measurements of mean diameter and polydispersion provide an indication of the stability of a colloidal suspension. The size distribution of the particles is given by the polydispersity index, with values below 0.2 usually being indicative of stable suspensions (Schaffazick *et al.* 2003, Mora-Huertas 2010).

Figure 2: Values obtained for (a) average diameter, (b) polydispersion, and (c) pH of the PCL-NC and SLN suspensions containing ATC during storage for 120 days at ambient temperature (n=3).
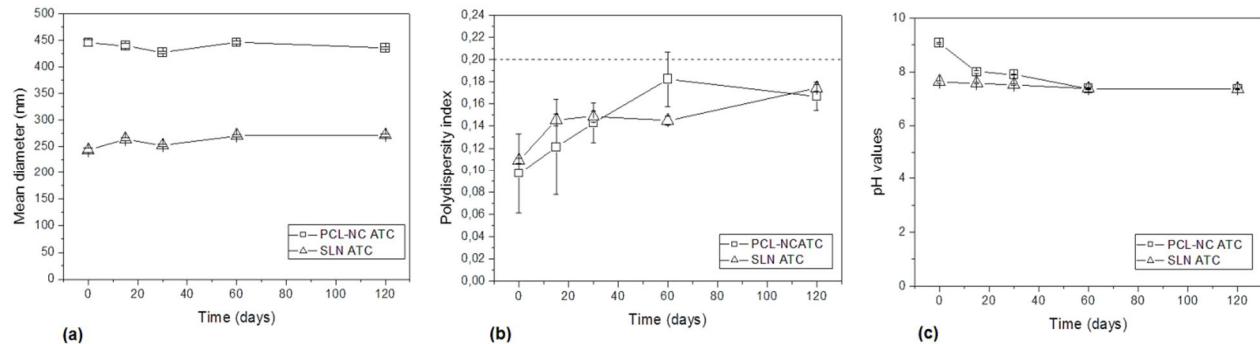
It can be seen from Figure 2(a) that the diameters of particles in the two suspensions analyzed remained almost constant throughout the period of 120 days, indicating that stability was maintained and that there was no formation of aggregates. Similar results have been reported previously for the size stability of nanoparticles (Das *et al.* 2011, de Melo *et al.* 2011, Moraes *et al.* 2011). Over time, there were small changes in polydispersion (Figure 2(b)), although neither formulation showed PI values greater than 0.2 during the trial period.

The pH values of the two formulations remained practically constant over 120 days (Figure 2(c)), in agreement with earlier work (Das *et al.* 2011, de Melo *et al.* 2011). Due to the buffering effect of the drug, the pH remained close to the pKa of ATC (7.8); hydrolysis of the polymer or lipid resulted in a shift in equilibrium from the neutral to the ionized form, which maintained a constant pH.

5.4.3. DSC Analysis

The nanoparticles and materials used in the preparation were investigated in terms of their glass transition and melting temperatures. Figure S1 shows the DSC curves obtained for ATC, the PCL polymer, the physical mixture (ATC + PCL), and the PCL-NC with and without ATC. Figure S2 shows the DSC curves obtained for ATC, glyceryl tripalmitate (TP), the physical mixture (ATC + TP), and the SLN with and without ATC.

Articaine showed an endothermic peak at 67.3 °C that corresponded to the melting point of the drug. For the PCL polymer, there was a thermal transition peak at 58.6 °C due to melting of the crystalline phase, consistent with previous work (Khatiwala *et al.* 2008). The PCL-NC showed an endothermic peak at around 55 °C, indicating that the PCL-NC manufacturing process increased the heterogeneity of the crystal polymer and produced less perfect structures with lower melting temperatures(Byrro *et al.* 2009). In the case of the PCL-NC containing ATC, there was a displacement of the endothermic peak from 55 to 49 °C. This decrease in melting temperature was indicative of an interaction between the drug and the carrier system that altered the crystal lattice. The endothermic melting point peak of ATC was not observed in the PCL-NC curve, suggesting that the drug was dispersed inside the NC or on their surfaces(Byrro *et al.* 2009). To investigate this hypothesis, the thermal behavior of a physical mixture of PCL and ATC was also evaluated. The curve for the physical mixture showed overlapping endothermic peaks for the polymer and the drug. Thus, even if the drug was in crystalline form, peak overlap could have prevented detection of the ATC peak in the curves for the PCL-NC containing ATC.

Glyceryl tripalmitate showed an endothermic peak at 64.0 ºC due to fusion of the lipid, involving the β form, in agreement with the literature (Helgason *et al.* 2009). Two endothermic peaks were observed for the SLN, at 45.7 and 61.9 ºC, due to the presence of the PVA surfactant. The presence of a surfactant alters the lipid packing arrangement, with the formation of new polymorphic forms. It has been suggested that the action of PVA involves the immobilization of lipid molecules in the interfacial region, preventing reestablishment of the β structural form (Vitorino *et al.* 2011). The peak at around 45 ºC could be attributed to the presence of coalescent lipid particles that crystallized by heterogeneous nucleation (α form), while the peak at around 61 ºC corresponded to the fusion temperature of tripalmitin (β form). Similar results have been obtained previously for SLN composed of glyceryl tripalmitate (Helgason *et al.* 2009, Vitorino *et al.* 2011). In the case of the SLN containing ATC, an endothermic peak occurred at 60.2 ºC. This decrease in the fusion temperature was suggestive of interaction between the drug and the carrier system, which altered the crystallization and fusion of the lipid. In addition, no ATC endothermic fusion peak was observed in the curve for SLN:ATC, indicating that the drug was dispersed in the interior or on the surface of the nanoparticles (Byrro *et al.* 2009). The curve obtained for the physical mixture of TP and ATC showed the presence of endothermic peaks for the lipid as well as the drug. This confirmed that

the technique was able to detect the peaks corresponding to ATC and TP, and that in the case of the SLN containing ATC, the drug was dispersed in the lipid matrix.

5.4.4. Cell viability

The yellow tetrazole (MTT) reduction test was used to determine cell viability. Figure 3 presents the results of cell viability tests using mouse 3T3 fibroblasts incubated with free ATC, PCL-NC:ATC, and SLN:ATC (0.1-1.2 mg/mL). Empty nanoparticles were also tested.

Figure 3: Cellular viability determined using the MTT test after exposure of Balb-c 3T3 cells to free ATC and ATC incorporated in PCL-NC and SLN suspensions (n=12). ** $p < 0.05$, one-way ANOVA with the Tukey-Kramer post-hoc test.
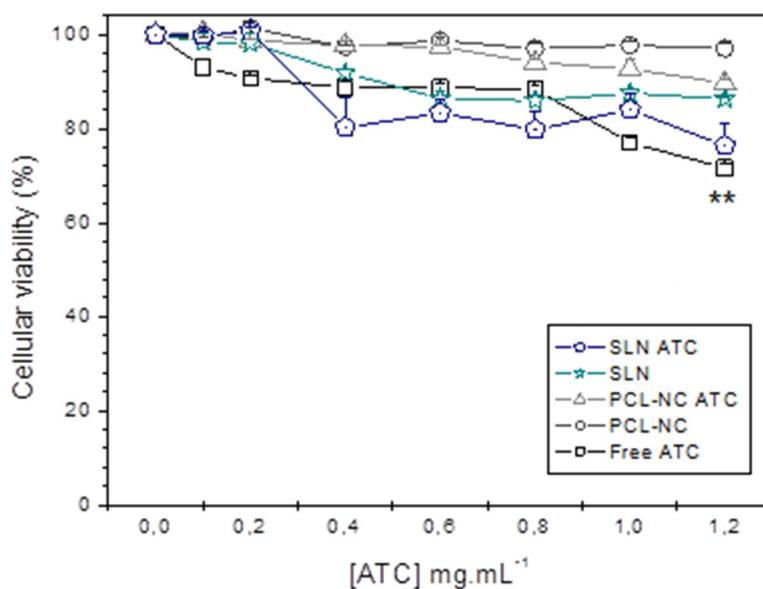
It is possible that the loaded polymers, lipids, and other components of the formulations could present some degree of toxicity due to their interaction with cell membranes (Nafee *et al.* 2009). However, at the concentrations tested, exposure to PCL-NC and SLN did not affect cell viability. One of the key aspects of the model used was that the in vitro cytotoxicity of ATC was dose-dependent. A protective effect was observed for treatment using ATC associated with the PCL-NC and SLN (at highest concentration tested), which can be explained by the lower availability of the drug due to its modified release from the nanoparticles. The cytotoxicity assay

results showed that the PCL-NC formulation containing ATC was less toxic, compared to the free drug and the SLN:ATC suspension (at 1.2 mg/mL) ($p<0.05$). Exposure of the cells to the free drug reduced cellular viability by around 30%, while exposure to PCL-NC:ATC and SLN:ATC resulted in reductions in viability of around 10% and 25%, respectively, at the highest concentration tested (1.2 mg/mL). These results are very promising since the desirable characteristics of a local anesthetic include low systemic toxicity. Similar results have been reported for PLGA nanospheres containing ropivacaine, alginate nanoparticles containing bupivacaine, and PCL nanospheres containing lidocaine, where insertion of the drug molecules into the nanocarriers resulted in reduced toxicity (Moraes *et al.* 2007e, Grillo *et al.* 2010, Campos *et al.* 2013b).

5.4.5. *In vitro* **permeation**

The release of ATC was investigated using free ATC, PCL-NC:ATC, and SLN:ATC (Figure 4(a)). In the two-compartment system described above, only free ATC molecules were able to traverse the cellulose acetate membrane, while the nanoparticles were unable to pass through the membrane. It was therefore possible to evaluate the interactions between ATC and the nanocarriers. Samples were collected from the acceptor compartment for quantification of ATC, and the results were expressed as the percentage of ATC released.

Figure 4: (a) Cumulative release of ATC, free or in suspensions of SLN or PCL-NC, at ambient temperature (n=3). (b) Permeation profiles of ATC for different gel formulations based on Aristoflex® AVC. Data presented as means and standard deviations (n=3). *** p<0.05, one-way ANOVA with the Tukey-Kramer post-hoc test.
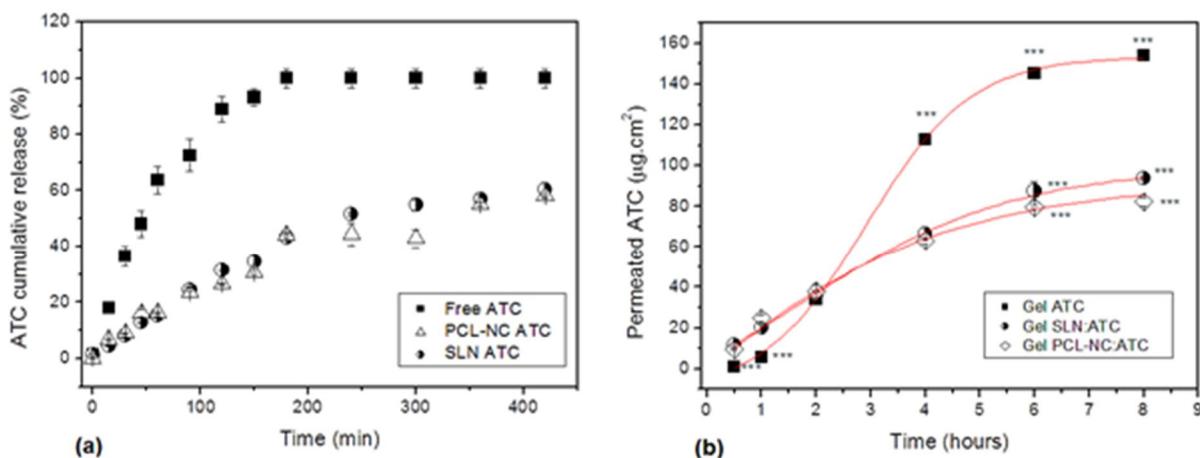
The release curve (a) showed that there was complete (100%) release of free ATC after 300 min, with 50% release ($t_{50\%}$) after 45 min, while the PCL-NC:ATC and SLN:ATC suspensions showed $t_{50\%}$ values of 400 and 300 min, respectively, demonstrating that both formulations were able to modify the ATC release profile. These differences in the release profiles could be attributed to the different mechanisms of ATC release from the nanoparticles, which was likely to initially involve desorption from the nanoparticle surfaces, followed by diffusion of the drug through the hydrophobic matrix (Siepmann and Siepmann 2008, Das *et al.* 2011).

Due to the lipophilic nature of uncharged ATC, the drug showed a high affinity for the hydrophobic matrices, which was reflected in the encapsulation efficiencies. The non-ionized form of the drug was released more slowly from the SLN, compared to free ATC, although the difference was smaller than obtained for PLC-NC:ATC. This can be explained by greater interaction of non-ionized ATC with the oily nucleus and polymeric wall of the PLC-NC, so that there was greater restriction of ATC release from the vesicular structure.

The Higuchi model was used to analyze the release profiles in order to identify the mechanism involved. The rate constants (*k*) and correlation coefficients (*r*) were calculated using linear regression. Values of *k* of 0.00552 min^{-1} (*r* = 0.991) and 0.08688 min^{-1} (*r* = 0.993) were

obtained for PCL-NC:ATC and SLN:ATC, respectively. These values indicated that the release of ATC occurred according to a Fickian diffusion mechanism. This kind of release mechanism has been reported previously for PCL nanocapsules loaded with lidocaine (Campos *et al.* 2013b).

5.4.6. Semi-solid formulation

After characterization, the nanoparticle suspensions were incorporated into semi-solid formulations composed of Aristoflex® AVC, a non-comedogenic vehicle that is not sticky and has pleasant sensorial characteristics. In addition, Aristoflex® AVC gel is anionic and was therefore compatible with the nanoparticle suspensions (Mendonça *et al.* 2009, Oliveira 2009, Farias 2011).

The semi-solid formulations containing ATC in free or encapsulated forms were evaluated in terms of their appearance, color, and odor, 24 h after preparation and then over a period of 30 days. All the formulations showed surfaces that were smooth, shiny, and homogeneous, indicating that the vehicle was suitable for the preparation of formulations containing articaine. An important point is that the products containing nanoparticles did not show the gelatine-like appearance common to formulations based on the Aristoflex® AVC polymer; this was due to the presence of surfactants in the nanoparticle formulations.

The formulations stored at ambient temperature (25 ºC) showed no changes in terms of color, odor, and appearance during the 30 days of the trial, indicating that they were suitable as carriers for free or encapsulated ATC. Similar findings have been reported for Aristoflex® gels containing hyaluronic acid (Oliveira 2009) or nanoparticles with adapalene (Farias 2011). The values obtained for the average particle diameter and polydispersity index of the suspensions incorporated in Aristoflex AVC® are provided in Table 2.

Table 2: Average diameter, polydispersity index, and zeta potential of nanoparticles containing ATC incorporated in Aristoflex AVC®.

Formulation	Average diameter (nm)	Polydispersity
Gel PCL-NC:ATC 2%	463.2 ± 24.7	0.190 ± 0.013
Gel SLN:ATC 2%	315.3 ± 20.1	0.206 ± 0.009

In the case of the SLN:ATC gel, there were increases in the average diameter and polydispersion of the nanoparticles after incorporation of the suspensions in the vehicle, compared to the values obtained for the suspensions. It is possible that interaction between the polymeric structure of the gel and the nanoparticles resulted in progressive aggregation of the particles (Farias 2011). For the PCL-NC:ATC gel formulation, there was no substantial change in the average particle diameter, compared to the values obtained for the suspension, indicating that there were no changes in the physico-chemical characteristics of this nanoparticulate system after incorporation in the gel.

It could be concluded that the average particle diameters and polydispersity indices of the nanoparticles loaded with ATC in semi-solid formulations remained stable, and that there was no significant aggregation or sedimentation of the particles after incorporation in the gel. It could therefore be concluded that the vehicle employed was suitable for the incorporation of these types of nanosystems.

The permeation profiles of semi-solid formulations were characterized under infinite dose conditions. The results obtained were expressed in terms of the cumulative amount of ATC permeated as a function of time (Figure 4(b)). The slope of the straight line for the period 1-8 h represented the permeation flux of ATC through the membrane, and the intersection with the x-axis indicated the time required for the initiation of permeation (the lag time)(Kaushik *et al.* 2010, Stoco 2011), as shown in Table 3. It is important to note that *sink* conditions were maintained in the diffusion cells throughout these experiments.

Application of the Higuchi mathematical model resulted in satisfactory fits to the release profiles (ATC gel: r^2 = 0.976; PCL-NC:ATC gel: r^2 = 0.999; SLN:ATC gel: r^2 = 0.997). This showed that the mechanism of release of free and encapsulated ATC in the semi-solid formulations was due to a diffusion process that could be described by Fick's First Law.

Table 3: Permeation parameter values obtained for permeation of different ATC gels through a cellulose acetate membrane (period: 1-8 h; 20 mg ATC/g of gel).

Formulation	Flux (μg/cm^2/h)	Lag time (h)	Permeability coefficient (cm^2/h)	Quantity of ATC permeated (μg/cm^2) (8 h)**
ATC gel	82.56 ± 1.41**	0.670 ± 0.013**	0.00357	154.06 ± 2.68
SLN:ATC gel	41.52 ± 0.66**	0.220 ± 0.078	0.00194	93.86 ± 1.17
PCL-NC:ATC gel	35.68 ± 1.98**	0.121 ± 0.044	0.00197	82.31 ± 3.91

** Statistically significant values ($p<0.05$; one-way ANOVA with the Tukey-Kramer post-hoc test).

It can be seen from Table 3 that the formulation containing 2% free ATC showed the highest permeation value (82.56 ± 0.35 μg/cm^2/h), lag time (0.670 ± 0.013 h), and permeability coefficient (0.00357 cm^2/h). This formulation therefore provided permeation of a greater quantity of ATC through the membrane, while the time required for onset of permeation was significantly longer, compared to the other formulations ($p<0.05$).

Much lower flux values were obtained for the formulations containing nanoparticles with ATC. There was a statistically significant difference between these two formulations in terms of the flux, which was lowest for the PCL-NC:ATC 2% gel, while no statistically significant difference was observed for the lag time. These results were in agreement with the release profiles of the suspensions of PCL-NC and SLN containing ATC.

The slower release of ATC from the PCL-NC than from the SLN was related to the efficiency with which ATC was encapsulated in these systems, with higher encapsulation efficiency leading to slower release. This pattern was repeated for the permeation of ATC in the semi-solid preparations, with the formulation containing PCL-NC:ATC presenting the lowest flux and the smallest permeability coefficient.

According to the literature, nanoparticle systems exhibit biphasic behavior, with an initial rapid release of the active agent (a burst effect), followed by a period of slower release (Cauchetier *et al.* 2003). The initial release phase can be attributed to the presence of the active agent in its free form, while the second phase corresponds to diffusion of the active substance following degradation of the nanoparticle matrix. This process of diffusion is governed by the

coefficient of partition of the agent between the polymer or lipid and the external aqueous medium, and by the concentration of surfactants (Farias 2011).

The gel containing ATC in its free form showed faster release, compared to the formulations containing the nanoencapsulated drug, with statistically significant differences for both the flux and the total amount released ($p < 0.05$), although there was a longer lag time, compared to the formulations containing nanoparticles. The shorter lag time for the nanoparticle formulations could be explained by the "burst effect" associated with the presence of free ATC that had not been encapsulated, and the lower fluxes could be attributed to the modification of the release profile induced by the presence of the nanoparticles.

In terms of clinical applications, the flux values exhibited by the formulations of ATC encapsulated in nanoparticles suggested the ability to provide a more prolonged anesthetic effect of ATC. The permeation kinetics data showed that the lag times were shorter for these formulations, which in clinical practice would help to minimize the time delay before onset of the anesthetic effect.

5.4.7. Rheological measurements

An important characteristic of semi-solid systems is that they preserve their shape when not under pressure, but flow or deform when submitted to an external force. Since conventional nanoparticle suspensions present low viscosity, alternative dosage forms (such as hydrogels) are required when a topical application is desired (Souto *et al.* 2004). However, the rheological properties of the final formulation need to be evaluated, because the components of the gel and the nanoparticle suspension can interact and affect the consistency of the resulting hydrogel (Souto *et al.* 2004). Evaluation of the rheological characteristics of semi-solid formulations designed for topical application is also very important in determination of in vivo performance, considering aspects including spreading ability, retention, drug delivery, and scalability (Souto *et al.* 2004, Vanic *et al.* 2014).

The rheological behaviors of the two different hydrogels containing SLN and PCL-NC, together with those of the control formulations (base gel and free articaine in the base gel), are illustrated in the flow curves shown in Figure 5.

Figure 5: Shear stress as a function of shear rate for the two different hydrogels containing SLN and PCL-NC, and the control formulations (base gel and free articaine in the base gel). The upper and lower curves correspond to ascending and descending measurements, respectively, for each formulation.
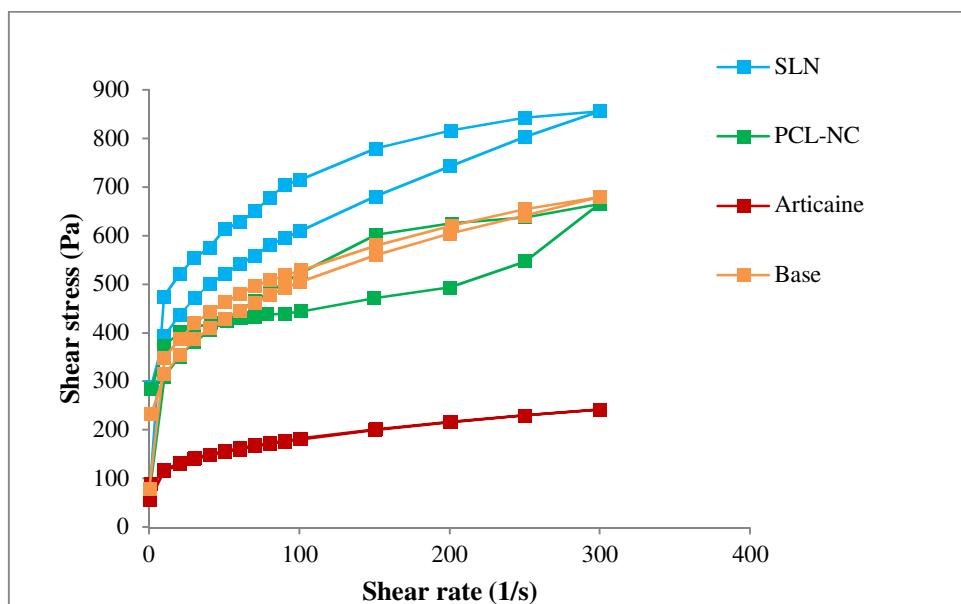
The flow rheograms reflected non-Newtonian pseudoplastic flows, where the shear rate increased with increasing shear stress (Picout and Ross-Murphy 2003, Lee *et al.* 2009). After achieving the maximum supported shear stress, the formulations started to flow and their viscosity decreased. These characteristics have been demonstrated previously for hydrogel-based formulations containing solid lipid nanoparticles and nanostructured lipid carriers (Souto *et al.* 2004, Silva *et al.* 2012).

Higher shear stress values were observed for the SLN and PCL-NC hydrogels, compared to the free articaine hydrogel, reflecting greater viscosity of the nanoparticle formulations. It has been suggested previously that this could be indicative of good storage stability of semi-solid formulations, as well as improved spreadability (Lippacher *et al.* 2004, Souto and Muller 2007).

Another property related to pseudoplastic systems is thixotropy, which is a time-dependent decrease in viscosity under shear stress, followed by a gradual recovery when the stress is removed (Lee *et al.* 2009). This is a common characteristic of formulations containing nanoparticles (Silva *et al.* 2012). It can be seen from Figure 5 that the SLN (22,090.23 Pa.s^{-1}) and PCL-NC (19,554.99 Pa.s^{-1}) hydrogels both presented thixotropy, while thixotropic behavior

114

was not observed for the base gel or the free articaine formulation. These observations could also be related to the presence of lipids in the formulations, which helps to ensure good spreadability in topical applications (Lippacher *et al.* 2004, Souto *et al.* 2004, Silva *et al.* 2012). Thixotropic properties contribute to increased retention times of topically applied formulations, leading to better therapeutic efficacy (Lee *et al.* 2009), which was an essential consideration in the case of the hydrogels developed in the present study.

5.5. Conclusions

This work provides new information concerning the preparation and characterization of nanoparticles and semi-solid formulations containing the local anesthetic articaine. Good encapsulation efficiencies were achieved, with values of around 78% for PCL-NC and 65% for SLN. In stability trials, measurements of colloidal parameters demonstrated that suspensions of these nanocarrier systems containing ATC remained stable for a period of 120 days. The encapsulation of ATC resulted in reduced toxicity of the drug, as shown by good values of cellular viability for the nanosystem formulations, compared to free ATC, which could be explained by the efficiency of encapsulation of the drug, resulting in smaller amounts of free ATC. The profile of ATC release was slower and more sustained for the PCL-NC and SLN formulations, compared to free ATC.

Semi-solid formulations incorporating ATC, either free or encapsulated in the nanocarriers, were prepared using Aristoflex® AVC gel. Sensorial evaluation of the formulations at time zero and after 30 days revealed no differences, confirming the suitability of this vehicle. Determination of the average diameter and polydispersion of the nanoparticles incorporated in the gel showed that there were no changes in the colloidal parameters and that the vehicle did not alter the stability of the suspensions of nanoparticles containing ATC. Rheological evaluation showed that the SLN and PCL-NC hydrogel formulations presented non-Newtonian pseudoplastic flows with thixotropy. In clinical practice, this should be reflected in better stability, increased retention time at the application site, and improved spreadability. The results of in vitro permeation experiments employing the semi-solid formulations demonstrated that the lag time was shorter for the preparations containing nanoparticles, compared to the preparation containing free ATC, and that the flow of ATC through the membrane was slower for the nanoparticle systems. The formulation containing ATC encapsulated in PCL-NC showed the best permeation characteristics. This study opens perspectives for the future use of

nanoparticulate carrier systems for the local anesthetic articaine, envisaging their infiltrative and/or topical use in skin.

Acnkowledgements

Abbreviation

PCL: poly(ε-caprolactone); PVA: polyvinyl alcohol; NC: nanocapsules; SLN: solid lipid nanoparticles; ATC: articaine; MTT: yellow tetrazole; TEM: transmission electron microscopy; DSC: differential scanning calorimetry.

5.6. Supplementary information

DSC curves of PCL nanocapsules

The DSC analyses were used to provide information concerning the interaction of the components of formulations. Figure S1 shows the thermal profiles obtained for the drug, raw materials, physical mixture and nanocapsules.

_____

Figure S1: DSC curves obtained for (a) ATC, (b) PCL polymer, (c) PCL nanocapsules, (d) PCL nanocapsules containing ATC, and (e) physical mixture of PCL and ATC.
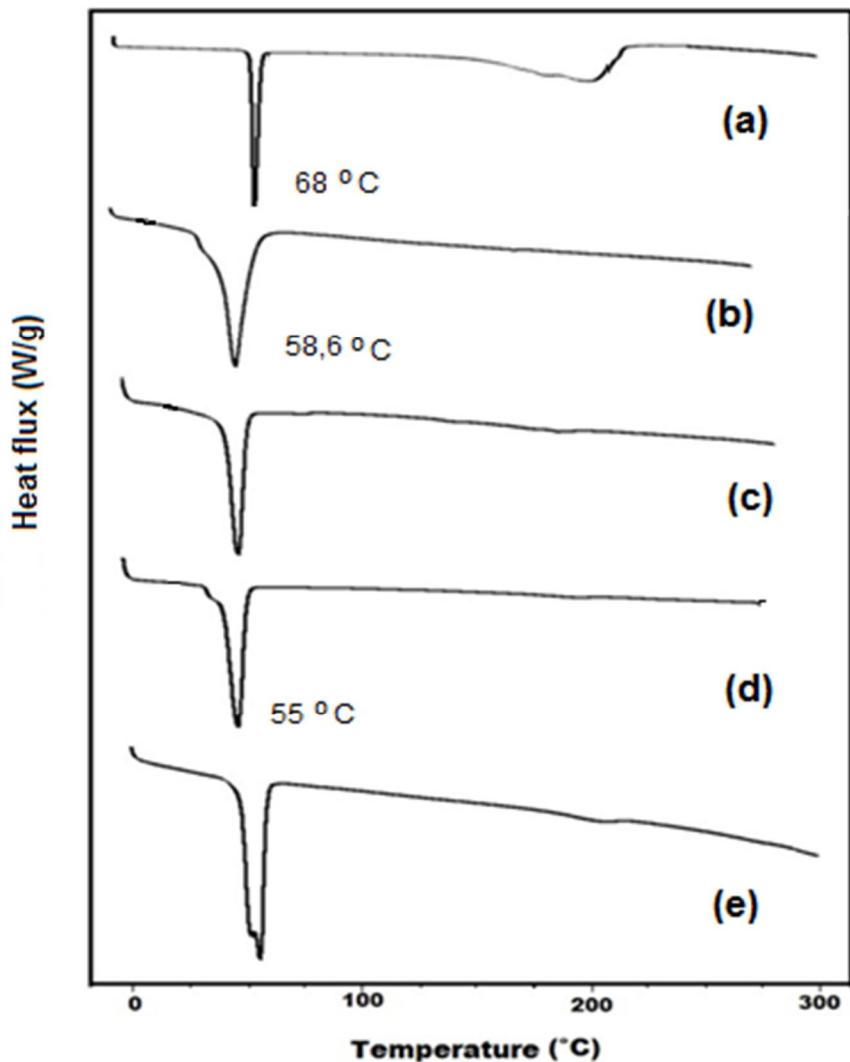
DSC curves of SLN

The thermal profiles were also obtained for the SLN loading ATC. Figure S2 shows the termal profile for the drug, raw materials, physical mixtures and nanoparticles.

Figure S2: DSC curves obtained for (a) ATC, (b) TP, (c) ATC + TP physical mixture, (d) SLN, and (e) SLN:ATC.
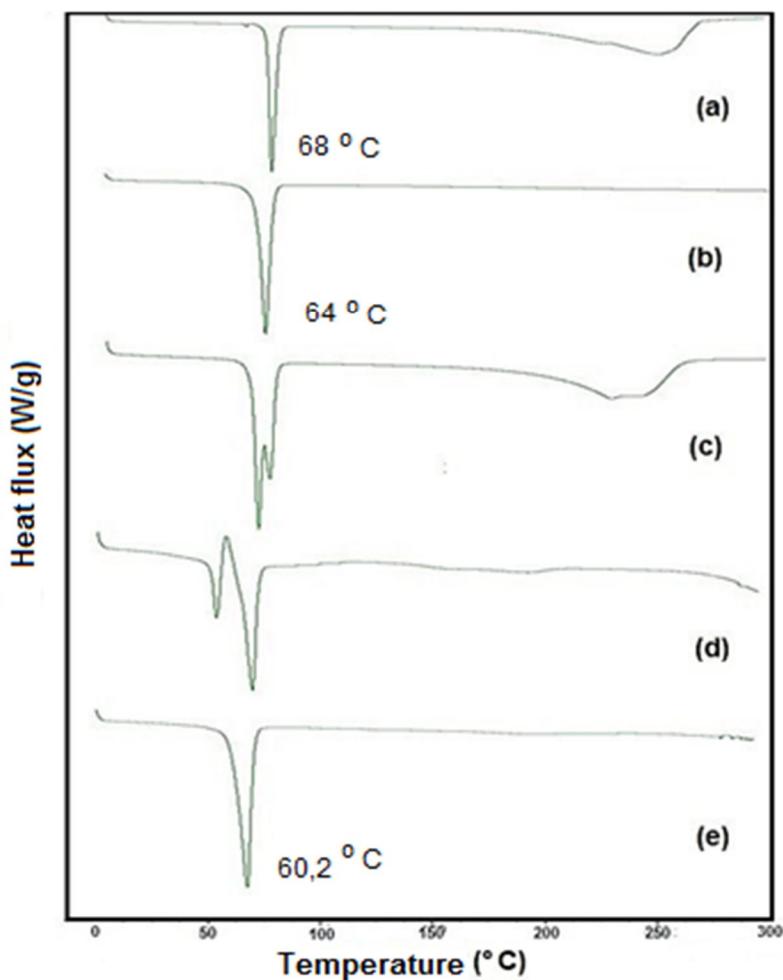
Capítulo 6 – Lipossomas contendo articaína na forma ionizada

Capítulo de livro:

de MELO, NFS; de PAULA, E; PASQUOTO, T; de LIMA, R; de ARAÚJO, DR, ROSA, AH; FRACETO, LF. Development of liposomes loaded with charged articaine using experimental design, in: "**Microspheres: Technologies, Applications and Role in Drug Delivery Systems"**, Editors: Daniele Ribeiro de Araújo e Leonardo Fernandes Fraceto, Nova Science Publishers Inc., USA, 2014.

6.1. Abstract

There has been increasing interest in the use of liposomes as carrier systems for pharmaceuticals. Advantages of these systems include protection of the active principle against degradation, modulation of the rate of drug release, and lower toxicity. Articaine (ATC) is a local anesthetic (LA) used in dental procedures, regional anesthesia, and the control of acute and chronic pain. The development of new liposomal formulations involves the stages of preparation, physicochemical characterization, and evaluation of stability. In this work, liposomal formulations were optimized using experimental design methodology, considering the following parameters: average particle diameter, polydispersion, zeta potential, and ATC encapsulation efficiency. The physicochemical properties of the suspensions (particle diameter, polydispersion, and encapsulation efficiency) were measured as a function of time in order to determine the stability of the formulations. The optimized formulation showed no substantial changes in these parameters during storage for up to 30 days at ambient temperature. The cytotoxicity of the formulations was evaluated using the MTT reduction test and was found to be lower compared to the free drug. The results demonstrated that it was possible to prepare liposomes as carriers for articaine, hence offering a new alternative for the management of pain.

Keywords: Liposomes, local anesthetics, experimental design, articaine.

6.2. Introduction

Advances in liposome research and development have resulted in improvements in formulation stability and better understanding of the physicochemical characteristics of these systems and their interaction with biological fluids (Lasic 1998, Batista *et al.* 2007). Liposomes are spherical colloidal vesicles composed of one or more concentric phospholipid bilayers, with sizes ranging from the micrometric to the submicrometric (Ranade 1989, Le Bourlais *et al.* 1998b, Cereda *et al.* 2004b, Batista *et al.* 2007, Elsayed *et al.* 2007), whose structures enable the incorporation of hydrophobic, hydrophilic, and amphiphilic molecules (Rose *et al.* 2005, Elsayed *et al.* 2007). Due to their similarity to biological membranes, due to the presence of phospholipids and cholesterol, liposomes do not present any risk of antigenicity or the occurrence of histological lesions after their administration (Cereda *et al.* 2004b, Dubey *et al.* 2007).

Liposomes can be composed of either a single bilayer (unilamellar) or multiple (multilamellar) lipid bilayers surrounding an aqueous internal compartment. In terms of size, the unilamellar vesicles are classified as either small unilamellar vesicles (SUV) or large unilamellar vesicles (LUV) (Vemuri and Rhodes 1995, Lasic 1998, Batista *et al.* 2007).

Qualitative and quantitative information concerning the composition of liposomes is important because their composition influences the stability of these systems, as well as the efficiency with which drugs can be encapsulated. The use of experimental design methodology has contributed to the development of liposomes that are more stable and provide better encapsulation of molecules, and offers advantages in terms of the number of the experiments required and the ability to evaluate the interactions between different factors (Woitiski *et al.* 2009, de Melo *et al.* 2013).

Articaine hydrochloride (ATC) is a local anesthetic (LA) that is widely used in clinical practice. The anesthetic effectiveness of this drug is related to its ability to easily diffuse between tissues, due to the presence of a thiophene ring in its structure. Nonetheless, a number of adverse reactions, such as permanent paresthesia and nerve lesions, have been reported when high concentrations (4%) of the compounds are used (Pogrel 2007, Paxton and Thome 2010). The use of liposomes as carriers for this LA could help to reduce adverse reactions as well as minimize the dosages required to achieve the desired effects. This chapter describes the optimization of liposomes using experimental design methodology, with ATC as a drug model, together with evaluation of the stability and cytotoxicity of the system.

6.3. Methods and results

6.3.1. Liposome preparation

The liposomes were produced using a procedure based on the hydration of a lipid film (Canfarotta *et al.*). A mixture of egg phosphatidylcholine (EPC), the sodium salt of 1,2–di(cis-9-octadecenoyl)-sn-glycerol-3-phosphate (phosphatidic acid, PA), cholesterol (CH), cholesterol sulfate (CHS), and α-tocopherol was used, at a molar ratio of 4:0.5:3:0.1:0.07. An aqueous solution of ATC (20 mg/mL) was added under agitation, forming multilamellar vesicles (MLV). This suspension was then submitted to sonication to obtain small unilamellar vesicles (SUV). The suspensions of SUV containing ATC (2%) were stored in amber flasks kept at ambient temperature (de Araujo *et al.* 2004, Rose *et al.* 2005, Cereda 2007).

6.3.2. Factorial design and liposome characterization

In previous studies, experimental design methodology and response surface analysis have been used to investigate the effects of different preparation variables on liposomal formulation parameters including particle size and drug encapsulation efficiency, amongst others (Padamwar and Pokharkar 2006, Ghanbarzadeh *et al.* 2013). Here, a factorial design with three levels (-1, +1, and two repetitions at the central point) was used to determine the influence of independent variables (PA concentration and CHS concentration) on the average particle diameter, polydispersion, zeta potential, and ATC encapsulation efficiency of the liposomal formulations. Each formulation was measured in triplicate (Table 1). An experimental matrix containing 10 formulations was obtained using the quadratic model:

$$Y = b_0 + b_1A + b_2B + b_{12}AB + b_{11}A^2 + b_{22}B^2 + E, \qquad \text{(Eq. 1)}$$

where b_0 is the arithmetic mean, b_1 and b_2 are the coefficients for the independent variables, b_{11}, b_{12}, and b_{22} are the coefficients for the interactions between the variables, Y corresponds to the factors, and E is the experimental error. The measurements of average diameter, polydispersion, and zeta potential were performed using photon correlation spectroscopy

(Cereda *et al.* 2004b, de Melo *et al.* 2013). Quantification of ATC employed high performance liquid chromatography, with an analytical curve that had been previously validated in accordance with the ICH recommendations (de Melo *et al.* 2013). The lipids used were selected in order to maximize the negative charge of the liposome and facilitate interaction with the positively charged ATC. Cholesterol sulfate plays an important role in cell membranes and helps to prevent their rupture (Schofield *et al.* 1998). The use of liposomes with greater negative charge therefore increases the efficiency of encapsulation of molecules with positive charge, due to electrostatic interaction, while at the same time the rate of release is reduced and the effect of the encapsulated active principle (in this case ATC) is prolonged.

Statistical analysis of the effects of the variables on the different parameters employed Statgraphics Centurion v. XVI software (with $p < 0.05$). This enabled construction of a quadratic mathematical model containing terms describing the effects of the experimental variables and their interactions.

Table 1: Experimental design matrix and results obtained for the average diameter, polydispersion (polydispersivity index - PDI), zeta potential, and encapsulation efficiency of liposomes containing articaine.

Formulation	A	B	Average size (nm) ± SD	PDI ± SD	Zeta potential (mV) ± SD	Encapsulation efficiency (%) ± SD
1	0	0	205.1±13.9	0.200±0.008	-56.4±10.2	9.77±1.43
2	0	1	196.9±17.8	0.321±0.012	-40.7±7.5	18.02±2.83
3	-1	1	222.8±7.2	0.276±0.008	-48.6±5.1	57.02±3.28
4	-1	0	192.1±7.1	0.299±0.013	-40.7±7.5	9.51±2.91
5	0	-1	148.6±11.1	0.230±0.011	-13.7±5.8	31.1±1.9
6	1	-1	180.4±7.7	0.217±0.009	-38.6±7.5	25.23±4.65
7	0	0	202.9±8.4	0.184±0.011	-47.6±1.7	8.67±2.02
8	0	-1	208.3±8.5	0.216±0.007	-38.5±0.9	27.17±1.93
9	-1	-1	187.2±13.8	0.231±0.005	-18.4±2.9	37.01±3.72
10	1	0	200.5±14.6	0.268±0.012	-31.9±2.8	35.03±3.11

A: cholesterol sulfate (-1 = 0 mg; 0 = 2 mg; 1 = 3 mg); B: phosphatidic acid (-1 = 0 mg; 0 = 2 mg; 1 = 4 mg).

The vesicles presented average diameters in the range 140-210 nm, polydispersivity index values of 0.2-0.3, zeta potentials in a range indicative of excellent colloidal stability, and good

encapsulation efficiency. The data were subjected to statistical analysis in order to evaluate the influence of variation of the factors at three levels (Table 2, Figure 1).

Table 2: Stardardized effects of factors on responses.

Mean diameter			
	Effect	Standard deviation (±)	*p*
Average	207.26	5.46	-
A: CHS	-24.60*	7.47*	0.0058*
B:[PA	-2.91	7.42	0.7026
AA	- 22,09	11.98	0.0881
AB	- 31,97*	9.15*	0.0040*
BB	- 21,24	11.94	0.0997
Experimental error	5.46	-	-
Polydispersion			
	Effect	Standard deviation (±)	*p*
Average	0.222		-
A: CHS	-0.034	0.024	0.1895
B: PA	0.052	0.022	0.0572
AA	0.045	0.039	0.2812
AB	-0.014	0.030	0.6540
BB	0.026	0.039	0.5199
Experimental error	0.018	-	-
Zeta potential			
	Effect	Standard deviation (±)	*p*
Average	-50.53		-
A: [CHS	8.95*	1.57*	0.0001*
B: [PA	- 1.75	1.53	0.2870
AA	27.25*	2.52*	0.0001*
AB	26.87*	1.93*	0.0001*
BB	18.05*	2.52*	0.0001*
Experimental error	1.15	-	-
Encapsulation efficiency			
	Effect	Standard deviation (±)	*p*
Average	8.41		-
A: CHS	-4.66	6.66	0,4964
B: PA	5.67	6.64	0.4102
AA	29.33*	10.68*	0.0167*
AB	6.34	8.16	0.4569
BB	29.12*	10.6*	0.0173*
Experimental error	4.87	-	-

*Significant at 95% confidence level.

Figure 1: Surface response plots for the effects of the factors CHS and PA on average diameter (A), polydispersion (B), zeta potential (C), and encapsulation efficiency (D).
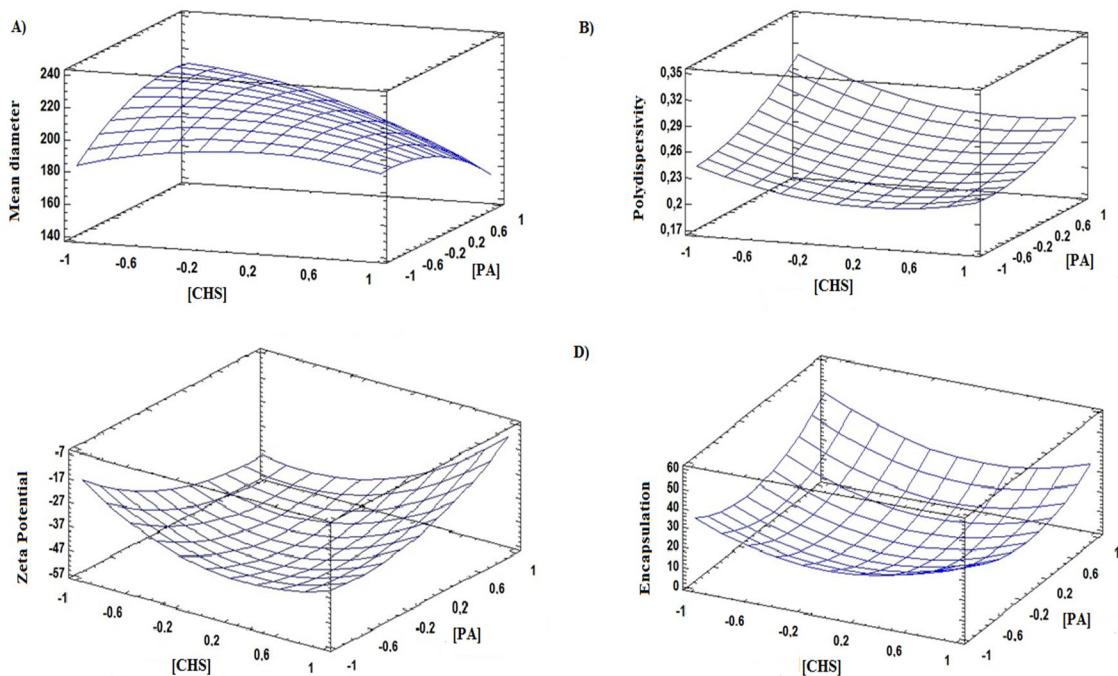
The CHS concentration (CHS), as well as the interaction between CHS and the phosphatidic acid concentration (PA) (represented by the term AB), showed statistically significant effects on the average diameter of the liposomes, which decreased at higher levels of CHS and PA. This could be explained by greater attraction between the non-polar lipid chains, which increased the degree of packing and interaction between the lipid molecules. It is important to point out that in this work there was no alteration of the lipid molar ratio. The decrease in the average diameter was probably related to the reduced fluidity of the bilayer induced by the presence of cholesterol sulfate (Padamwar and Pokharkar 2006, Ghanbarzadeh *et al.* 2013).

None of the factors investigated had any statistically significant effect on the polydispersion of the liposomes, although there was an observed tendency towards greater polydispersion at higher PA concentrations. The final lipid concentration was maintained fixed, which probably accounted for the lack of any substantial changes in polydispersion, which is

known to be affected by the lipid concentration. It was not necessary to use additional surfactants during preparation of the liposomes, because the egg phosphatidylcholine used is an amphiphilic phospholipid involved in formation of the lamellar phase (Frézard *et al.* 2005). Since the quantity of this phospholipid employed in the formulation remained invariant, no effect on the polydispersion of the formulations was expected.

The concentration of CHS and the quadratic polynomial fits of the factors (terms AA, BB, and AB) had significant effects on the zeta potential of the liposomes containing ATC, due to the negative charges of the components, with higher concentrations resulting in higher zeta potential values. Liposomes produced using EPC generally show negative zeta potentials, indicative of high electrostatic stabilization of the vesicles in suspension, with little tendency towards aggregation. In this study, a negatively charged phospholipid (PA) was used, together with CHS, so that the surfaces of the liposomes became even more negative. Similar results have been reported in the literature for liposomes containing vitamin E (Padamwar and Pokharkar 2006).

The same phospholipid/cholesterol molar ratio was maintained for all the formulations. Both CHS and PA possess negative charges, and the resulting high negative charge on the liposomes favored their electrostatic interaction with ATC (which possesses a positive charge), hence increasing the encapsulation efficiency. The value obtained here for the encapsulation efficiency (58%) was higher than the values reported for liposomes containing other local anesthetics (Cereda *et al.* 2004b, de Araujo *et al.* 2004), once again indicating that increased negative charge favors the encapsulation of drugs carrying positive charges. Changes in the concentrations of CHS and PA, using adjustment of the quadratic polynomial, caused statistically significant changes in the encapsulation efficiency. An increase in the concentration of each of these components therefore caused an enhancement of the ATC encapsulation efficiency. This can be explained by the fact that cholesterol has the effect of reducing the fluidity of the phospholipid bilayer, causing the vesicles to become slightly more rigid (Padamwar and Pokharkar 2006), resulting in more effective interaction of the active principle within the liposomes.

Empirical quadratic models were constructed for the variables that displayed significant effects, described by Equations 2, 3, and 4.

Mean diameter = 207.26 - 24.60 (SCH) - 31.97 (SCH).(PA) - 21.24 (PA^2)+ 5.46

(Eq. 2)

Zeta potential = -50.53 + 8.95 (SCH) + 27.25 (SCH^2)+ 26.87 (SCH).(PA) + 18.05 (PA^2)+ 1.15   (Eq. 3)

Encapsulation efficiency = 8.41 + 29.33 (SCH^2)+ 29.12 (PA^2)+ 4.97   (Eq. 4)

Formulations containing liposomes are relatively expensive compared to conventional pharmaceutical formulations. The most important parameter considered here for selection of a suitable formulation was therefore the encapsulation efficiency. The formulation used in subsequent experiments corresponded to formulation 3 of the factorial design, which showed the highest ATC encapsulation efficiency as well as satisfactory colloidal properties.

6.3.3. Colloidal stability

The colloidal stability of liposomes can be affected by processes that may be chemical (hydrolysis and oxidation), physical (aggregation and fusion of the vesicles), and biological (time of circulation in the bloodstream). Depending on their composition, liposomal formulations can have short useful lifetimes, in part due to the inherent instability of these systems (Sharma *et al.* 1997, Batista *et al.* 2007).

The stability of the vesicles containing ATC was evaluated using measurements of average diameter, polydispersion, zeta potential, and encapsulation efficiency as a function of time. The results obtained for the SUV/ATC formulation are shown in Figure 2.

Figure 2: Changes in (a) average diameter and polydispersion, and (b) zeta potential and encapsulation efficiency of liposomes containing ATC (formulation 3) during 90 days of storage at ambient temperature (n=3).
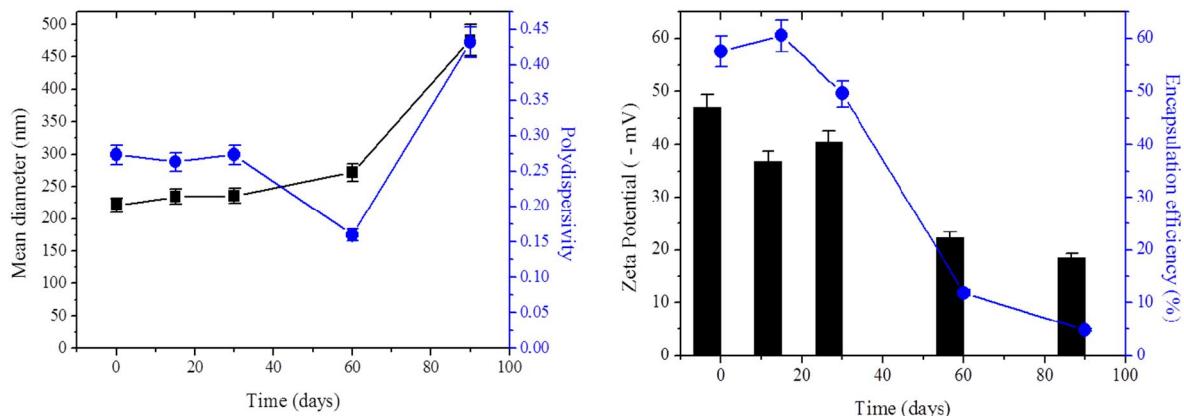
All the parameters analyzed showed changes during the storage period. The values of the average diameter and polydispersion increased substantially after 60 days, and were approximately twice the initial values after 90 days, indicating aggregation of the vesicles and a more heterogeneous size distribution. In previous work investigating the physicochemical instability of liposomes, it was found that aggregation and reduced performance of the vesicles as modified release systems was determined by their chemical composition as well as the conditions and duration of storage (Vemuri and Rhodes 1995, Sharma *et al.* 1997, Diniz 2008). Similar results have been reported for liposomes containing local anesthetics produced using the same primary materials (EPC, cholesterol, and α-tocopherol) (de Araujo *et al.* 2004, Cereda 2007, Vieira 2012).

Changes in the zeta potential were also investigated, since this parameter provides an important indication of the stability of liposomes in suspension. The zeta potential increased from -40 to -18 mV during the storage period, providing further evidence of aggregation of the vesicles over the course of time. Despite the presence of PA in the formulation, which increased the negative charge on the surface and generated greater repulsion between the particles, this was not sufficient to maintain the vesicles in a stable state over 90 days. Similar findings in relation to negative charge have been reported for liposomes containing the local anesthetic ropivacaine (Vieira 2012).

The efficiency of encapsulation of ATC in the liposomes diminished from 57% at the beginning of the trial to 5% after 90 days (Figure 2(b)). Despite this substantial reduction, the encapsulation of ATC in the liposomal vesicles still remained high relative to the values obtained for the encapsulation of other local anesthetics in liposomes, which could be attributed to the different compositions of the formulations. The reduction in encapsulation efficiency could be explained by the hydrolysis and oxidation of the phospholipids, leading to changes in the permeability of the bilayer and release of the drug to the external medium, hence prejudicing the integrity of the formulation (Diniz 2008).

It could be concluded that after optimization using experimental design, the liposomal formulation showed satisfactory colloidal stability for up to 30 days of storage, while after this period, the vesicles suffered a loss of integrity associated with aggregation and leakage of the drug to the exterior.

6.3.4. Cell viability

The goal of a modified release system is to maintain the concentration of a drug between two set levels for as long as possible in order to reduce the frequency of administration and minimize toxicity (Kuzma *et al.* 1997). In the present work, cellular viability was evaluated using the MTT (a yellow tetrazole) reduction test. The principle of this test is based on the capture of MTT by the cells, followed by its reduction to formazan by the action of mitochondrial dehydrogenases, resulting in the accumulation of this compound in viable cells. Solubilization of the cells then causes the release of formazan, which can be easily detected by spectrophotometry in the visible region (at a wavelength of 570 nm) (Welder 1992).

The cytotoxicity of the liposomal formulation was evaluated using CHO cells incubated with free ATC, liposomes without ATC, and liposomes containing ATC, at concentrations from 0.02 to 1 mg/mL (Figure 3).

Figure 3: Cytotoxicity determined using the MTT test after exposure of CHO cells to SUV, free ATC, and SUV/ATC.
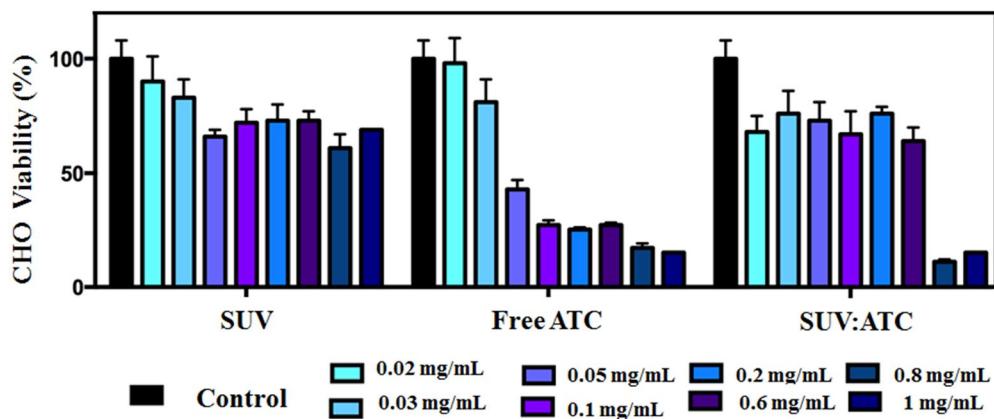
An important point concerning this *in vitro* cytotoxicity model is that the toxicity of ATC is dose-dependent, so the protective effects observed using the SUV/ATC formulation can be explained by the lower availability of free drug, due to the modified release of ATC from the liposomes.

Exposure of the CHO cells to SUV alone had little effect on cellular viability, at the concentrations employed. However, exposure to the free drug reduced the viability of the cells to 30%, at the highest concentration employed (1 mg/mL), demonstrating the toxicity of the local anesthetic. At low ATC concentrations, the SUV/ATC formulation was less toxic than the free drug, while the toxicities were similar at the two highest concentrations tested. It has been found previously that exposure of the cell membrane to certain ionizable groups present in pharmaceuticals can lead to the loss of its integrity (Nafee *et al.* 2009). It should be noted that the SUV/ATC formulation showed an encapsulation efficiency of 58%, so that there was still a considerable quantity of free drug available to interact with components of the membrane. As a result, the reductions in cellular viability observed after exposure of the cells to the formulations containing ATC at higher concentrations were similar to the reductions observed for free ATC alone. Nonetheless, the formulation containing ATC encapsulated in SUV may be suitable for future use in clinical practice, since at lower ATC concentrations it was less toxic, compared to the free drug. Similar findings have been reported previously for liposomal vesicles containing ropivacaine (Vieira 2012).

6.4. Conclusions

Use of experimental design enabled determination of the proportions of the components of SUV formulations that provided the best ATC encapsulation efficiency and suspension stability. An encapsulation efficiency of around 58% was achieved, and the colloidal parameter values for the SUV containing ATC indicated that the suspensions were stable for 30 days. Cytotoxicity evaluation using the MTT reduction test revealed that encapsulation of the drug reduced its toxicity, compared to free ATC. The findings of this work suggest that the SUV could be used as a carrier for articaine in clinical applications involving infiltrative and/or topical administration.

Acknowledgements

Capítulo 7 – Comparação entre as formulações estudadas

Os sistemas de liberação modificada possuem inúmeras vantagens, dentre elas a redução da toxicidade de fármacos uma vez que a liberação torna-se mais lenta ou então existe a possibilidade de veicular uma menor concentração do fármaco e proporcionar, no mínimo, o mesmo efeito terapêutico. Os sistemas de liberação modificada presentes neste estudo foram diferentes quanto a sua composição química e estruturação. As NC PCL possuem uma conformação vesicular, ou seja, um núcleo oleoso circundado por uma parede polimérica. Já as NC PEG-PCL apesar de possuírem estrutura vesicular, seu núcleo é de natureza aquosa. As NE Alg/Quit e SLN possuem uma estrutura matricial sólida de polímero e lipídio, respectivamente. Os lipossomas SUV são vesículas compostas por uma bicamada de fosfolipídios, que apresentam arranjo espontâneo no meio aquoso. A ATC na forma não ionizada apresenta uma estrutura mais apolar do que na forma cloridrato (ionizada), sendo assim, a forma não ionizada foi escolhida para os sistemas mais hidrofóbicos (NC PCL e SLN) e a forma ionizada para os sistemas mais hidrofílicos (NC PEG-PCL, NE Alg/Quit e lipossomas). As Figuras 1, 2, 3, 4 e 5 mostram um resumo dos principais resultados alcançados para cada uma das formulações desenvolvidas neste estudo.

Figura 1: Representação esquemática da estrutura da NC PCL com ATC e dos principais resultados obtidos no estudo desta formulação.
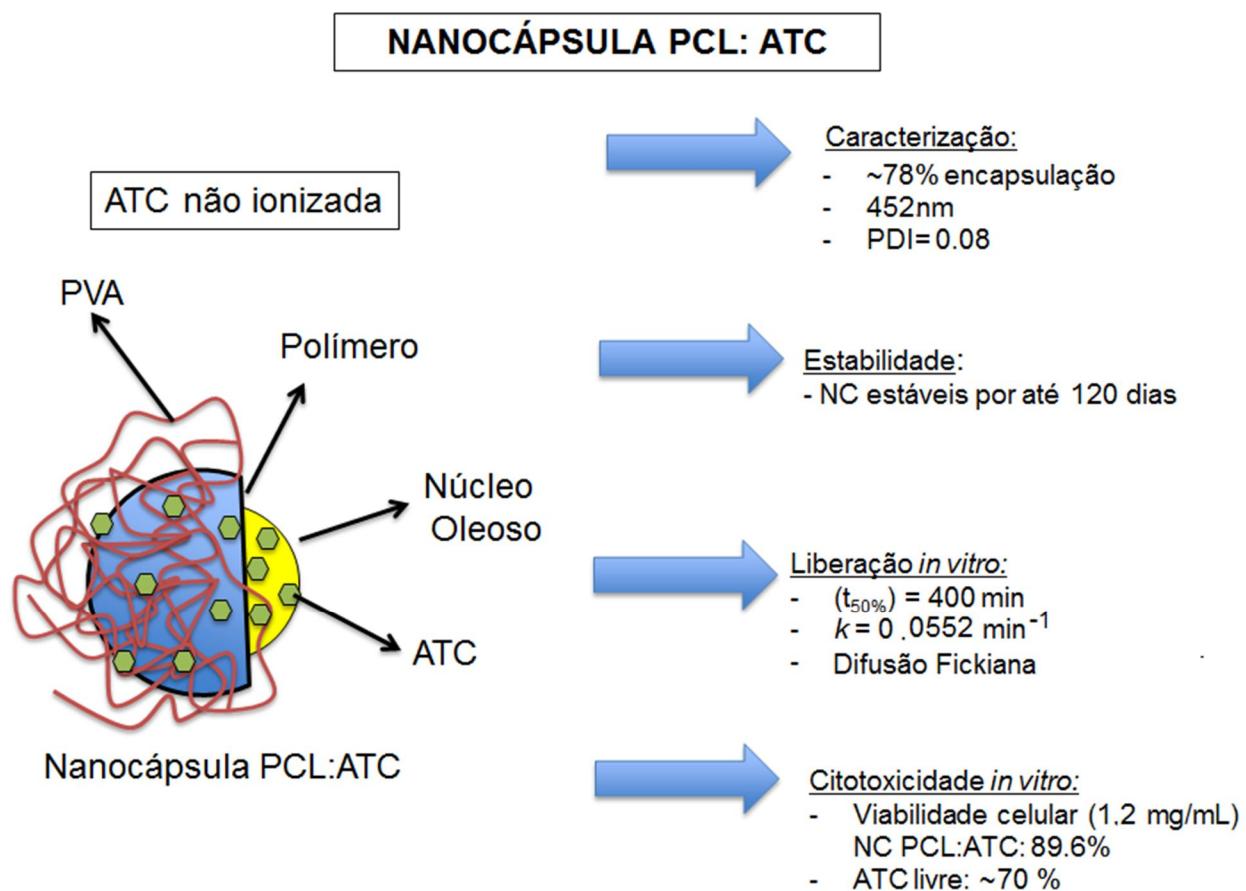
Figura 2: Representação esquemática da estrutura da NC PEG-PCL com ATC e dos principais resultados obtidos no estudo desta formulação.
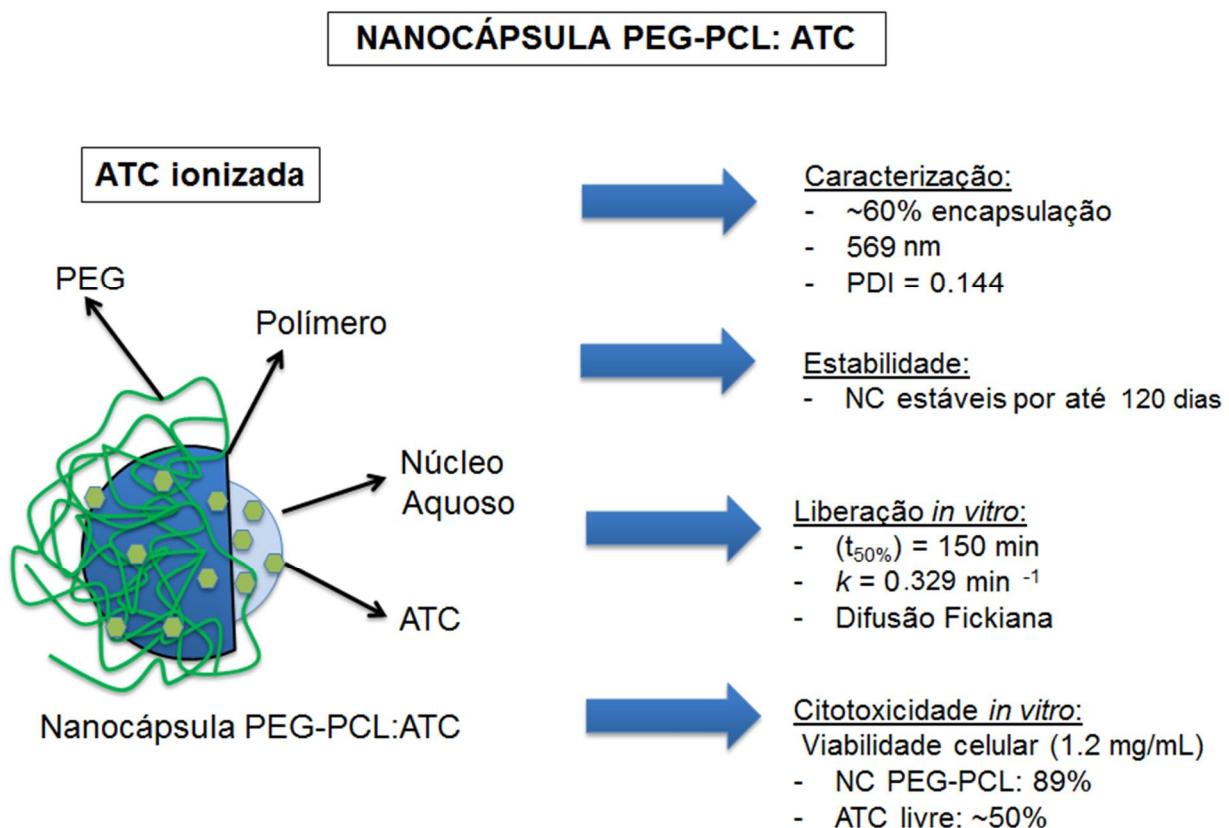
Figura 3: Representação esquemática da estrutura da NE Alg/Quit com ATC e dos principais resultados obtidos no estudo desta formulação.
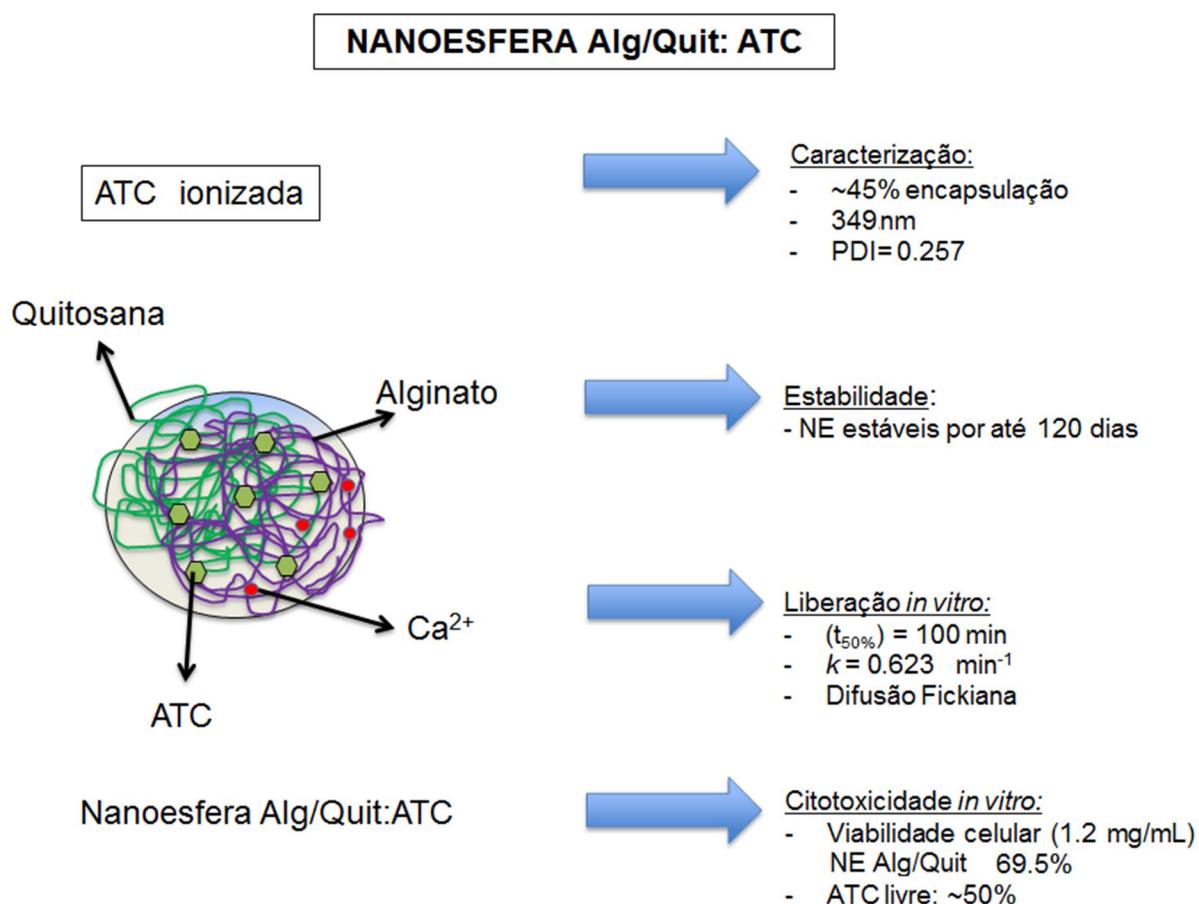
Figura 4: Representação esquemática da estrutura da NLS com ATC e dos principais resultados obtidos no estudo desta formulação.

NANOPARTÍCULA LIPÍDICA SÓLIDA: ATC

ATC não ionizada

PVA

Lipídio

ATC

Nanopartícula lipídica sólida:ATC

Caracterização:
- ~65% encapsulação
- 244 nm
- PDI= 0.109

Estabilidade:
- SLN estáveis por até 120 dias

Liberação *in vitro:*
- $(t_{50\%})$ = 300 min
- k = 0.0868 min^{-1}
- Difusão Fickiana

Citotoxicidade *in vitro:*
- Viabilidade celular (1.2 mg/mL) SLN:ATC: 79,3 %
- ATC livre: ~ 70 %

_____
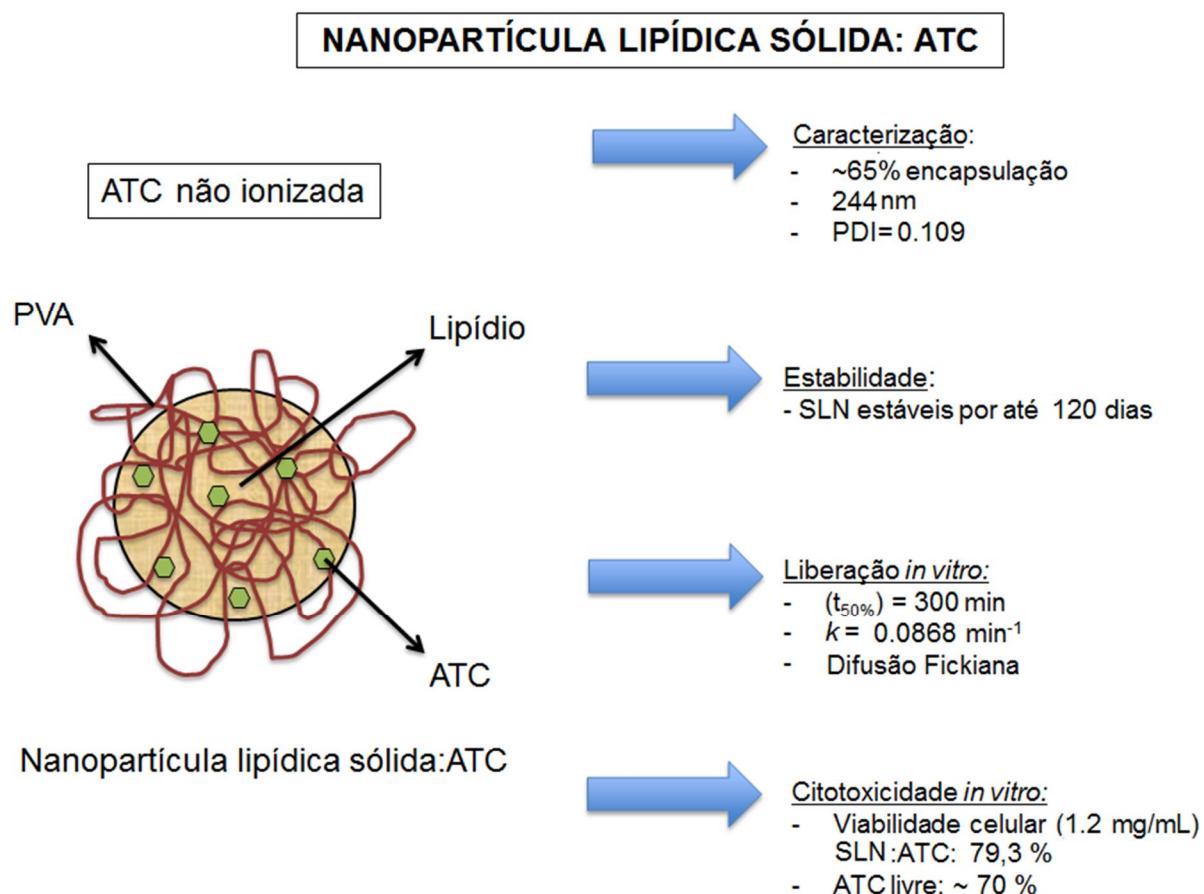
Figura 5: Representação esquemática da estrutura da SUV com ATC e dos principais resultados obtidos no estudo desta formulação.
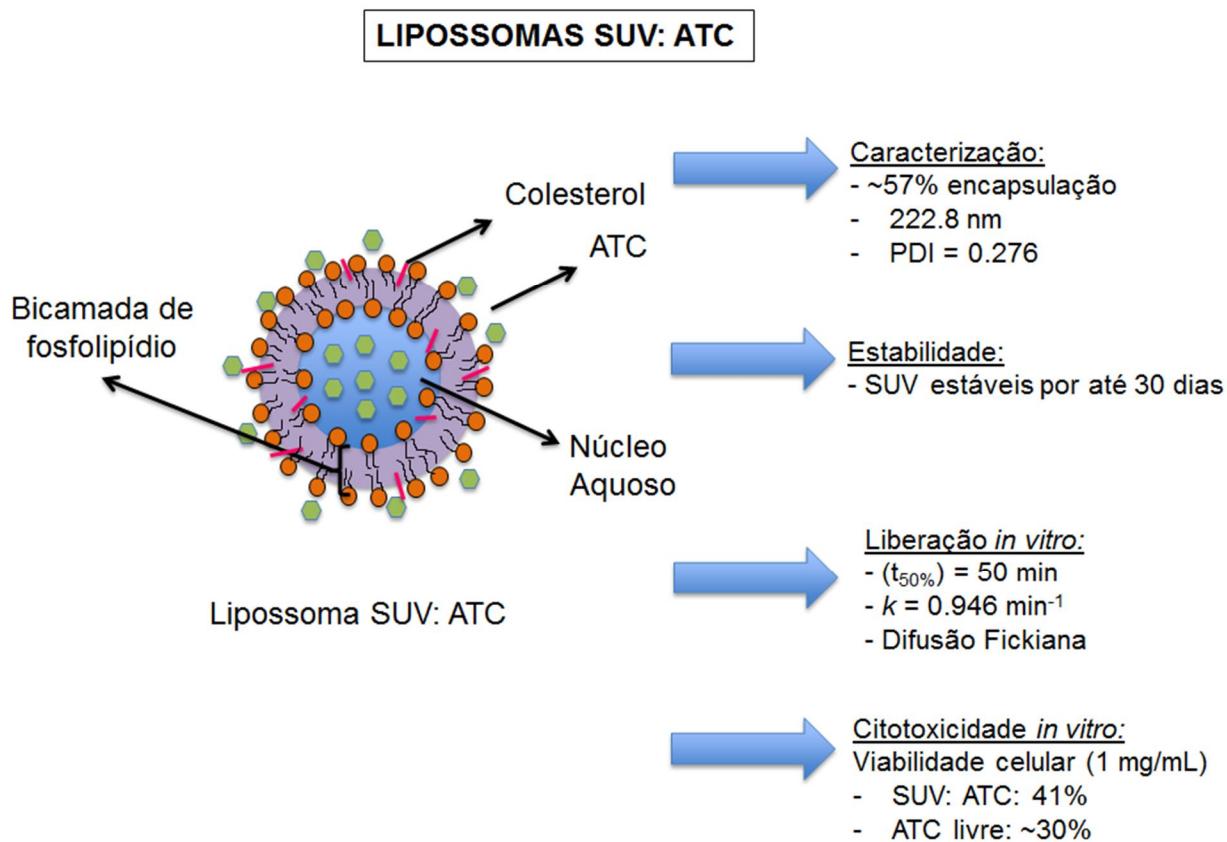
Tabela 1: Resumo dos principais dados obtidos das formulações (NC PCL, NE Alg/Quit, SLN, NC PEG-PCL e SUV) as quais foram otimizadas, todas contendo ATC. Relação dos dados físico-químicos e a forma do AL presente em cada uma das formulações.

Parâmetro	NC PCL	NLS	NE Alg/Quit	NC PEG-PCL	SUV
Forma do AL	Não ionizada	Não ionizada	Ionizada	Ionizada	Ionizada
Diâmetro médio (nm)	452.9	244.1	349.4	569.2	222.8
Polidispersão	0.08	0.109	0.257	0.144	0.276
Potencial zeta (mV)	-5.2	-14.9	-23.1	-18.9	- 48.6
Encapsulação (%)	~78	~65	~45	~60	~57

De acordo com a Tabela 1, pode-se ver um resumo dos principais resultados obtidos para as formulações. Neste sentido, todas elas obtiveram bons parâmetros coloidais. As formulações produzidas com a forma não ionizada da ATC apresentaram eficiência de encapsulação maior do que as formulações feitas com a forma ionizada. Provavelmente isto deve-se ao fato de que a forma não ionizada possui uma solubilidade aquosa menor e assim, durante a formação da nanopartícula, o fármaco interage melhor com os componentes mais hidrofóbicos, ficando a maior parte retida no núcleo oleoso ou na parede polimérica (no caso das NC PCL) ou na matriz lipídica (no caso das NLS). As NC PEG-PCL, as NE Alg/Quit e as SUV obtiveram valores menores de encapsulação devido a uma possível interação mais superficial da forma ionizada com os componentes das formulações. Com relação a estabilidade das suspensões, todas as estudadas apresentaram valores satisfatórios dos parâmetros (diâmetro médio, polidispersão, pH e eficiência de encapsulação) durante o período analisado (180 dias), porém a formulação de SUV apresentou valores dos parâmetros coloidais estáveis por apenas 30 dias.

Tabela 2: Resumo dos principais dados obtidos com o experimento de cinética de liberação *in vitro* para os sistemas NC PCL, NC PEG-PCL, NE Alg/Quit, NLS e SUV todos contendo ATC. Relação dos dados de liberação com a eficiência de encapsulação e a forma do AL presente em cada uma das formulações.

Parâmetro	NC PCL	NLS	NE Alg/Quit	NC PEG-PCL	SUV
Forma do AL	Não ionizada	Não ionizada	Ionizada	Ionizada	Ionizada
Encapsulação (%)	~78	~65	~45	~60	~57
$t_{50\%}$(min)	400	300	100	150	50
Mecanismo	Difusão	Difusão	Difusão	Difusão	Difusão
Constante (k)	$0,0052$ min^{-1}	$0,0868$ min^{-1}	$0,623$ min^{-1}	$0,329$ min^{-1}	$0,946$ min^{-1}

$t_{50\%}$ = tempo para liberação do 50% do total de fármaco presente no sistema.

Comparando os sistemas nanoparticulados (Tabela 2), foi possível observar que as NC PCL foram as que obtiveram maior eficiência de encapsulação do fármaco ATC, e perfil de liberação mais lento ($t_{50\%}$ = 400 min, k = 0,0052 min^{-1}), seguido das NLS ($t_{50\%}$ = 300 min, k = 0,08688 min^{-1}), NC PEG-PCL ($t_{50\%}$ = 150 min, k = 0,329 min^{-1}) e por último as NE Alg/Quit ($t_{50\%}$ = 100 min, k = 0,623 min^{-1}). Os resultados da cinética de liberação estão relacionados com os

valores alcançados para eficiência de encapsulação. Provavelmente as NE Alg/Quit obtiveram um perfil de liberação mais rápido devido a menor eficiência de encapsulação e a interação da ATC ocorrer de forma mais superficial por interação eletrostática. As NC PEG-PCL e NLS obtiveram parâmetros comparáveis aos parâmetros das NC PCL, uma vez que estão veiculando a mesma forma de ATC (não ionizada) e possuírem eficiência de encapsulação relativamente alta. As NC PCL mostraram um perfil mais lento devido a uma possível interação maior da ATC com o núcleo oleoso, dificultando a liberação do fármaco para o meio.

Tabela 3: Resumo dos principais dados obtidos com o experimento de citotoxicidade *in vitro* através da avaliação da viabilidade celular em células 3T3 (fibroblastos de camundongo) pela redução de MTT para os sistemas NC PCL, NC PEG-PCL, NE Alg/Quit e NLS, todos contendo ATC. Relação dos dados de citotoxicidade com a cinética de liberação, eficiência de encapsulação e a forma do AL presente em cada uma das formulações.

Parâmetro	ATC livre		NC PCL	NLS	NE Alg/Quit	NC PEG-PCL
Forma do AL	Não ionizada	Ionizada	Não ionizada	Não ionizada	Ionizada	Ionizada
Encapsulação (%)	-	-	~78	~65	~45	~60
$t_{50\%}$ (min)	45	45	400	300	100	150
Viabilidade Celular (%)	~70	~50	~89,6	~79,3	~65,9	~89

Com relação à citotoxicidade (Tabela 3), todas as formulações foram satisfatórias uma vez que conseguiram reduzir a toxicidade do fármaco ATC. Neste sentido, pode-se observar que a formulação com maior eficiência de encapsulação (NC PCL) foi aquela que obteve maior porcentagem de viabilidade celular. Isto corrobora com o efeito protetor da encapsulação de fármacos em sistemas de liberação modificada, uma vez que há uma menor quantidade de fármaco disponível no meio, a toxicidade é menor quando comparada ao fármaco livre em solução. Assim, como as NC PCL possuem uma menor quantidade de ATC livre, a toxicidade desta formulação é menor quando comparada a ATC livre e as outras formulações estudadas com eficiência de encapsulação menor. Porém é visível que todas as formulações tiveram uma toxicidade menor quando comparadas com ATC livre (*p<0,05*).

A viabilidade celular para as formulações de SUV foi testada em outra linhagem celular (a CHO, Chinese Hamster Ovary), não sendo possível uma comparação direta dos valores de

citotoxicidade com as demais formulações testadas. Ainda assim, os valores de viabilidade celular obtidos não foram satisfatórios para redução da toxicidade da ATC (~41%, 1 mg/mL de ATC)

Uma vez caracterizados, os sistemas nanoparticulados foram dispersos em gel de Aristoflex® AVC. Este veículo semissólido demonstrou-se apropriado para veiculação de suspensões de nanopartículas contendo ATC uma vez que suas características organolépticas não foram alteradas ao longo do tempo para todas as formulações e os parâmetros coloidais das nanopartículas não se modificaram. Os experimentos de permeação *in vitro* demonstraram que o gel contendo ATC livre possui em tempo para início de permeação maior do que para os géis contendo nanopartículas (*time lag* = 0,670h), bem como fluxo e coeficiente de permeabilidade maior. O gel que obteve *time lag* (0,121 h), fluxo (35,68 µg/cm^2/h) e coeficiente de permeabilidade (0,00197 cm^2/h) menor foi o gel contendo NC PCL. Estes resultados são condizentes com os dados de cinética de liberação da ATC em suspensão de NC PCL, demonstrando mais uma vez que este sistema foi o mais adequado para modificar o perfil de liberação da ATC, fazendo com que ela seja liberada em um tempo maior do que formulações com este anestésico livre. Os sistemas de NE Alg/Quit, NC PEG-PCL e SUV contendo ATC não foram estudados em formulações semissólidas.

Analisando as suspensões de nanopartículas, pensando em uma futura aplicação clínica por via infiltrativa, a formulação NC PCL com ATC mostra-se a mais promissora para o controle da dor em procedimentos cirúrgicos de longa duração, uma vez que ela possui o perfil de liberação mais lento e sustentado de todas as suspensões estudadas. Acredita-se que esta suspensão poderia ser capaz de manter um maior tempo de anestesia sustentada. Por outro lado, as suspensões de NE Alg/Quit, NC PEG-PCL e NLS mostram-se mais promissoras para utilização de procedimentos cirúrgicos de curta duração. Neste caso, essas suspensões possuem um perfil de liberação mais lento do que a ATC livre e acredita-se que seria capaz de reduzir a quantidade de ATC nas formulações usuais (4 para 2%) para atingir um mesmo tempo de anestesia. Assim, o risco de toxicidade e ocorrência de reações adversas seria menor. As formulações de SUV apresentaram resultados considerados pouco satisfatórios com relação à estabilidade físico-química e citotoxicidade *in vitro* comparado com as demais formulações estudadas, por este motivo o estudo de cinética de liberação não foi realizado.

Com relação às formulações semissólidas de Aristoflex®AVC contendo ATC livre e nanoencapsulada, vislumbrando uma futura aplicação clínica tópica em pele, as formulações contendo nanopartículas foram notadamente melhores do que a formulação contendo ATC livre

_____

nos quesitos início da permeação (*time lag*), coeficiente de permeabilidade e fluxo. Isto significa que as formulações com nanopartículas promovem um início de ação mais rápido e mantém a permeação por muito mais tempo tornando a liberação sustentada, sendo assim mais promissoras para uso em procedimentos clínicos e controle da dor.

Capítulo 8 – Conclusões gerais

Este estudo revelou importantes informações referentes à preparação e caracterização de nanopartículas e formulações semissólidas contendo o anestésico local ATC. Através da aplicação da metodologia de superfície de resposta foi possível determinar as proporções ideais das formulações de NC PCL, NE Alg/Quit, e SUV para alcançar uma maior eficiência de encapsulação de ATC e estabilidade das suspensões. A eficiência de encapsulação da ATC foi alta, com valores em torno de 78% para NC PCL, 45% para NE Alg/Quit, 60% para NC PEG-PCL, 65% para NLS e 57% para SUV.

Os estudos de estabilidade demostraram que as NC PCL, NE Alg/Qui, NC PEG-PCL e NLS contendo ATC apresentaram parâmetros coloidais compatíveis com suspensões estáveis por um período de 120 dias. As SUV apresentaram estabilidade por apenas 30 dias.

A análise morfológica através das imagens obtidas por microscopia eletrônica de transmissão para NC PCL, NE Alg/Quit, NC PEG-PCL e NLS contendo ATC, pode-se observar que as partículas apresentam-se com formato esférico e diâmetro na faixa entre 200 e 500 nm.

A citotoxicidade das NC PCL, NE Alg/Quit, NC PEG-PCL e NLS contendo ATC foi avaliada através da técnica de viabilidade celular através da redução de MTT. A encapsulação da ATC demonstrou redução da toxicidade do fármaco uma vez que foram observados valores maiores de viabilidade celular para a formulação quando comparado com ATC livre. Isto ocorre devido à eficiência de encapsulação de ATC. Sendo assim, há menor quantidade de ATC livre, fazendo com que a toxicidade seja diminuída. As SUV não foram capazes de reduzir a toxicidade da ATC de forma satisfatória quando comparada com os outros sistemas.

O perfil de liberação da ATC foi modificado quando comparado com as NC PCL, NE Alg/Quit, NC PEG-PCL e NLS apresentando uma liberação mais lenta e sustentada comparada com a cinética da ATC livre. A aplicação de um modelo matemático permitiu calcular o valor das constantes de liberação (k) e mostrou que o perfil de liberação da ATC nas nanopartículas se deu por de difusão fickiana.

Os experimentos de infravermelho e calorimetria exploratória diferencial demonstraram que existe interação entre o fármaco e as nanopartículas uma vez que houve diminuição da temperatura de fusão sugerindo alterando na organização cristalina do polímero.

As formulações semissólidas foram preparadas com gel de Aristoflex® AVC e foram incorporadas ATC livre e encapsulada em NC PCL e NLS. A análise sensorial das formulações

143

no tempo zero e 30 dias demonstrou que não houve alteração das características iniciais de cor, odor e aparência indicando que o veículo escolhido foi adequado. A análise do diâmetro médio e polidispersão das nanopartículas incorporadas no gel demonstrou que não houve alteração dos parâmetros coloidais indicando que o veículo não alterou a estabilidade das suspensões de nanopartículas contendo ATC. Os ensaios de permeação *in vitro* para as formulações de géis demostraram que as preparações contendo nanopartículas obtiveram *time lag* menor do que a preparação contendo ATC livre e também apresentaram fluxo menor de ATC através da membrana. Isto se deve ao fato das nanopartículas modificarem o perfil de liberação do fármaco, deixando-o mais lento e sustentado. A formulação que obteve melhores parâmetros de permeação foi a que continha NC PCL com ATC. Os testes reológicos demonstraram que os géis contendo nanopartículas com ATC apresentaram fluxo não-Newtoniano psedoplástico com tixotropia, fenômeno este que não foi observado para o gel contendo ATC livre.

Este estudo abre assim perspectivas para o futuro uso de diferentes sistemas nanocarredores para o anestésico local articaína visando uma futura aplicação por via infiltrativa e/ou tópica em pele na prática clínica.

Referências Bibliográficas

Abdelbary, G. and Fahmy, R. H. (2009). "Diazepam-loaded solid lipid nanoparticles: design and characterization." *AAPS PharmSciTech* **10**(1): 211-219.

Agnihotri, S. A., Mallikarjuna, N. N. and Aminabhavi, T. M. (2004). "Recent advances on chitosan-based micro- and nanoparticles in drug delivery." *J Control Release* **100**(1): 5-28.

Alexis, F., Rhee, J. W., Richie, J. P., Radovic-Moreno, A. F., Langer, R. and Farokhzad, O. C. (2008). "New frontiers in nanotechnology for cancer treatment." *Urol Oncol* **26**(1): 74-85.

Ali, H., Shirode, A. B., Sylvester, P. W. and Nazzal, S. (2010). "Preparation and in vitro antiproliferative effect of tocotrienol loaded lipid nanoparticles." *Colloids Surf A* **353**: 43-51.

Alonso, M. J. (2004). "Nanomedicines for overcoming biological barriers." *Biomed Pharmacother* **58**(3): 168-172.

Alvarez-Román, R., Naik, A., Kalia, N., Guya, H. and Fessi, H. (2004). "Skin penetration and distribution of polymeric nanoparticles." *J Control Release* **99**: 53-62.

Alves, M. P., Scarrone, A. L., Santos, M., Pohlmann, A. R. and Guterres, S. S. (2007). "Human skin penetration and distribution of nimesulide from hydrophilic gels containing nanocarriers." *Int J Pharm* **341**(1-2): 215-220.

Andrews, G. P., Donnelly, L., Jones, D. S., Curran, R. M., Morrow, R. J., Woolfson, A. D. and Malcolm, R. K. (2009). "Characterization of the rheological, mucoadhesive, and drug release properties of highly structured gel platforms for intravaginal drug delivery." *Biomacromolecules* **10**(9): 2427-2435.

Ansel, H. C., Popovich, N. G. and Allen, L. V. (2000). *Formas farmacêuticas e sistemas de liberação de fármacos.* São Paulo, Premier Editorial.

Anton, N., Benoit, J. P. and Saulnier, P. (2008). "Design and production of nanoparticles formulated from nano-emulsion templates-a review." *J Control Release* **128**(3): 185-199.

Aranha, I. B. and Lucas, E. F. (2001). "Poli(Álcool Vinílico) modificado com cadeias hidrocarbônicas: avaliação do balanço hidrófilo/lipófilo." *Polímeros* **11**(4): 174-181.

Ashraf, H., Kazem, M., Dianat, O. and Noghrehkar, F. (2013). "Efficacy of articaine versus lidocaine in block and infiltration anesthesia administered in teeth with irreversible pulpitis: a prospective, randomized, double-blind study." *Journal of Endodontics* **39**(1): 6-10.

Assis, L. M., Zavareze, E. R., Prentice-Hernandez, C. and Souza-Soares, L. A. (2012). "Características de nanopartículas e potenciais de aplicação em alimentos." *Brazilian Journal of Food Technology* **15**: 99-109.

Attama, A. A., Reichl, S. and Muller-Goymann, C. C. (2009). "Lipid nanoparticles as drug/gene delivery systems to the retina." *Curr Eye Res* **34**: 698-705.

Avgoustakis, K., Beletsi, A., Panagi, Z., Klepetsanis, P., Livaniou, E., Evangelatos, G. and Ithakissios, D. S. (2003). "Effect of copolymer composition on the physicochemical characteristics, in vitro stability, and biodistribution of PLGA-mPEG nanoparticles." *Int J Pharm* **259**(1-2): 115-127.

Barros-Neto, B., Scarminio, I. S. and Bruns, R. E. (2007). *Como fazer experimentos*. Campinas, Editora Unicamp.

Basso, R. C., Ribeiro, A. P. B., Masuchi, M. H., Gioelli, L. A., Gonçalves, L. A. G., dos Santos, A. O., Cardoso, L. P. and Grimaldi, R. (2010). "Tripalmitin and monoacylglycerols as modifiers in the crystallisation of palm oil." *Food Chem* **122**: 1185-1192.

Batheja, P., Sheihet, L., Kohn, J., Singer, A. J. and Michniak-Kohn, B. (2011). "Topical drug delivery by a polymeric nanosphere gel: Formulation optimization and in vitro and in vivo skin distribution studies." *J Control Release* **149**(2): 159-167.

Batista, C. M., Carvalho, C. M. B. and Magalhães, N. S. S. (2007). "Lipossomas e suas aplicações terapêuticas: Estado da arte." *Rev Bras Cienc Farm* **43**: 167-179.

Bawa, R. (2007). "Patents and nanomedicine." *Nanomedicine* **2**(3): 351-374.

Box, G. E. P. and Drapper, N. R. (1987). *Empirical model building and response surfaces*. NY, John Wiley and Sons.

Brasil (2003). Resolution RE 899. A. N. d. V. Sanitária. Brasil.

Brown, M. B., Martin, G. P., Jones, S. A. and Akomeah, F. K. (2006). "Dermal and transdermal drug delivery systems: current and future prospects." *Drug Deliv* **13**(3): 175-187.

Buse, J. and El-Aneed, A. (2010). "Properties, engineering and applications of lipid-based nanoparticle drug-delivery systems: current research and advances." *Nanomedicine* **5**(8): 1237-1260.

Butterworth, J. F. t., Brownlow, R. C., Leith, J. P., Prielipp, R. C. and Cole, L. R. (1993). "Bupivacaine inhibits cyclic-3',5'-adenosine monophosphate production. A possible contributing factor to cardiovascular toxicity." *Anesthesiology* **79**(1): 88-95.

Byrro, R. M. D., Miyashita, D., Albulquerque, V. B., Cruz, A. A. V. and Cunha Jr, A. S. (2009). "Sistemas biodegradáveis contendo acetato de prednisolona para administração orbitária." *Arq Bras Oftalmol* **72**: 444-450.

Calvo, P., Remunan-Lopez, C., Vila-Jato, J. L. and Alonso, M. J. (1997). "Chitosan and chitosan/ethylene oxide-propylene oxide block copolymer nanoparticles as novel carriers for proteins and vaccines." *Pharm Res* **14**(10): 1431-1436.

Campos, E. V. R., de Melo, N. F. S., de Paula, E., Rosa, A. H. and Fraceto, L. F. (2013a). "Screening of conditions for the preparation of poly(epsilon-caprolactone) nanocapsules containing the local anesthetic articaine." *J Colloid Sci Biotechnol* **2**(2): 106-111.

Campos, E. V. R., de Melo, N. F. S., Guilherme, V. A., de Paula, E., Rosa, A. H., de Araujo, D. R. and Fraceto, L. F. (2013b). "Preparation and characterization of poly(epsilon-caprolactone) nanospheres containing the local anesthetic lidocaine." *J Pharm Sci* **102**(1): 215-226.

Canfarotta, F., Whitcombe, M. J. and Piletsky, S. A. (2013). "Polymeric nanoparticles for optical sensing." *Biotechnol Adv* **31**(8): 1585-1599.

Catteral, W. and Mackie, K. (1996). Anestésicos locais. *As bases farmacológicas da terapêutica.* L. S. Goodmann and A. G. Gilman. Rio de Janeiro, McGraw-Hill.

Cauchetier, E., Deniau, M., Fessi, H., Astier, A. and Paul, M. (2003). "Atovaquone-loaded nanocapsules: influence of the nature of the polymer on their in vitro characteristics." *Int J Pharm* **250**(1): 273-281.

Cereda, C. M., Brunetto, G. B., de Araujo, D. R. and de Paula, E. (2006). "Liposomal formulations of prilocaine, lidocaine and mepivacaine prolong analgesic duration." *Can J Anaesth* **53**(11): 1092-1097.

Cereda, C. M., de Araujo, D. R., Brunetto, G. B. and De Paula, E. (2004a). "Liposomal prilocaine: preparation, characterization, and in vivo evaluation." *J Pharm Pharm Sci* **7**(2): 235-240.

Cereda, C. M., Tofoli, G. R., Maturana, L. G., Pierucci, A., Nunes, L. A., Franz-Montan, M., de Oliveira, A. L., Arana, S., de Araujo, D. R. and de Paula, E. (2012). "Local neurotoxicity and myotoxicity evaluation of cyclodextrin complexes of bupivacaine and ropivacaine." *Anesth Analg* **115**(5): 1234-1241.

Cereda, C. M. S. (2007). *Sistema de liberação prolongada com o anestésico local prilocaína em lipossomas: preparo, caracterização e testes biológicos.* PhD, Universidade Estadual de Campinas.

Cereda, C. M. S., de Araujo, D. R., Brunetto, G. B. and de Paula, E. (2004b). "Liposomal prilocaine: preparation, characterization, and in vivo evaluation." *J Pharm Pharm Sci* **7**: 235-240.

Cevc, G. and Vierl, U. (2010). "Nanotechnology and the transdermal route: A state of the art review and critical appraisal." *J Controlled Release* **141**: 277-299.

Ch'ng, H. S., Park, H., Kelly, P. and Robinson, J. R. (1985). "Bioadhesive polymers as platforms for oral controlled drug delivery II: synthesis and evaluation of some swelling, water-insoluble bioadhesive polymers." *J Pharm Sci* **74**(4): 399-405.

Chen, H., Chang, X., Du, D., Li, J., Xu, H. and Yang, X. (2006). "Microemulsion-based hydrogel formulation of ibuprofen for topical delivery." *Int J Pharm* **315**(1-2): 52-58.

Chopra, S., Patil, G. V. and Motwani, S. K. (2007). "Release modulating hydrophilic matrix systems of losartan potassium: optimization of formulation using statistical experimental design." *Eur J Pharm Biopharm* **66**(1): 73-82.

Cohen, S. M. (2012). "Extended pain relief trial utilizing infiltration of Exparel((R)), a long-acting multivesicular liposome formulation of bupivacaine: a Phase IV health economic trial in adult patients undergoing open colectomy." *J Pain Res* **5**: 567-572.

Collins, V. J. (1993). *Principles of Anesthesiology: general and regional.* USA, Lea & Febiger.

Colombo, G., Padera, R., Langer, R. and Kohane, D. S. (2005). "Prolonged duration local anesthesia with lipid-protein-sugar particles containing bupivacaine and dexamethasone." *J Biomed Mater Res A* **75**(2): 458-464.

Coppi, G., Iannuccelli, V., Leo, E., Bernabei, M. T. and Cameroni, R. (2002). "Protein immobilization in crosslinked alginate microparticles." *J Microencapsul* **19**(1): 37-44.

Corrêa, N. M., Camargo Junior, F. B., Ignácio, R. F. and Leonardi, G. R. (2005). "Avaliação do comportamento reológico de diferentes géis hidrofílicos." *Rev Bras Cienc Farm* **41**(1): 73-78.

Costa, I. M. (2005). *Estudo de pré-formulação com composto polifenólico quercetina*. Master, Universidade Federal do Rio Grande do Sul.

Costa, P. J. C. (2002). "Avaliação in vitro da lioequivalência de formulações farmacêuticas." *Rev Bras Cienc Farm* **38**(2): 141-153.

Covino, B. G. and Vassalo, H. G. (1985). *Anestésicos locais: mecanismos de ação e uso clínico.* Rio de Janeiro, Colina.

Das, S., Ng, W. K., Kanaujia, P., Kim, S. and Tan, R. B. (2011). "Formulation design, preparation and physicochemical characterizations of solid lipid nanoparticles containing a hydrophobic drug: effects of process variables." *Colloids Surf B* **88**(1): 483-489.

de Araujo, D. R., Cereda, C. M., Brunetto, G. B., Pinto, L. M., Santana, M. H. and de Paula, E. (2004). "Encapsulation of mepivacaine prolongs the analgesia provided by sciatic nerve blockade in mice." *Can J Anaesth* **51**(6): 566-572.

de Araújo, D. R., Fraceto, L. F., Braga, A. F. A. and de Paula, E. (2005). "Sistemas de liberação controlada com bupivacaína racêmica (S50-R50) e mistura enantiomérica de bupivacaína (S75-R25): efeitos da complexação com ciclodextrinas no bloqueio do nervo ciático em camundongos." *Rev Bras Anestesiol* **55**(3): 316-328.

de Araujo, D. R., Padula, C., Cereda, C. M., Tofoli, G. R., Brito, R. B., Jr., de Paula, E., Nicoli, S. and Santi, P. (2010). "Bioadhesive films containing benzocaine: correlation between in vitro permeation and in vivo local anesthetic effect." *Pharm Res* **27**(8): 1677-1686.

de Araujo, D. R., Pinto Lde, M., Braga Ade, F. and de Paula, E. (2003). "Drug-delivery systems for local anesthetics: therapeutic applications." *Rev Bras Anestesiol* **53**(5): 663-671.

de Araujo, D. R., Tsuneda, S. S., Cereda, C. M., Del, G. F. C. F., Prete, P. S., Fernandes, S. A., Yokaichiya, F., Franco, M. K., Mazzaro, I., Fraceto, L. F., de, F. A. B. A. and de Paula, E. (2008). "Development and pharmacological evaluation of ropivacaine-2-hydroxypropyl-beta-cyclodextrin inclusion complex." *Eur J Pharm Sci* **33**(1): 60-71.

de Jong, R. H. (1994). *Local Anesthesics*. Springfield, Illinois, C. C. Thomas.

de Lima, R., Feitosa, L. O., Maruyama, C. R., Barga, M. A., Yamawaki, P. C., Vieira, I. J., Teixeira, E. M., Corrêa, A. C., Mattoso, L. H. and Fraceto, L. F. (2012). "Evaluation of the genotoxicity of cellulose nanofibers " *Int J Nanomedicine* **7**: 3555-3565.

de Melo, N. F. S., Campos, E. V. R., de Paula, E., Rosa, A. H. and Fraceto, L. F. (2013). "Factorial design and characterization studies for articaine hydrochloride loaded alginate/chitosan nanoparticles." *J Colloid Sci Biotechnol* **2**(2): 146-152.

de Melo, N. F. S., Campos, E. V. R., Gonçalves, C. M., De Paula, E., Pasquoto, T., De Lima, R., Rosa, A. H. and Fraceto, L. F. (2014). "Development of hydrophilic nanocarriers for the charged form of the local anesthetic articaine. ." *Colloids Surf B* **121**: 66-73.

de Melo, N. F. S., de Araujo, D. R., Grillo, R., Moraes, C. M., de Matos, A. P., de Paula, E., Rosa, A. H. and Fraceto, L. F. (2012). "Benzocaine-loaded polymeric nanocapsules: study of the anesthetic activities." *J Pharm Sci* **101**(3): 1157-1165.

de Melo, N. F. S., Grillo, R., Guilherme, V. A., de Araujo, D. R., de Paula, E., Rosa, A. H. and Fraceto, L. F. (2011). "Poly(lactide-co-glycolide) nanocapsules containing benzocaine: influence of the composition of the oily nucleus on physico-chemical properties and anesthetic activity." *Pharm Res* **28**(8): 1984-1994.

de Melo, N. F. S., Grillo, R., Rosa, A. H., Dias Filho, N. L., de Paula, E., de Araujo, D. R. and Fraceto, L. F. (2010). "Desenvolvimento e caracterização de nanocápsulas de poli (L-lactídeo) contendo benzocaína." *Quim Nova* **33**(1): 65-69.

de Oliveira, E. F., Paula, H. C. and Paula, R. C. (2014). "Alginate/cashew gum nanoparticles for essential oil encapsulation." *Colloids Surf B* **113**: 146-151.

de Paula, E. and Schreier, S. (1995). "Use of a novel method for determination of partition coefficients to compare the effect of local anesthetics on membrane structure." *Biochim Biophys Acta* **1240**(1): 25-33.

De, S. and Robinson, D. (2003). "Polymer relationships during preparation of chitosan-alginate and poly-l-lysine-alginate nanospheres." *J Control Release* **89**(1): 101-112.

de Santis, A. K. (2008). *Formas farmacêuticas emi-sólidas de uso tópico contendo nifedipina: Desenvolvimento galênico e avaliação biofarmacotécnica*. Master, Universidade Federal do Rio de Janeiro.

Derakhshandeh, K., Erfan, M. and Dadashzadeh, S. (2007). "Encapsulation of 9-nitrocamptothecin, a novel anticancer drug, in biodegradable nanoparticles: factorial design, characterization and release kinetics." *Eur J Pharm Biopharm* **66**(1): 34-41.

Diaz, M. (2009). "Is it safe to use articaine? ." *TeamWork* **2**: 28-35.

Diniz, D. G. A. (2008). *Obtenção, caracterização e avaliação da citotoxicidade sobre células neoplásicas da isotretinoína encapsulada em lipossomas e nanocápsulas poliméricas* PhD, Universidade de Brasília.

Doustgani, A., Farahani, E. V., Imani, M. and Doulabi, A. H. (2012). "Dexamethasone sodium phosphate release from chitosan nanoparticles prepared by ionic gelation method." *J Colloid Sci Biotechnol* **1**(1): 42-50.

Dower, J. S., Jr. (2003). "A review of paresthesia in association with administration of local anesthesia." *Dent Today* **22**(2): 64-69.

Dubey, V., Mishra, D. and Jain, J. N. (2007). "Melatonin loaded ethanolic liposomes: Physicochemical characterization and enhanced transdermal delivery." *Eur J Pharm Biopharm* **607**: 398-405.

Durán, N., Mattoso, L. H. C. and Morais, P. C. (2006). *Nanotecnologia: Inrodução, preparação e caracterização de nanomateriais e exemplos de aplicação*. São Paulo, Artliber.

El Maghraby, G. M., Williams, A. C. and Barry, B. W. (2006). "Can drug-bearing liposomes penetrate intact skin?" *J Pharm Pharmacol* **58**(4): 415-429.

Eldem, T., Speiser, P. and Hincal, A. (1991). "Optimization of spray-dried and -congealed lipid micropellets and characterization of their surface morphology by scanning electron microscopy." *Pharm Res* **8**(1): 47-54.

Eldsater, C., Erlandsson, B., Renstad, R., Albertsson, A.-C. and Karlsson, S. (2001). "The biodegradation of amorphous and crystalline regions in fiml-blown poly(ε caprolactone)." *Polymer* **41**: 1297-1304.

Elsayed, M. M., Abdallah, O. Y., Naggar, V. F. and Khalafallah, N. M. (2007). "Deformable liposomes and ethosomes as carriers for skin delivery of ketotifen." *Pharmazie* **62**: 133-137.

Farias, G. D. (2011). *Formulações semissólidas contendo nanocápsulas de adapaleno: determinação da estabilidade, avaliação da liberação in vitro e ensaios utilizando biometria cutânea*. Master, Centro Universitário Franciscano de Santa Maria.

Ferreira, S. L., Bruns, R. E., Ferreira, H. S., Matos, G. D., David, J. M., Brandao, G. C., da Silva, E. G., Portugal, L. A., dos Reis, P. S., Souza, A. S. and dos Santos, W. N. (2007). "Box-Behnken design: an alternative for the optimization of analytical methods." *Anal Chim Acta* **597**(2): 179-186.

Fraceto, L. F., de Araujo, D. R. and de Paula, E. (2008). "Anestésicos locais: interação com membranas biológicas e com o canal de sódio voltagem-dependente." *Quim Nova* **31**: 1775-1783.

Fraceto, L. F., Oyama, S., Jr., Nakaie, C. R., Spisni, A., de Paula, E. and Pertinhez, T. A. (2006). "Interaction of local anesthetics with a peptide encompassing the IV/S4-S5 linker of the Na+ channel." *Biophys Chem* **123**(1): 29-39.

Franchi, L. P., Santos, R. A., Matsubara, E. Y., de Lima, J. C., Rosolen, J. M. and Takahashi, C. S. (2012). "Citotoxicidade e genotoxicidade de nanotubos de carbono. ." *Quim Nova* **35**: 571-580.

Franz-Montan, M., Silva, A. L., Fraceto, L. F., Volpato, M. C., Paula, E., Ranali, J. and Groppo, F. C. (2010). "Liposomal encapsulation improves the duration of soft tissue anesthesia but does not induce pulpal anesthesia." *J Clin Anesth* **22**(5): 313-317.

Frézard, F., Schettini, D. A., Rocha, O. G. F. and Demicheli, C. (2005). "Lipossomas: propriedades físico-químicas e farmacológicas, aplicações na quimioterapia à base de antimônio." *Quim Nova* **28**: 511-518.

Gamisans, F., Lacoulonche, F., Chauvet, A., Espina, M., Garcia, M. L. and Egea, M. A. (1999). "Flurbiprofen-loaded nanospheres: analysis of the matrix structure by thermal methods." *Int J Pharm* **179**(1): 37-48.

Ganguly, S. and Dash, A. K. (2004). "A novel in situ gel for sustained drug delivery and targeting." *Int J Pharm* **276**(1-2): 83-92.

Gazori, T., Khoshayand, M. R., Azizi, E., Yazdizade, P., Nomani, A. and Haririan, I. (2009). "Evaluation of Alginate/Chitosan nanoparticles as antisense delivery vector: Formulation, optimization and in vitro characterization." *Carbohyd Polym* **77**(3): 599-606.

George, M. and Abraham, T. E. (2006). "Polyionic hydrocolloids for the intestinal delivery of protein drugs: alginate and chitosan--a review." *J Control Release* **114**(1): 1-14.

Ghanbarzadeh, S., Valizadeh, H. and Zakeri-Milani, P. (2013). "Application of response surface methodology in development of sirolimus liposomes prepared by thin film hydration technique." *Bioimpacts* **3**(2): 75-81.

Gonzalez-Rodriguez, M. L., Holgado, M. A., Sanchez-Lafuente, C., Rabasco, A. M. and Fini, A. (2002). "Alginate/chitosan particulate systems for sodium diclofenac release." *Int J Pharm* **232**(1-2): 225-234.

Gopferich, A. (1996). "Mechanisms of polymer degradation and erosion." *Biomaterials* **17**(2): 103-114.

Gorner, T., Gref, R., Michenot, D., Sommer, F., Tran, M. N. and Dellacherie, E. (1999). "Lidocaine-loaded biodegradable nanospheres. I. Optimization Of the drug incorporation into the polymer matrix." *J Control Release* **57**(3): 259-268.

Govender, T., Riley, T., Ehtezazi, T., Garnett, M. C., Stolnik, S., Illum, L. and Davis, S. S. (2000). "Defining the drug incorporation properties of PLA-PEG nanoparticles." *Int J Pharm* **199**(1): 95-110.

Govender, T., Stolnik, S., Garnett, M. C., Illum, L. and Davis, S. S. (1999). "PLGA nanoparticles prepared by nanoprecipitation: drug loading and release studies of a water soluble drug." *J Control Release* **57**(2): 171-185.

Grillo, R., De Melo, N. F. S., de Araújo, D. R., de Paula, E., Dias Filho, N. L., Rosa, A. H. and Fraceto, L. F. (2009). "Validation of an HPLC Method for quantitative Determination of Benzocaine in PHBV-Microparticles and PLA-Nanoparticles." *Lat Am J Pharm* **28**: 393-399.

Grillo, R., de Melo, N. F. S., de Araujo, D. R., de Paula, E., Rosa, A. H. and Fraceto, L. F. (2010). "Polymeric alginate nanoparticles containing the local anesthetic bupivacaine." *J Drug Target* **18**(9): 688-699.

Gupta, S. P. (1991). "QSAR studies on local anesthetics." *Chem Rev* **91**: 1109-1119.

Guterres, S. S., Fessi, H., Barratt, G., Puisieux, F. and Devissaguet, J. P. (1995). "Poly(D,L-lactide) nanocapsules containing non-steroidal anti-inflammatory drugs: gastrointestinal tolerance following intravenous and oral administration." *Pharm Res* **12**(10): 1545-1547.

Haug, A. and Larsen, B. (1962). "Quantitative determination of the uronic acid composition of alginates." *Acta Chem Scand* **16**: 1908–1918

Helgason, T., Awad, T. S., Kristbergsson, K., McClements, D. J. and Weiss, J. (2009). "Effect of surfactant surface coverage on formation of solid lipid nanoparticles (SLN)." *J Colloid Interface Sci* **334**(1): 75-81.

Heuschkel, S., Goebel, A. and Neubert, R. H. (2008). "Microemulsions--modern colloidal carrier for dermal and transdermal drug delivery." *J Pharm Sci* **97**(2): 603-631.

Hotza, D. (1997). "Colagem de folhas cerâmicas " *Cêramica* **43**(283-284): 159-166.

Hsu, S. H., Tang, C. M. and Lin, C. C. (2004). "Biocompatibility of poly(epsilon-caprolactone)/poly(ethylene glycol) diblock copolymers with nanophase separation." *Biomaterials* **25**(25): 5593-5601.

Hu, L., Xing, Q., Meng, J. and Shang, C. (2010). "Preparation and enhanced oral bioavailability of cryptotanshinone-loaded solid lipid nanoparticles." *AAPS PharmSciTech* **11**(2): 582-587.

ICH (2005). Validation of Analytical Procedures: Text and Methodology (Q2R1). I. C. o. Harmonization. Geneva.

Igartua, M., Saulnier, P., Heurtault, B., Pech, B., Proust, J. E., Pedraz, J. L. and Benoit, J. P. (2002). "Development and characterization of solid lipid nanoparticles loaded with magnetite." *Int J Pharm* **233**(1-2): 149-157.

Isen, D. A. (2000). "Articaine: pharmacology and clinical use of a recently approved local anesthetic." *Dent Today* **19**(11): 72-77.

Jain, S. K., Chourasia, M. K., Masuriha, R., Soni, V., Jain, A., Jain, N. K. and Gupta, Y. (2005). "Solid lipid nanoparticles bearing flurbiprofen for transdermal delivery." *Drug Deliv* **12**(4): 207-215.

Janes, K. A., Calvo, P. and Alonso, M. J. (2001a). "Polysaccharide colloidal particles as delivery systems for macromolecules." *Adv Drug Deliv Rev* **47**(1): 83-97.

Janes, K. A., Fresneau, M. P., Marazuela, A., Fabra, A. and Alonso, M. J. (2001b). "Chitosan nanoparticles as delivery systems for doxorubicin." *J Control Release* **73**(2-3): 255-267.

Jenning, V. and Gohla, S. H. (2001). "Encapsulation of retinoids in solid lipid nanoparticles (SLN)." *J Microencapsul* **18**(2): 149-158.

Johansen, O. (2004). *Comparison of articaine and lidocaine used as dental local anesthetics*, University of Oslo.

Kalo, P. and Kemppinen, A. (2003). Triglycerides/structures and properties. *Encyclopedia of food sciences and nutrition*. B. Caballero, L. Turgo and P. M. Finglas. London, Academic Press**:** 5857-5868.

Kaushik, D., Costache, A. and Michniak-Kohn, B. (2010). "Percutaneous penetration modifiers and formulation effects." *Int J Pharm* **386**(1-2): 42-51.

Kellens, M., Meeussen, W. and Reynaers, H. (1990). "Crystallization and phase studies os tripalmitin. ." *Chem Phys Lipids* **55**: 163-178.

Khatiwala, V. K., Shekhar, N., Aggarwal, S. and Mandal, U. K. (2008). "Biodegradation of Poly(e-caprolactone) (PCL) Film by Alcaligenes Faecalis." *J Polym Environ* **16**(1): 61-67.

Knudsen, K., Beckman Suurkula, M., Blomberg, S., Sjovall, J. and Edvardsson, N. (1997). "Central nervous and cardiovascular effects of i.v. infusions of ropivacaine, bupivacaine and placebo in volunteers." *Br J Anaesth* **78**(5): 507-514.

Koo, O. M., Rubinstein, I. and Onyuksel, H. (2005). "Role of nanotechnology in targeted drug delivery and imaging: a concise review." *Nanomedicine* **1**(3): 193-212.

Kumar, A. and Sawant, K. (2013). "Encapulation of exemestane in polycaprolactone nanoparticles: optimization, characterization and release kinetics. ." *Cancer Nano* **4**: 57-71.

Kumari, A., Yadav, S. K. and Yadav, S. C. (2010). "Biodegradable polymeric nanoparticles based drug delivery systems." *Colloids Surf B* **75**: 1-18.

Kuo, Y. C. and Chen, H. H. (2009). "Entrapment and release of saquinavir using novel cationic solid lipid nanoparticles." *Int J Pharm* **365**(1-2): 206-213.

Kuzma, P. J., Kline, M. D., Calkins, M. D. and Staats, P. S. (1997). "Progress in the development of ultra-long-acting local anesthetics." *Reg Anesth* **22**(6): 543-551.

Lamprecht, A., Rodero Torres, H., Schafer, U. and Lehr, C. M. (2000). "Biodegradable microparticles as a two-drug controlled release formulation: a potential treatment of inflammatory bowel disease." *J Control Release* **69**(3): 445-454.

Larsen, D. B., Parshad, H., Fredholt, K. and Larsen, C. (2002). "Characteristics of drug substances in oily solutions. Drug release rate, partitioning and solubility." *Int J Pharm* **232**(1-2): 107-117.

Lasic, D. D. (1998). "Novel applications of liposomes." *Trend Biotechnol* **16**: 302-321.

Le Bourlais, C. A., Zia, H., Sado, P. A., Needham, T. and Leverge, R. (1998a). "Ophtalmic drug delivery systems recent advanceds." *Prog Retin Eye Res* **17**: 33-58.

Le Bourlais, C. A., Zia, H., Sado, P. A., Needham, T. and Leverge, R. (1998b). "Ophtalmic drug delivery systems recent advanceds. ." *Prog. Retin. Eye Res* **17**: 33-58.

Le Guevello, P., Le Corre, P., Chevanne, F. and Le Verge, R. (1993). "High-performance liquid chromatographic determination of bupivacaine in plasma samples for biopharmaceutical studies and application to seven other local anaesthetics." *J Chromatogr* **622**(2): 284-290.

Lee, C. H., Moturi, V. and Lee, Y. (2009). "Thixotropic property in pharmaceutical formulations." *J Control Release* **136**(2): 88-98.

Leng, F., Wan, J., Liu, W., Tao, B. and Chen, X. (2012). "Prolongation of epidural analgesia using solid lipid nanoparticles as drug carrier for lidocaine." *Reg Anesth Pain Med* **37**(2): 159-165.

Lertsutthiwong, P., Rojsitthisak, P. and Nimmannit, U. (2009). "Preparation of turmeric oil-loaded chitosan-alginate biopolymeric nanocapsules." *Mat Sci Eng C* **29**(3): 856-860.

Li, H. L., Hadid, D. and Ragsdale, D. S. (2002). "The batrachotoxin receptor on the voltage-gated sodium channel is guarded by the channel activation gate." *Mol Pharmacol* **61**(4): 905-912.

Lippacher, A., Muller, R. H. and Mader, K. (2004). "Liquid and semisolid SLN dispersions for topical application: rheological characterization." *Eur J Pharm Biopharm* **58**(3): 561-567.

Liu, Y., Seipel, C., Lopez, M. E., Nuchtern, J. G., Brandt, M. L., Fallon, S. C., Manyang, P. A., Tjia, I. M., Baijal, R. G. and Watcha, M. F. (2013). "A retrospective study of multimodal analgesic treatment after laparoscopic appendectomy in children." *Paediatr Anaesth* **23**(12): 1187-1192.

Löffler, M., Miller, D. and Hening, T. (2001). Stabilizing O/W systems with a polymeric sulfonic acid as a gateway to new formulation platforms with new sensoric properties. Frankfurt, Clariant GmbH.

Lu, Y. and Chen, S. C. (2004). "Micro and nano-fabrication of biodegradable polymers for drug delivery." *Adv Drug Deliv Rev* **56**(11): 1621-1633.

Ma, J., Feng, P., Ye, C., Wang, Y. and Fan, Y. (2001). "An improved interfacial coacervation technique to fabricate biodegradable nanocapsules of an aqueous peptide solution from polylactide and its block copolymers with poly(ethylene glycol)." *Colloid Polym Sci* **279**(4): 387-392.

Maia Campos, P. M. B. G., Bontempo, E. B. M. G. and Leonardi, G. R. (1999). *Formulário Dermocosmético*. São Paulo, Tecopress.

Malamed, S. F. (2001). *Manual de Anestesia Local,* Elsevier.

Malamed, S. F. (2004). *Handbook of local anesthesia*, Elsevier.

Malamed, S. F. (2006). "Local anesthetics: dentistry's most important drugs, clinical update 2006." *J Calif Dent Assoc* **34**(12): 971-976.

Mandawage, S. D. and Patravale, V. B. (2008). "Development of SLNs from natural lipids: application to topical delivery of tretinoin." *Int J Pharm* **363**: 132-138.

Manjunath, K., Reddy, J. S. and Venkateswarlu, V. (2005). "Solid lipid nanoparticles as drug delivery systems." *Methods Find Exp Clin Pharmacol* **27**(2): 127-144.

Martinsen, A. A., Skajak-Break, G. and Smidsrod, O. (1997). "Comparison of different methods for determination of molecular weight and molecular weight distribution of alginates." *Carbohydr Polym* **15**: 171-193.

Marzzoco, A. and Torres, B. B. (2007). *Bioquímica Básica*, Guanabara Koogan.

McLure, H. A. and Rubin, A. P. (2005). "Review of local anaesthetic agents." *Minerva Anestesiol* **71**(3): 59-74.

Mehnert, W. and Mäder, K. (2012). "Solid lipid nanoparticles. Production, characterization and applications." *Adv Drug Deliv Rev* **64**((Suppl).): 83-101.

Mendonça, C. C., Silva, I. C. L., Rodrigues, K. A., Campos, M. A. L., Medeiros, M. C. M., Casteli, V. C., Ferrari, M., Musis, C. R. and Machado, S. R. P. (2009). "Emulsões O/A contendo Cetoconazol 2,0%: avaliação da estabilidade acelerada e estudos de liberação in vitro." *Rev Ciên Farm Básica Apl* **30**: 35-46.

Mi, F. L., Sung, H. W. and Shyu, S. S. (2002). "Drug release from chitosan– alginate complex beads reinforced by a naturally occurring crosslinking agent." *Carbohydr Polym* **48**: 61-72.

Mishra, B., Patel, B. B. and Tiwari, S. (2010). "Colloidal nanocarriers: a review on formulation technology, types and applications toward targeted drug delivery." *Nanomedicine* **6**(1): 9-24.

Mohanraj, V. J. and Chen, Y. (2006). "Nanoparticles – A review." *Trop J Pharm Res* **5**: 561-573.

Mondal, N., Samanta, A., Pal, T. K. and Ghosal, S. K. (2008). "Effect of different formulation variables on some particle characteristics of poly (DL-lactide-co-glycolide) nanoparticles." *Yakugaku Zasshi* **128**(4): 595-601.

Mora-Huertas, C. E. F., H.; Elaissari, A. (2010). "Polymer based nanocapsules for drug delivery." *Int J Pharm* **385**: 113-142.

Moraes, C. M., Abrami, P., De Araujo, D. R., Braga, A. F., Issa, M. G., Ferraz, H. G., De Paula, E. and Fraceto, L. F. (2007a). "Characterization of Lidocaine:Hydroxypropyl-β-Cyclodextrin Inclusion Complex." *J Inclus Phenom Macroc Chem* **57**: 313-316.

Moraes, C. M., Abrami, P., De Paula, E., Andreo Filho, N. and Fraceto, L. F. (2007b). "Preparo e caracterização físico-química de complexos de inclusão entre anestésicos locais e hidróxipropil-β-ciclodextrina." *Quim Nova* **30**: 777-784.

Moraes, C. M., Abrami, P., De Paula, E., Braga, A. F. and Fraceto, L. F. (2007c). "HPLC and solubility study of the interaction between S (-) Bupivacaine and Hydroxypropyl-β-Cyclodextrin." *Int J Pharm* **331**: 99-106.

Moraes, C. M., Abrami, P., de Paula, E., Braga, A. F. and Fraceto, L. F. (2007d). "Study of the interaction between S(--) bupivacaine and 2-hydroxypropyl-beta-cyclodextrin." *Int J Pharm* **331**(1): 99-106.

Moraes, C. M., de Matos, A. P., de Lima, R., Rosa, A. H., de Paula, E. and Fraceto, L. F. (2007e). "Initial development and characterization of PLGA nanospheres containing ropivacaine." *J Biol Phys* **33**(5-6): 455-461.

Moraes, C. M., de Matos, A. P., de Paula, E., Rosa, A. H. and Fraceto, L. F. (2009). "Benzocaine loaded biodegradable poly-(d,l-lactide-co-glycolide) nanocapsules: factorial design and characterization." *Mater Sci Eng B* **165**: 243-246.

Moraes, C. M., de Matos, A. P., Grillo, R., de Melo, N. F. S., de Paula, E., Dias Filho, N. L., Rosa, A. H. and Fraceto, L. F. (2011). "Screening of formulation variables for the preparation of poly(epsilon-caprolactone) nanocapsules containing the local anesthetic benzocaine." *J Nanosci Nanotechnol* **11**(3): 2450-2457.

Morales, M. M. (2007). *Terapias avançadas: células-tronco, terapia gênia e nanotecnologia aplicada à saúde*, Editora Atheneu.

Moreira, K., Miranda, L. N., Zétola, M., Pezzini, B. R. and Bazzo, G. C. (2012). "Comprimidos contendo microesferas de cetoprofeno como sistema de liberação bifásica." *Rev Cien Farm Básica Apl* **33**(1): 71-76.

Muller, R. H., Mehnert, W., Lucks, J. S., Schwarz, C., Zur Muhlen, A., Weyhers, H., Freitas, C. and Ruhl, D. (1995). "Solid lipid nanoparticles (SLN)—an alternative colloidal carrier system for controlled drug delivery." *Eur J Pharm Biopharm* **41**: 62-69.

Munoz-Bonilla, A., Cerrada, M. L., Fernandez-Garcia, M., Kubacka, A., Ferrer, M. and Fernandez-Garcia, M. (2013). "Biodegradable polycaprolactone-titania nanocomposites: preparation, characterization and antimicrobial properties." *Int J Mol Sci* **14**(5): 9249-9266.

Mura, P., Faucci, M. T., Manderioli, A., Bramanti, G. and Ceccarelli, L. (1998). "Compatibility study between ibuproxam and pharmaceutical excipients using differential scanning calorimetry, hot-stage microscopy and scanning electron microscopy." *J Pharm Biomed Anal* **18**(1-2): 151-163.

Nafee, N., Schneider, M., Schaefer, U. F. and Lehr, C. M. (2009). "Relevance of the colloidal stability of chitosan/PLGA nanoparticles on their cytotoxicity profile." *Int J Pharm* **381**(2): 130-139.

Nagarwal, R. C., Kumar, R. and Pandit, J. K. (2012). "Chitosan coated sodium alginate-chitosan nanoparticles loaded with 5-FU for ocular delivery: in vitro characterization and in vivo study in rabbit eye." *Eur J Pharm Sci* **47**(4): 678-685.

Nair, L. S. and Laurencin, C. T. (2007). "Biodegradable polymers as biomaterials." *Prog Polym Sci* **32**: 762-798.

Neckel, G. L. and Lemos-Senna, E. (2005). "Preparação e caracterização de nanocápsulas contendo camptotecina a partir do ácido poli (D,L-lático) e de copolímeros diblocos do ácido poli (D,L-lático) e polietilenoglicol." *Acta Farm Bonaerense* **24**(4): 504-511.

Némati, F., Dubernet, C., Fessi, H., Colin de Verdiere, A. and Poupon, M. F. (1996). "Reversion of multidrug resistance using nanoparticles in vitro: influence of the nature of the polymer." *Int J Pharm* **138**: 237-246.

Nicoli, S., Colombo, P. and Santi, P. (2005). "Release and permeation kinetics of caffeine from bioadhesive transdermal films." *AAPS J* **7**(1): E218-223.

Oliveira, A. Z. M. (2009). *Desenvolvimento de formulações cosméticas com ácido hialurônico*. Master, Universidado do Porto.

Paavola, A., Yliruusi, J., Kajimoto, Y., Kalso, E., Wahlstrom, T. and Rosenberg, P. (1995). "Controlled release of lidocaine from injectable gels and efficacy in rat sciatic nerve block." *Pharm Res* **12**(12): 1997-2002.

Padamwar, M. N. and Pokharkar, V. B. (2006). "Development of vitamin loaded topical liposomal formulation using factorial design approach: drug deposition and stability." *Int J Pharm* **320**(1-2): 37-44.

Parveen, S., Misra, R. and Sahoo, S. K. (2012). "Nanoparticles: a boon to drug delivery, therapeutics, diagnostics and imaging." *Nanomedicine* **8**(2): 147-166.

Pathak, P. and Nagarsenker, M. (2009). "Formulation and evaluation of lidocaine lipid nanosystems for dermal delivery." *AAPS PharmSciTech* **10**(3): 985-992.

Patil, J. S., Kamalapur, M. V., Marapur, S. C. and Kadam, D. V. (2010). "Ionotropic gelation and polyelectrolyte complexation: the novel techniques to design hydrogel particulate sustained, modulated drug delivery system: a review." *Dig. J. Nanomater. Bios.* **5**(1): 241-248.

Paxton, K. and Thome, D. E. (2010). "Efficacy of articaine formulations: quantitative reviews." *Dent Clin North Am* **54**(4): 643-653.

Picos, D. R., Carril, M. G., Mena, D. F. and Fuente, L. N. (2000). "Microesferas biodegradables de liberación controlada para administración parenteral." *Rev Cubana Farm* **34**: 70-77.

Picout, D. R. and Ross-Murphy, S. B. (2003). "Rheology of biopolymer solutions and gels." *ScientificWorldJournal* **3**: 105-121.

Pinto, L. M., Fraceto, L. F., Santana, M. H., Pertinhez, T. A., Junior, S. O. and de Paula, E. (2005). "Physico-chemical characterization of benzocaine-beta-cyclodextrin inclusion complexes." *J Pharm Biomed Anal* **39**(5): 956-963.

Pogrel, M. A. (2007). "Permanent nerve damage from inferior alveolar nerve blocks--an update to include articaine." *J Calif Dent Assoc* **35**: 271-273.

Polakovic, M., Gorner, T., Gref, R. and Dellacherie, E. (1999). "Lidocaine loaded biodegradable nanospheres. II. Modelling of drug release." *J Control Release* **60**(2-3): 169-177.

Poletto, F. S., Jager, E., Re, M. I., Guterres, S. S. and Pohlmann, A. R. (2007). "Rate-modulating PHBHV/PCL microparticles containing weak acid model drugs." *Int J Pharm* **345**(1-2): 70-80.

Preetz, C., Rube, A., Reiche, I., Hause, G. and Mader, K. (2008). "Preparation and characterization of biocompatible oil-loaded polyelectrolyte nanocapsules." *Nanomedicine* **4**(2): 106-114.

Rampino, A., Borgogna, M., Blasi, P., Bellich, B. and Cesaro, A. (2013). "Chitosan nanoparticles: preparation, size evolution and stability." *Int J Pharm* **455**(1-2): 219-228.

Ranade, V. V. (1989). "Drug delivery systems: site-specific drug delivery using liposomes as carriers." *J Clin Pharmacol* **29**(8): 685-694.

Rang, H. P., Dale, M. M., Ritter, J. M. and Moore, P. K. (2004). *Farmacologia*. Rio de Janeiro, Elservier.

Rawat, M., Singh, D., Saraf, S. and Saraf, S. (2006). "Nanocarriers: Promising vehicle for bioactive drugs." *Biol Pharm Bull* **29**(9): 1790-1798.

Reis, C. P., Neufeld, R. J., Ribeiro, A. J. and Veiga, F. (2006). "Nanoencapsulation I: Methods preparation of drug-loaded polymeric nanoparticles." *Nanomedicine* **2**: 8-21.

Remant Bahadur, K. C., Bhattari, S. R., Aryal, S., Khil, M. S., Dharmaraj, N. and Kim, H. Y. (2007). "Novel amphiphilic triblock copolymer based on PPDO, PCL, and PEG: Synthesis, characterization, and aqueous dispersion." *Colloids Surf A* **292**(1): 69-78.

Renehan, E. M., Enneking, F. K., Varshney, M., Partch, R., Dennis, D. M. and Morey, T. E. (2005). "Scavenging nanoparticles: an emerging treatment for local anesthetic toxicity." *Reg Anesth Pain Med* **30**(4): 380-384.

Richter, K. and Oertel, R. (1999). "Solid-phase extraction and high-performance liquid chromatographic determination of articainic and its metabolite articainic acid in human serum." *J Chromatogr B Biomed Sci Appl* **724**(1): 109-115.

Roco, M. C. (1999). "Nanoparticles and nanotechnology research." *J Nanopart Research* **1**: 1-6.
Rose, J. S., Neal, J. M. and Kopacz, D. J. (2005). "Extended-duration analgesia: update on microspheres and liposomes." *Reg Anesth Pain Med* **30**(3): 275-285.

Rotthauser, B., Kraus, G. and Schmidt, P. C. (1998). "Optimization of an effervescent tablet formulation containing spray dried L-leucine and polyethylene glycol 6000 as lubricants using a central composite design." *Eur J Pharm Biopharm* **46**(1): 85-94.

Saboktakin, M. R., Tabatabaie, R. M., Maharramov, A. and Ramazanov, M. A. (2011). "Synthesis and characterization of pH-dependent glycol chitosan and dextran sulfate nanoparticles for effective brain cancer treatment." *Int J Biol Macromol* **49**(4): 747-751.

Sankalia, M. G., Mashru, R. C., Sankalia, J. M. and Sutariya, V. B. (2007). "Reversed chitosan-alginate polyelectrolyte complex for stability improvement of alpha-amylase: optimization and physicochemical characterization." *Eur J Pharm Biopharm* **65**(2): 215-232.

Sarmento, B., Ferreira, D. C., Jorgensen, L. and van de Weert, M. (2007). "Probing insulin's secondary structure after entrapment into alginate/chitosan nanoparticles." *Eur J Pharm Biopharm* **65**(1): 10-17.

Schaffazick, S. R., Guterres, S. S., Freitas, L. L. and Pohlmann, A. R. (2003). "Caracterização e estabilidade fisico-química de sistemas poliméricos nanoparticulados para administração de fármacos." *Quim Nova* **26**: 726-737.

Schofield, M., Jenski, L. J., Dumaual, A. C. and Stillwell, W. (1998). "Cholesterol versus cholesterol sulfate: effects on properties of phospholipid bilayers containing docosahexaenoic acid." *Chem Phys Lipids* **95**(1): 23-36.

Seaton, A. and Donaldson, K. (2005). "Nanoscience, nanotoxicology, and the need to think small." *Lancet* **365**(9463): 923-924.

Sharma, U. S., Sharma, A., Chau, R. I. and Straubinger, R. M. (1997). "Liposome-mediated therapy of intracranial brain tumors in a rat model." *Pharm Res* **14**(8): 992-998.

Shegokar, R., Singh, K. K. and Muller, R. H. (2011). "Production & stability of stavudine solid lipid nanoparticles--from lab to industrial scale." *Int J Pharm* **416**(2): 461-470.

Shimizu, T., Yamato, M., Kikuchi, A. and Okano, T. (2003). "Cell sheet engineering for myocardial tissue reconstruction." *Biomaterials* **24**(13): 2309-2316.

Siepmann, J. and Siepmann, F. (2008). "Mathematical modeling of drug delivery." *Int J Pharm* **364**(2): 328-343.

Silva, A. C., Amaral, M. H., Gonzalez-Mira, E., Santos, D. and Ferreira, D. (2012). "Solid lipid nanoparticles (SLN)--based hydrogels as potential carriers for oral transmucosal delivery of risperidone: preparation and characterization studies." *Colloids Surf B* **93**: 241-248.

Silva, A. C., Gonzalez-Mira, E., Garcia, M. L., Egea, M. A., Fonseca, J., Silva, R., Santos, D., Souto, E. B. and Ferreira, D. (2011a). "Preparation, characterization and biocompatibility studies on risperidone-loaded solid lipid nanoparticles (SLN): high pressure homogenization versus ultrasound." *Colloids Surf B* **86**(1): 158-165.

Silva, M. S., Cocenza, D. S., de Melo, N. F. S., Grillo, R., Rosa, A. H. and Fraceto, L. F. (2010). "Nanopartículas de alginato como sistema de liberação para o herbicida clomazone." *Quim Nova* **33**(9): 1868-1873.

Silva, M. S., Cocenza, D. S., Grillo, R., de Melo, N. F. S., Tonello, P. S., de Oliveira, L. C., Cassimiro, D. L., Rosa, A. H. and Fraceto, L. F. (2011b). "Paraquat-loaded alginate/chitosan nanoparticles: Preparation, characterization and soil sorption studies." *J Hazard Mater* **190**(1-3): 366-374.

Singh, N., Manshian, B., Jenkins, G. J., Griffiths, S. M., Williams, P. M., Maffeis, T. G., Wright, C. J. and Doak, S. H. (2009). "NanoGenotoxicology: the DNA damaging potential of engineered nanomaterials." *Biomaterials* **30**(23-24): 3891-3914.

Singla, A. K. and Chawla, M. (2001). "Chitosan: some pharmaceutical and biological aspects--an update." *J Pharm Pharmacol* **53**(8): 1047-1067.

Sinha, V. R., Bansal, K., Kaushik, R., Kumria, R. and Trehan, A. (2004). "Poly-epsilon-caprolactone microspheres and nanospheres: an overview." *Int J Pharm* **278**(1): 1-23.
Smidsrod, O. and Skjak-Braek, G. (1990). "Alginate as immobilization matrix for cells." *Trends Biotechnol* **8**(3): 71-78.

Sonaje, K., Italia, J. L., Sharma, G., Bhardwaj, V., Tikoo, K. and Kumar, M. N. (2007). "Development of biodegradable nanoparticles for oral delivery of ellagic acid and evaluation of their antioxidant efficacy against cyclosporine A-induced nephrotoxicity in rats." *Pharm Res* **24**(5): 899-908.

Song, S. I. and Kim, B. C. (2004). "Characteristic rheological features of PVA solutions in water-containing solvents with different hydration state." *Polymer* **45**: 2381-2386.

Souto, E. B. and Doktorovova, S. (2009). "Chapter 6 - Solid lipid nanoparticle formulations pharmacokinetic and biopharmaceutical aspects in drug delivery." *Methods Enzymol* **464**: 105-129.

Souto, E. B. and Muller, R. H. (2007). "Rheological and in vitro release behaviour of clotrimazole-containing aqueous SLN dispersions and commercial creams." *Pharmazie* **62**(7): 505-509.

Souto, E. B., Severino, P. and Santana, M. H. A. (2012). "Preparação de nanopartículas poliméricas a partir da polimerização de monômeros - parte I." *Polímeros* **22**(1): 96-100.

Souto, E. B., Severino, P., Santana, M. H. A. and Pinho, S. C. (2011). "Nanopartículas de lipídios sólidos: métodos clássicos de produção laboratorial." *Quim Nova* **34**: 1762-1769.

Souto, E. B., Wissing, S. A., Barbosa, C. M. and Muller, R. H. (2004). "Evaluation of the physical stability of SLN and NLC before and after incorporation into hydrogel formulations." *Eur J Pharm Biopharm* **58**(1): 83-90.

_____

Stoco, S. M. (2011). *Liberação de ropivacaína através da pele: aspectos biofarmacêuticos da incorporação de promotores de absorção e encapsulação em nanopartículas*. Master, Universidade Estadual de Campinas.

Sun, J. and Tan, H. (2013). "Alginate-based biomaterials for regenerative medicine applications. ." *Materials* **6**: 1285-1309.

Taddio, A., Soin, H. K., Schuh, S., Koren, G. and Scolnik, D. (2005). "Liposomal lidocaine to improve procedural success rates and reduce procedural pain among children: a randomized controlled trial." *CMAJ* **172**(13): 1691-1695.

Torchilin, V. P. (2006). "Multifunctional nanocarriers." *Adv Drug Deliv Rev* **58**(14): 1532-1555.

Vandervoort, J., Yoncheva, K. and Ludwig, A. (2004). "Influence of the homogenisation procedure on the physicochemical properties of PLGA nanoparticles." *Chem Pharm Bull (Tokyo)* **52**(11): 1273-1279.

Vanic, Z., Hurler, J., Ferderber, K., Golja Gasparovic, P., Skalko-Basnet, N. and Filipovic-Grcic, J. (2014). "Novel vaginal drug delivery system: deformable propylene glycol liposomes-in-hydrogel." *J Liposome Res* **24**(1): 27-36.

Varshosaz, J., Tabbakhian, M. and Mohammadi, M. Y. (2010). "Formulation and optimization of solid lipid nanoparticles of buspirone HCl for enhancement of its oral bioavailability." *J Liposome Res* **20**(4): 286-296.

Vasconcelos, R. J. H., Nogueira, R. V. B., Leal, A. K. R., Oliveira, C. T. V. and Bezerra, J. G. B. (2002). "Alterações sistêmicas decorrentes do uso de lidocaína e prilocaína na prática odontológica." *Rev Cir Traumat Buco-Maxilo Facial* **2**: 13-19.

Vemuri, S. and Rhodes, C. T. (1995). "Preparation and characterization of liposomes as therapeutic delivery systems: a review." *Pharm Acta Helv* **70**: 95-111.

Venkatraman, S. S., Jie, P., Min, F., Freddy, B. Y. and Leong-Huat, G. (2005). "Micelle-like nanoparticles of PLA-PEG-PLA triblock copolymer as chemotherapeutic carrier." *Int J Pharm* **298**(1): 219-232.

Venter, J. P., Muller, D. G., du Plessis, J. and Goosen, C. (2001). "A comparative study of an in situ adapted diffusion cell and an in vitro Franz diffusion cell method for transdermal absorption of doxylamine." *Eur J Pharm Sci* **13**(2): 169-177.

Venturini, C. G., Jager, E., Oliveira, C. P., Bernardi, A., Battastini, A. M. O., Guterres, S. S. and Pohlmann, A. R. (2011). "Formulation of lipid core nanocapsules." *Colloids Surf A* **375**(1-3): 200-208.

Vieira, A. L. N. (2012). *Complexo de inclusão do anestésico local ropivacaína em ciclodextrina, encapsulado em lipossomas*. Master, Universidade Estadual de Campinas.

Vila, A., Sánchez, A., Tobío, M., Calvo, P. and Alonso, M. (2002). "Design of biodegradable particles for protein delivery." *J Control Release* **78**: 15-24.

Vitorino, C., Carvalho, F. A., Almeida, A. J., Sousa, J. J. and Pais, A. A. (2011). "The size of solid lipid nanoparticles: an interpretation from experimental design." *Colloids Surf B* **84**(1): 117-130.

Vree, T. B. and Gielen, M. J. (2005). "Clinical pharmacology and the use of articaine for local and regional anaesthesia." *Best Pract Res Clin Anaesthesiol* **19**(2): 293-308.

Vrignaud, S., Benoit, J. P. and Saulnier, P. (2011). "Strategies for the nanoencapsulation of hydrophilic molecules in polymer-based nanoparticles." *Biomaterials* **32**(33): 8593-8604.

Wang, Q., Guan, Y. X., Yao, S. J. and Zhu, Z. Q. (2010). "Microparticle formation of sodium cellulose sulfate using supercritical fluid assisted atomization introduced by hydrodynamic cavitation mixer." *Chem Eng J* **159**: 220-229.

Wei, X., Gong, C., Gou, M., Fu, S., Guo, Q., Shi, S., Luo, F., Guo, G., Qiu, L. and Qian, Z. (2009). "Biodegradable poly(epsilon-caprolactone)-poly(ethylene glycol) copolymers as drug delivery system." *Int J Pharm* **381**(1): 1-18.

Weinschenk, S. (2012). "Neural therapy—A review of the therapeutic use of local anesthetics." *Acupuncture and Related Therapies* **1**(1): 5-9.

Welder, A. A. (1992). "A primary culture system of postnatal rat heart cells for the study of cocaine and methamphetamine toxicity." *Toxicol Lett* **60**(2): 183-196.

Wiles, M. D. and Nathanson, M. H. (2010). "Local anaesthetics and adjuvants--future developments." *Anaesthesia* **65 Suppl 1**: 22-37.

Woitiski, C. B., Carvalho, R. A., Ribeiro, A. J., Neufeld, R. J. and Veiga, F. (2008). "Strategies toward the improved oral delivery of insulin nanoparticles via gastrointestinal uptake and translocation." *BioDrugs* **22**(4): 223-237.

Woitiski, C. B., Veiga, F., Ribeiro, A. and Neufeld, R. (2009). "Design for optimization of nanoparticles integrating biomaterials for orally dosed insulin." *Eur J Pharm Biopharm* **73**(1): 25-33.

Woodruff, M. A. and Hutmacher, D. W. (2010). "The return of a forgotten polymer : Polycaprolactone in the 21st century." *Prog Polym Sci* **35**(10): 1217-1256.

Yadav, A. K., Mishra, P., Jain, S., Mishra, P., Mishra, A. K. and Agrawal, G. P. (2008). "Preparation and characterization of HA-PEG-PCL intelligent core-corona nanoparticles for delivery of doxorubicin." *J Drug Target* **16**(6): 464-478.

Yang, S. J., Lin, F. H., Tsai, H. M., Lin, C. F., Chin, H. C., Wong, J. M. and Shieh, M. J. (2011). "Alginate-folic acid-modified chitosan nanoparticles for photodynamic detection of intestinal neoplasms." *Biomaterials* **32**(8): 2174-2182.

Yoo, J. H., Shanmugam, S., Thapa, P., Lee, E. S., Balakrishnan, P., Baskaran, R., Yoon, S. K., Choi, H. G., Yong, C. S., Yoo, B. K. and Han, K. (2010). "Novel self-nanoemulsifying drug

delivery system for enhanced solubility and dissolution of lutein." *Arch Pharm Res* **33**(3): 417-426.

You, J. and Peng, C. (2005). "Calcium-alginated nanoparticles formed by reverse microemulsion as gene carriers." *Macromol Symp* **219**: 147-153.

Zahoor, A., Sharma, S. and Khuller, G. K. (2007). "Chemotherapeutic evaluation of alginate nanoparticle-encapsulated azole antifungal and antitubercular drugs against murine tuberculosis." *Nanomedicine* **3**: 239–243.

Zandanel, C. and Vauthier, C. (2012). "Poly(isobutylcyanoacrylate) nanoparticles decorated with chitosan: effect of conformation of chitosan chains at the surface on complement activation properties." *J Colloid Sci Biotechnol* **1**(1): 68-81.

Zanini, M. (2007). "Gel de ácido tricloroacético - Uma nova técnica para um antigo ácido." *Med Cutan Ibero Lat Am* **35**(1): 14-17.

Zhang, L., He, Y., Ma, G., Song, C. and Sun, H. (2012). "Paclitaxel-loaded polymeric micelles based on poly(varepsilon-caprolactone)-poly(ethylene glycol)-poly(varepsilon-caprolactone) triblock copolymers: in vitro and in vivo evaluation." *Nanomedicine* **8**(6): 925-934.

Zhou, Z., Ye, J., Chen, L., Ma, A. and Zou, F. (2010). "Simultaneous determination of ropivacaine, bupivacaine and dexamethasone in biodegradable PLGA microspheres by high performance liquid chromatography." *Yakugaku Zasshi* **130**(8): 1061-1068.

Zhu, R. R., Qin, L. L., Wang, M., Wu, S. M., Wang, S. L., Zhang, R., Liu, Z. X., Sun, X. Y. and Yao, S. D. (2009). "Preparation, characterization, and anti-tumor property of podophyllotoxin-loaded solid lipid nanoparticles." *Nanotechnology* **20**(5): 055702.